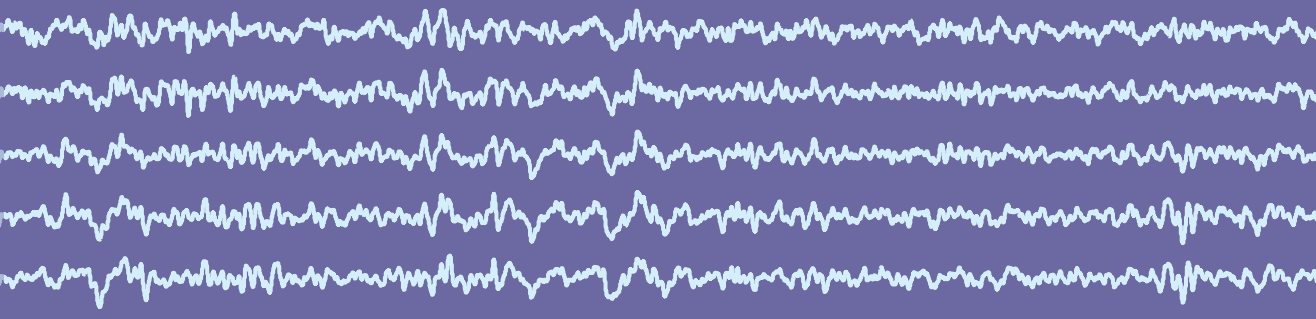

Identification of Connectivity in Human Motor Control

Exciting the Afferent Pathways

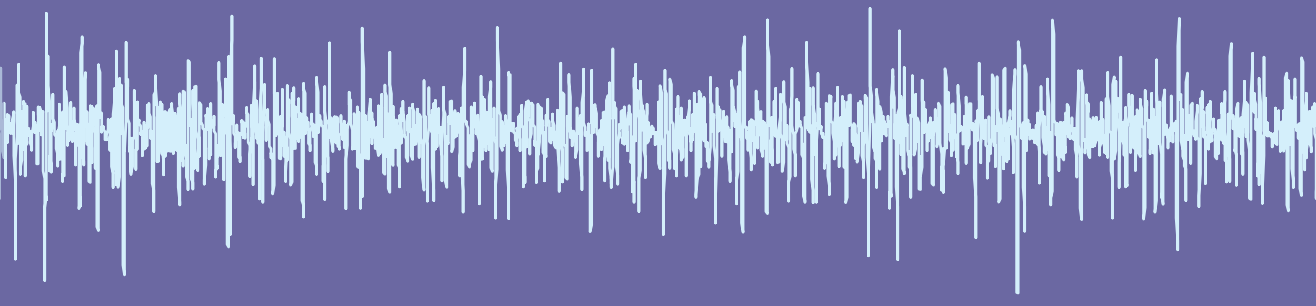

Floor Campfens

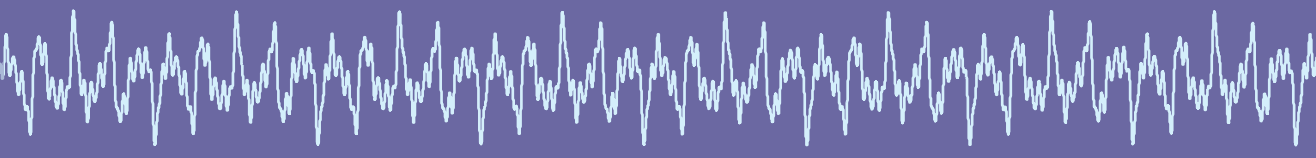

Identification of Connectivity in Human Motor Control: Exciting the Afferent Pathways

Sanne Floor Campfens, MSc

Samenstelling promotiecommissie:

Voorzitter / Secretaris

prof. dr. ir. J.W.M. Hilgenkamp	Universiteit Twente

Promotoren

prof. dr. ir. H. van der Kooij	Universiteit Twente
prof. dr. ir. M.J.A.M. van Putten	Universiteit Twente

Co-promotor

dr. ir. A.C. Schouten	Universiteit Twente

Referent

dr. G. Nolte	Universitätsklinikum Hamburg-Eppendorf

Leden

prof. dr. ir. P.H. Veltink	Universiteit Twente
prof. dr. R.J.A. van Wezel	Universiteit Twente
prof. dr. ir. D.F. Stegeman	Vrije Universiteit Amsterdam
prof. dr. G. Kwakkel	Vrije Universiteit Amsterdam

Paranimfen
Tjitske Boonstra
Thijs Maalderink

Ontwerp omslag en binnenwerk:
Floor Campfens

Drukwerk:
Ipskamp Drukkers

ISBN: 978-90-365-3721-6
DOI: 10.3990/1.9789036537216

Identification of Connectivity in Human Motor Control: Exciting the Afferent Pathways

Proefschrift

ter verkrijging van
de graad van doctor aan de Universiteit Twente,
op gezag van de rector magnificus,
prof. dr. H. Brinksma,
volgens besluit van het College voor Promoties
in het openbaar te verdedigen
op donderdag 9 oktober 2014 om 14.45 uur.

door

Sanne Floor Campfens

geboren op 18 januari 1985
te Amsterdam

Dit proefschrift is goedgekeurd door de promotoren:
prof. dr. ir. H. van der Kooij
prof. dr. ir. M.J.A.M. van Putten

en door de copromotor:
dr.ir. A.C. Schouten

Summary

Motor control involves various parts of the central nervous system (CNS) and requires the exchange of information between neural populations in the CNS. Information exchange in facilitated by the formation of functional networks between populations of neurons, relying on the synchronization of neural oscillations. This thesis presents the development and evaluation of techniques that quantify the corticomuscular connectivity (i.e. connectivity between cortex and muscles) in motor control.

Intramuscular coherence (IMC) quantifies the common (supra-spinal) drive to different parts of a single muscle. While IMC analyses does not require complex measurement techniques, IMC analysis is an attractive technique to apply during functional tasks like walking. However, the applicability of IMC analysis is limited due low reliability and agreement of IMC variables between sessions (chapter 2). The smallest real difference indicated that large differences in IMC variables are needed to detect changes in common drive to muscles between sessions.

Corticomuscular coherence (CMC) is the coherence between cortical activity, recorded by EEG or MEG, and muscle activity, recorded by EMG. This is a widely applied measure of corticomuscular connectivity. The phase of the complex corticomuscular coherency is often interpreted as a transmission delay between cortex and muscles. We showed that phase analysis for the estimation of transmission delay gives unreliable results in closed loop systems (chapter 3). As evidence is accumulating that CMC arises in a closed loop system, phase analysis of corticomuscular coherency is not a valid measure of the transmission delay between cortex and muscles.

Based on techniques from the field of system identification, two measures of pathway connectivity were presented (chapter 4 and 6). External mechanical perturbations were applied to 'open' the closed loop motor control system. Two connectivity measures were derived from the application of joint position perturbations during a static motor task: position-cortical coherence (PCC) and muscle stretch evoked potentials (StrEPs). Because the mechanical perturbations 'enter' the motor control system at the beginning of the afferent sensory pathways, integrity of the afferent sensory pathways is required and sufficient for the detection of PCC and StrEP. Indeed, in the normal subject group all subjects presented PCC as well as a StrEP, consistent with a normal integrity of the afferent sensory pathways.

Position-cortical coherence quantifies the correlation between a joint position perturbation and cortical activity, recorded by EEG, in the frequency domain. Presence of significant PCC at a specific frequency indicates that the cortical activity is synchronized to the position perturbation at that frequency. In normal young subjects ($n = 22$) significant PCC

was localized at the sensorimotor area contralateral to the position perturbation.

Position-cortical coherence has an important advantage over CMC measured during an unperturbed task. Significant CMC is detected in only 40% of a normal healthy populations. Significant PCC was detected in all healthy subjects. In addition, because CMC is affected by both afferent and efferent pathways it is not possible to relate changes in CMC to specific pathway connectivity. Position-cortical coherence primarily reflects afferent pathway connectivity.

The muscle stretch evoked potential represents the time course of cortical activation in response to transient joint movement. Peaks in the StrEP at different latencies allow the separation between the arrival of sensory feedback at the cortex and subsequent processing of this information. In normal young subjects ($n = 22$), the StrEP was characterized by an early peak within 60ms after movement onset localized at the contralateral primary motor cortex and a complex of late peaks between 60 and 300ms after movement onset over the vertex. Stretch evoked potential waveforms and features were consistent across different tasks and sessions.

Also in (subacute) stroke survivors afferent pathway connectivity can be assessed by PCC or the StrEP. All (subacute) stroke survivors presented PCC (chapter 4) and a StrEP (chapter 6), even those with very poor motor function who were unable to perform an isotonic wrist flexion task. Abnormal and heterogeneous StrEP waveforms were seen in subacute stroke subjects, but no significant difference was found between StrEP features of subjects with good and poor function. However, presence of PCC did differ between subacute subjects with good and poor motor function. Future research should show whether PCC could aid in giving stroke survivors a more detailed prognosis of their potential motor function recovery or allow applying rehabilitation therapy targeted to critical time windows.

Samenvatting

Verschillende onderdelen van het centraal zenuwstelsel zijn betrokken bij het aansturen van bewegingen. Zo vereist bewegingsaansturing de uitwisseling van informatie tussen groepen neuronen op verschillende plekken in het centraal zenuwstelsel. De informatie-uitwisseling komt tot stand door de formatie van functionele netwerken van groepen neuronen die de oscillaties in hun activiteit met elkaar synchroniseren. In dit proefschrift wordt de ontwikkeling en evaluatie beschreven van technieken om corticomusculaire connectiviteit (connectiviteit tussen cortex en spieren) te kwantificeren.

Intramusculaire coherentie (IMC) kwantificeert de centrale (supra-spinale) aansturing richting verschillende delen van een spier. Omdat IMC analyse geen complexe meettechnieken vereist is het een aantrekkelijke techniek om toe te passen tijdens functionele motorische taken zoals lopen. Echter, de toepasbaarheid van IMC analyse is beperkt door de lage betrouwbaarheid en overeenstemming van IMC variabelen tussen meetsessies (hoofdstuk 2). Evaluatie van het onderscheidend vermogen van de IMC variabelen liet zien dat er grote verschillen tussen IMC variabelen nodig zijn om een verschil tussen meetsessies aan te tonen.

Corticomusculaire coherentie (CMC) is de coherentie tussen corticale activiteit, gemeten met EEG of MEG, en spieractiviteit, gemeten met EMG. Het is een veelvuldig toegepaste maat voor corticomusculaire connectiviteit. De fase van de complexe CMC wordt vaak geïnterpreteerd als een tijdsvertraging ten gevolge van het transport van informatie tussen cortex en spieren. Wij hebben laten zien dat fase-analyse om tijdsvertragingen te schatten onbetrouwbare resultaten geeft binnen gesloten-lussystemen (hoofdstuk 3). Er wordt steeds meer bewijs gepresenteerd dat CMC ontstaat binnen een gesloten-lussysteem, daardoor is fase-analyse van CMC geen valide methode om tijdsvertragingen te schatten tussen cortex en spieren.

Gebaseerd op technieken uit de systeem identificatie, zijn er twee maten voor richting-specifieke gepresenteerd (hoofdstuk 4 en 6). Externe mechanische verstoringen zijn toegepast om het gesloten-lussysteem van bewegingsaansturing 'open' te maken. Twee connectiviteitsmaten zijn afgeleid van de toepassing van externe positieverstoringen tijdens een statische motorische taak: positie-corticale coherentie (PCC) en door spier-rek opgewekte potentialen (StrEPs). Omdat de externe mechanische verstoringen het bewegingsaansturingssysteem 'binnen' komen aan het begin van de van de afferente sensorische banen, is integriteit van de van de afferente sensorische banen een voorwaarde voor de detectie van PCC en StrEPs.

Positie-corticale coherentie kwantificeert de correlatie in het frequentiedomein tussen de positieverstoring en corticale activiteit, gemeten door middel van EEG. Aanwezigheid

van significante PCC op een specifieke frequentie geeft aan dat de corticale activititeit is gesynchroniseerd met de positieverstoring op de betreffende frequentie. In gezonde proefpersonen (n = 22) is significante PCC gelocaliseerd sensorische-motorische cortex contralateraal aan de positieverstoring.

Positie-corticale coherentie heeft een belangrijk voordeel ten opzichte van CMC gemeten tijdens een onverstoorde motorische taak. Significante CMC wordt gevonden in slechts 40% van een normale gezonde populatie. Significante PCC werd gevonden in alle normale gezonde proefpersonen. Daarnaast is het niet mogelijk om onderscheid te maken tussen efferente en afferente paden bij veranderingen in CMC. Positie-corticale coherentie reflecteert specifiek connectiviteit via de afferente paden.

De spier-rek opgewekte potentialen representeren het tijdsverloop van de corticale activatie in reactie op kortdurende positieverstoringen. Pieken in de StrEP op verschillende latenties maken het het mogelijk om verschil te maken tussen de aankomst van sensorische feedback op de cortex en de daarop volgende verwerking van die informatie. In gezonde proefpersonen (n = 22), wordt de StrEP gekarakteriseerd door een vroege piek, binnen 60ms na de inzet van de beweging, gelocaliseerd op de contralaterale motorische cortex. De vroege piek wordt gevolgd door een complex van latere pieken tussen 60 en 300ms na de inzet van de beweging. Spier-rek opgewekte potentialen hadden een consistente vorm en eigenschappen tussen verschillende taken en sessies.

Ook na een herseninfarct kan connectiviteit via de afferente paden gemeten worden met PCC of StrEPs. Alle proefpersonen die een herseninfarct hadden meegemaakt lieten PCC (hoofdstuk 5) en StrEP (hoofdstuk 6) zien. Integriteit van de afferente paden kon zelfs gemeten worden in proefpersonen met een zeer slechte motorische functie, zij waren niet in staat om een motorische taak uit te voeren. Proefpersonen na een herseninfarct lieten abnormale StrEP vormen zien, maar er was geen significant verschil tussen individuen met goede en slechte motorische functie. Echter, de aanwezigheid van PCC verschilde wel tussen proefpersonen met goede en slechte functie. Toekomstig onderzoek moet uitwijzen of PCC kan bijdragen in het beter voorstellen van het potentiele herstel van motorische functie na een CVA. Mogelijk zou PCC ook kunnen worden toegepast om revalidatietherapie specifiek aan te bieden binnen kritische tijdsvensters van herstel.

Table of contents

Chapter 1

Introduction

Humans are capable of performing extremely complex movement patterns. From gracious ballet dancers, bending their joints to nearly impossible angles, to skilled pianists, moving their fingers across the keyboard faster than the eye can see. These artists are specialists in specific movement skills.

Movement control is vital in the everyday life of all of us. We are able to move around, manipulate objects and express ourselves through the control of our muscles. With movement being such an essential part of everyday life it is easy to understand that diseases affecting the ability to move have a major impact on the quality of life.

The performance of movement involves our joints, muscles and central nervous system (CNS). The CNS acts as the control centre that sends out commands to muscles and receives feedback about the resulting movement of the joints. A large body of research is dedicated to understanding how movement is controlled in the normal physiological situation as well as in the context of (neurological) diseases affecting motor control, such as stroke. The research presented in this thesis contributes to this field by evaluating methods that quantify the *connectivity* between muscles and the CNS.

In this introductory chapter, some background and concepts are described that provide the basis for the research presented in this thesis. This chapter is concluded by the research aims and an outline of this thesis.

1.1 Motor control

The control of movement (motor control) involves our CNS, muscles, and several types of sensors. The CNS (consisting of the spinal cord, brain stem, cerebellum and the brain) sends motor commands that reach the muscles via the descending efferent pathways. The muscles contract, generating torque around the joints and resulting in a change of joint angles. Special sensors in the muscles (muscle spindles) and tendons (Golgi tendon organs) sense changes in muscle length and tendon force. Via the ascending afferent pathways the sensory feedback signals are sent back to the CNS where they lead to adjustment of the motor commands.

Motor control thus relies on a circular flow of information and forms a so-called closed loop feedback system. One of the reasons that motor control is so versatile is that motor control does not consist of a single loop. Several parts of the CNS are involved in motor control and they form multiple nested and interacting loops (Scott, 2004). Figure 1.1 depicts which parts of the CNS are involved in motor control and gives an indication of the complex structure. The spinal cord is at the lowest hierarchical level: the level of the 'simple' spinal reflex loop. At higher hierarchical levels the brain stem, basal ganglia, cerebellum and several cortical areas are involved in motor control.

At the cortical level, the primary motor cortex can be considered the starting point of the efferent pathways. The primary motor cortex has direct connections with interneurons in the spinal cord and with the α-motor neurons (Scott, 2004) which are the final section of the efferent pathways: their axons terminate at the neuromuscular junction. The primary motor cortex receives input from several subcortical and cortical areas involved in sensory integration and motor planning (Kandel et al., 2000).

Just posterior of the primary motor cortex the primary sensory cortex is located, which can be considered the endpoint of the afferent pathways. The primary sensory cortex receives input from the various peripheral sensors. The primary motor cortex and primary sensory cortex are connected via direct connections, but also indirectly via other cortical and subcortical brain areas (Kandel et al., 2000). The cortical areas are needed for a proper functioning of the closed loop motor control system. Damage to these cortical areas affects the ability to perform movement.

1.2 Stroke

A stroke is the loss of brain function due to insufficient blood supply to a part of the brain. Stroke is a major cause for adult onset disability in the Western world. Each year approximately 41.000 people have a stroke in the Netherlands[1]. The loss of blood supply can either be caused by obstruction of a blood vessel supplying the brain (ischemic stroke, 80% of the strokes) or by rupture of a blood vessel (hemorrhagic stroke). Depending on the severity and the location of the stroke, a stroke survivor may experience loss of various functions including motor function, sensory function, sight and cognitive functions.

Rehabilitation after stroke aims at improving the patient's quality of life. When a stroke survivor experiences motor impairment, i.e. partial or complete paralysis of parts of the

[1] Website of the Hersenstichting
`www.hersenstichting.nl/alles-over-hersenen/hersenaandoeningen/beroerte`, accessed April 2014

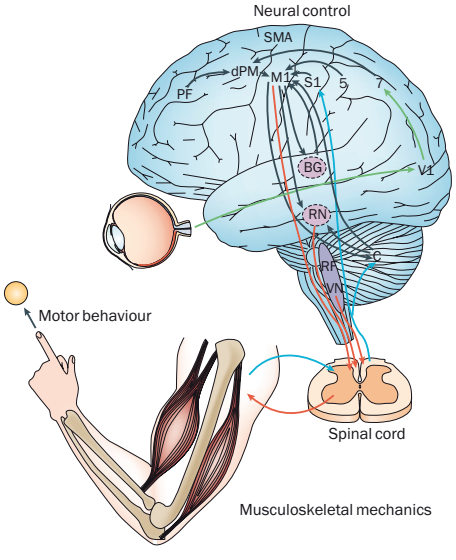

Figure 1.1: Overview of central nervous system involved in motor control. At the lowest hierarchical level there is the spinal cord; at a higher level there are neural populations in the brain stem. The cortex provides the highest level of motor control; multiple cortical areas and subcortical neural populations interact in motor control. In this figure red lines represent the efferent pathways, blue lines the afferent pathways. Green lines indicate the visual pathways and black lines the local cortical and subcortical pathways. Abbreviations: RF: reticular formation, VN: vestibular nuclei, M1: primary motor cortex, S1: primary sensory cortex, 5: parietal cortex area 5, dPM: dorsal premotor cortex, SMA: supplementary motor area, PF: prefrontal cortex, V1: primary visual cortex, 7: posterior parietal cortex area 7, BG: basal ganglia, RN: red nucleus, C: cerebellum.

body, rehabilitation therapy is aimed at reducing this motor impairment. Nearly all stroke survivors with initial motor deficits experience some degree of improvement of motor function within the first six months after stroke. Motor function may improve due to restitution mechanisms: the actual recovery of lost functions. In addition, also compensation strategies, i.e. the emergence of new movement patterns, can lead to a reduction of motor impairment (Kwakkel et al., 2004). Various processes act on different time scales and interact with each other, making the recovery of motor function a complex and time-dependent process.

It has been shown that both sensory and motor areas in the cortex can reorganise during motor function recovery after stroke (Grefkes and Ward, 2014; Roiha et al., 2011). Monitoring the efferent and afferent pathways during recovery can provide valuable insight in how possible reorganization is related to the functioning of closed loop motor control. This requires techniques that quantify how activity at the various CNS levels are functionally connected.

1.3 Connectivity between neural populations

It has become clear that motor control involves different parts of the CNS. Motor control is only possible when neural population in different parts of the CNS are able to exchange information. This requires both anatomical and functional connections between the various neural populations. The anatomical connections are formed by the wired connection infrastructure between the neural populations. The functional connection represents the exchange of information across these anatomical connections (Fries, 2005).

The group activity of a population of neurons has an oscillatory character and these

oscillations are thought to play an important role in the formation of functional networks. Populations of neurons involved in a certain task synchronize their oscillations allowing the integration of information relevant for that specific task (Varela et al., 2001; Fries, 2005; Stam and van Straaten, 2012). By synchronizing oscillatory activity, neural populations are able to form functional networks including populations necessary for the task at hand. The formation of functional connections has been shown for different types of tasks (several examples are described in the review of Varela et al., 2001), including motor control tasks (Kristeva-Feige et al., 2002; Schoffelen et al., 2005, 2011).

Although it is accepted that synchronization of oscillations contributes to the functional connectivity between populations of neurons, there are different views on what is being coded and how this synchronization should be quantified (Horwitz, 2003). Although many methods have been presented, the following brief overview will be limited to three groups of measures that are widely applied in experimental studies on connectivity in motor control.

The first group of measures is based on the correlation between activity of different neural populations. Often the frequency domain equivalent of correlation is applied: *coherence* (Rosenberg et al., 1989; Bruns, 2004; Nolte et al., 2004). Coherence between two signals expresses the amount of linear coupling between the two signals at each frequency. If there is no linear coupling the coherence is zero; if there is perfect linear coupling the coherence is one. Perfect linear coupling means there is a constant phase difference and a constant amplitude ratio between the signals. Related to coherence is the (complex) *coherency*. Coherence is the magnitude squared of the complex coherency.

The second group of measures takes only the phase of oscillations into account: *phase synchronization*, which has various versions and implementations (Tass et al., 1998; Lachaux et al., 1999; Stam et al., 2007; Vinck et al., 2010). In phase synchronization measures, the amplitude ratio between two signals is ignored. Phase synchronization and coherence can be related: at a single frequency phase synchronization between two signals is a necessary and sufficient condition for the presence of significant coherence between the signals (Bruns, 2004). However, unlike coherence, phase synchronization can also be quantified across frequencies (Tass et al., 1998).

The third group of measures is based on the concept of *Granger causality* (Granger, 1969). While coherence and phase synchronization based measures directly quantify synchronization from time series of neural activity, most measures based on Granger causality require a modelling step. First a multivariate autoregressive model is fitted to time series of neural activity. Subsequently, connectivity measures are calculated from the model parameters. Granger causality measures express how well the future of a signal can be predicted by taking into account the past of another signal. Modelling the data has the added advantage that, in addition to quantifying the strength of connectivity, the directionality of the information flow can de determined and quantified (Kaminski and Blinowska, 1991; Baccalá and Sameshima, 2001). Disentangling the directionality of the information flow is not possible with coherence or phase synchronization measures.

Connectivity in motor control

Using invasive techniques (e.g. electrocorticography), the activity of cortical areas involved in motor control can be recorded separately, which allows studying the role of these

Box 1.1: Electrophysiological measurements

Electroencephalography
The electroencephalogram (EEG) records the potential differences arising due to synaptic activity of the pyramidal cells in the cortex. Dendrites of pyramidal neurons receive input via their synapses, causing changes in the membrane potential of the dendrites. Each change in this postsynaptic potential gives rise to a small extracellular current. When the input to large groups of pyramidal cells is sufficiently synchronized, these extracellular currents sum up to current dipoles large enough to allow the recording of potential differences by electrodes on the scalp.
Due to the volume conducting properties of the tissue separating the current dipoles and the recording electrodes, the spatial resolution of the EEG is limited. However, a very attractive property of EEG, compared with other functional brain imaging techniques, is the high time resolution: changes in cortical activity can be recorded on a millisecond time scale.

Electromyography
The electromyogram (EMG) records the electrical activity of muscles. Muscle fibres belonging to one motor unit receive input from one α-motor neuron. When an action potential is transferred to the muscle fibres via the neuromuscular junction, the outer membrane of the muscle fibre is depolarized. The depolarization travels as an action potential along the muscle fibres in two directions away from the neuromuscular junction, triggering the contraction of the muscle fibre.
Because the depolarization of all muscle fibres in one motor unit is synchronized, the depolarization wave can result in extracellular currents that cause potential differences large enough to be measured outside of the muscles. In case of superficial muscles, the summed electrical signals from different motor units can even be recorded by electrodes placed on the skin overlying the muscle: surface EMG.

different areas in motor control (Baker, 2007). Using non-invasive electrophysiological recordings (box 1.1), the number of different cortical and subcortical areas that can be distinguished is limited. The various cortical and subcortical areas contributing to motor control are lumped and the electroencephalogram (EEG) acts as a measure for the activity of the lumped cortical control level. Electromyography (EMG) acts as a measure of the motor commands sent by the spinal cord to the muscles via the α-motor neurons.

When relying on traditional non-invasive measurements of CNS activity, the scheme of motor control needs to be simplified (figure 1.2). In the simplified scheme two levels are discriminated in the CNS: the cortex and the spinal cord.

This scheme greatly simplifies the complexity of motor control and the number of pathways. Nevertheless, this scheme is implicitly adopted when connectivity in motor control is studies using non-invasive techniques. Also in the work presented in this thesis the simplified scheme of motor control will serve as a general framework.

Connectivity between the neural populations at the cortical level and populations at the level of the spinal cord is measured by applying connectivity measures on recorded EEG and EMG. Because these signals originate from the cortex and the muscles this is referred to as *corticomuscular connectivity*. Most often corticomuscular connectivity is measured by coherence between EEG and EMG: *corticomuscular coherence* (CMC). Significant CMC is found in the beta band (15 to 30Hz) during static isometric contractions (Halliday et al., 1998; Conway et al., 1995; Mima et al., 2000; Baker, 2007).

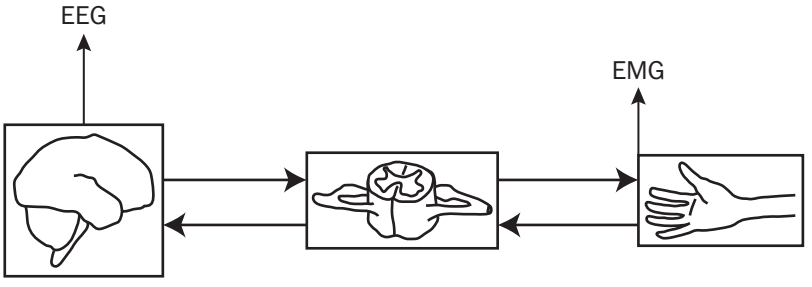

Figure 1.2: Simplified scheme of motor control consisting of two levels in the central nervous system (CNS), the cortex and the spinal cord. Left to right arrows indicate the efferent pathways, right to left arrows indicate the afferent pathways. The electroencephalogram (EEG) records cortical activity. The electromyogram (EMG) records muscle activity.

To study the coordination between muscles during complex movement tasks, coherence between pairs of EMG channels is measured. *Intermuscular coherence* is the coherence between recordings from different muscles while *intramuscular coherence* is the coherence between signals recorded from different parts of a single muscle. Coherence between (parts of) muscles can represent the amount of common (supra-spinal) input the α-motor neurons receive but may also represent connectivity between neural populations in the spinal cord (Grosse et al., 2002).

The applicability of current measures of corticomuscular connectivity is limited. First of all, significant CMC cannot be detected in all subjects (Ushiyama et al., 2011; Mendez-Balbuena et al., 2011). Furthermore, current measures of connectivity in motor control do not allow separation between the efferent and afferent pathways. To study the role of efferent and afferent pathways in physiological and pathophysiological motor control, new techniques must be developed that can reliably be obtained from all subjects acknowledge the closed loop structure of motor control.

1.4 Aim and outline of this thesis

This thesis evaluates and develops techniques to quantify pathway specific connectivity in motor control. The newly developed techniques are based on a concept from the field of system identification: the application of external (mechanical) perturbations to 'open' the closed loop of motor control (Ljung, 1999; Pintelon and Schoukens, 2001). Previously this approach has successfully been applied to identify different types of reflexes in posture control (van der Helm et al., 2002; Schouten et al., 2008; Mugge et al., 2010) and to separate the contribution of the legs and joints involved in upright balance control (van Asseldonk et al., 2006; Pasma et al., 2012; Boonstra et al., 2013).

This thesis contains the following original contributions:

- Evaluation of test-retest reliability and agreement of tibialis anterior intramuscular coherence during walking (chapter 2).

- Demonstration of a pitfall in the application of connectivity measures to estimate transmission delays in closed loop motor control (chapter 3).
- Presentation of a novel connectivity measure in motor control based on coherence and the application of continuous joint position perturbations: position-cortical coherence (PCC, chapter 4).
- Evaluation of the consistency of specific features of cortical responses to transient external joint position perturbations (muscle stretch evoked potentials, StrEPs, chapter 6).
- First exploration of afferent pathway connectivity with the newly developed measures, PCC and StrEP, in stroke survivors with various levels of motor function (chapters 5 and 6).

Chapter 2 and chapter 3 present the results on an evaluation of connectivity measures that are often applied in studies on (aspects of) motor control. Chapter 2 assesses the test-retest reliability and agreement of intramuscular coherence. Chapter 3 describes a simulation study where we investigate which measures of corticomuscular connectivity are suitable to estimate transmission delays in a closed-loop system.

Chapters 4 and 5 introduce and evaluate a new measure of connectivity between sensorimotor cortex and muscles. The new measure relies on the application of continuous external perturbations during a motor task. Chapter 4 describes the results from healthy young subjects and chapter 5 describes the results from a group of stroke survivors.

Chapter 6 contains the results of an evaluation of the cortical response (evoked potential) resulting from transient external perturbations during a motor task. We identify and evaluate specific features of the evoked potentials in healthy subjects and explored the evoked potentials in subacute stroke survivors.

The thesis is concluded with a general discussion in chapter 7.

1

Chapter 2

Reliability and agreement of intramuscular coherence in the tibialis anterior muscle

Edwin H.F. van Asseldonk, **S. Floor Campfens**, Stan J.F. Verwer, Michel J.A.M. van Putten and Dick F. Stegeman. *PloS ONE* 6(2): e88428, 2014

ABSTRACT

Neuroplasticity drives recovery of walking after a lesion of the descending tract. Intramuscular coherence analysis provides a way to quantify corticomotor drive during a functional task, like walking and changes in coherence serve as a marker for neuroplasticity. Although intramuscular coherence analysis is already applied and rapidly growing in interest, the reproducibility of variables derived from coherence is largely unknown. The purpose of this study was to determine the test-retest reliability and agreement of intramuscular coherence variables obtained during walking in healthy subjects.

Ten healthy participants walked on a treadmill at a slow and normal speed in three sessions. Area of coherence and peak coherence were derived from the intramuscular coherence spectra calculated using rectified and non-rectified m. tibialis anterior electromyography (EMG). Reliability, defined as the ability of a measurement to differentiate between subjects and established by the intra-class correlation coefficient, was on the limit of good for area of coherence and peak coherence when derived from rectified EMG during slow walking. Yet, the agreement defined as the degree to which repeated measures are identical was low as the measurement error was relatively large. The smallest change to exceed the measurement error between two repeated measures was 66% of the average value. For normal walking and/or other EMG processing settings, not rectifying the EMG and/or high-pass filtering with a high cutoff frequency (100Hz) the reliability was only moderate to poor and the agreement was considerably lower.

Only for specific conditions and EMG-processing settings, the derived coherence variables can be considered to be reliable measures. However, large changes (> 66%) are needed to indicate a real difference. So, although intramuscular coherence is an easy to use and a sufficiently reliable tool to quantify intervention-induced neuroplasticity, the large effects needed to reveal a real change limit its practical use.

2.1 Introduction

Recovery of walking after a lesion of the descending tract relies on neuroplasticity, reorganization of the function, structure and connections of the central nervous system in response to internal or external (i.e. training) stimuli (Cramer et al., 2011). Human walking requires integrated action of neural control circuitries at the spinal cord and brain (Bo Nielsen, 2002). Changes in these circuitries, reflecting neuroplasticity, can be obtained using coherence analysis of motor unit firing behaviour during walking.

Coherence derived from a pair of EMG signals, EMG-EMG coherence, quantifies the common oscillatory drive to a pair of muscles (intermuscular coherence) or to two parts of the same muscle (intramuscular coherence). EMG-EMG coherence in the beta (15−35Hz) bands is considered to reflect the common corticospinal drive from the primary motor cortex to the muscles (Hansen et al., 2001; Grosse et al., 2003; Halliday et al., 2003; Grosse et al., 2002; Petersen et al., 2010; Brown et al., 1999) whereas also spinal circuitries could potentially contribute (Norton et al., 2004, 2003). EMG-EMG coherence is an attractive approach to assess this common drive since it is easy to measure, requiring only the recording of EMG signals without the need to perturb or stimulate the system (Bo Nielsen, 2002; Barthélemy et al., 2010; Hansen et al., 2005; Norton, 2008).

EMG-EMG coherence can be applied during functional tasks like walking. Early studies explored the cortical involvement in the control of walking (Hansen et al., 2001; Halliday et al., 2003; Petersen et al., 2010). More clinically oriented studies showed that the EMG-EMG coherence in the beta band in patients with motor deficits resulting from stroke (Bo Nielsen et al., 2008) or spinal cord injury (Barthélemy et al., 2010; Hansen et al., 2005; Norton and Gorassini, 2006) is decreased. These decreases indicate that beta-band EMG-EMG coherence depends largely on the integrity of the corticospinal tract. In spinal cord injury subjects, the decreased intramuscular coherence is related to impairments during walking (Barthélemy et al., 2010). Furthermore, quantification of EMG-EMG coherence has been used to monitor corticospinal drive as a result of a gait rehabilitation intervention. Norton and Gorassini (2006) demonstrated that changes in locomotor function in spinal cord injury subjects after an extensive treadmill training program were accompanied by increases in corticospinal drive. This was considered to reflect neuroplasticity. These studies illustrate that EMG-EMG coherence can quantify the effects of interventions that aim to improve walking ability through promoting neuroplasticity like intensive (robot-aided) gait training or non-invasive brain stimulation (Rogers et al., 2011).

Different variables are derived from the coherence spectra to capture changes in these spectra in a single value and assess effects on corticospinal drive. A commonly used derived variable is the area of coherence (Coh_{area}) (Barthélemy et al., 2010; Norton and Gorassini, 2006; Power et al., 2006) which is the area under the coherence spectrum dwelling above the 95% confidence limit within a certain frequency band. Another typical variable is the peak coherence (Coh_{peak}) which is the peak value of the spectrum within a certain frequency band (Petersen et al., 2010; Perez et al., 2006).

While EMG acquisition is relatively easy, the processing of the signals for the calculation of coherence includes several choices. These may include (high-pass) filtering and rectification. Most experimental studies reporting EMG-EMG coherence used rectification of EMG signals before calculating the coherence. The need for this processing step is debated in recent studies (Farina et al., 2013; McClelland et al., 2012b; Stegeman et al.,

2010; Halliday and Farmer, 2010; Neto and Christou, 2010; Yao et al., 2007; Myers et al., 2003; Boonstra and Breakspear, 2012). Rectification has been suggested to enhance information about motor unit firing rate (Cramer et al., 2011; Halliday and Farmer, 2010; Yao et al., 2007; Myers et al., 2003; Boonstra and Breakspear, 2012; Ward et al., 2013). However, recent studies have stressed that rectification is a non-linear operation which has an inconsistent effect on power spectra and may obscure the detection of a common oscillatory drive to the muscle(s) (McClelland et al., 2012b; Stegeman et al., 2010; Neto and Christou, 2010). The effect of high-pass filtering on EMG-EMG coherence has only recently attracted attention. High-pass filtering improves the "information density" of the signals as the filtered signals allow for better force estimation (Potvin and Brown, 2004; Staudenmann et al., 2007). Recently, Boonstra and Breakspear (2012) were the first to explore the effect of high-pass filtering on EMG-EMG coherence. They showed that high-pass filtering with cutoff frequencies between 100 and 300Hz increased the coherence.

To be able to use coherence variables to assess the effect of interventions, the reproducibility of these variables for repeated measurements should be assessed including the processing settings that result in the best reproducibility. In the current study we focus on intramuscular coherence. To our knowledge, there has not been an extensive study on the reproducibility of coherence variables. Reproducibility is the degree to which repeated measurements in stable study objects provide similar results and can be split up in reliability and agreement. Reliability assesses how well subjects can be distinguished from each other and is quantified by the intra-class correlation coefficient. Agreement is the degree to which repeated measures are identical and is quantified by the standard error of measurement and the smallest real difference (de Vet et al., 2006; Kottner et al., 2011). In order for a measure to be well suited for application in intervention studies, especially the agreement should be large, indicating that small effects can be shown (de Vet et al., 2006). Here we assessed the test-retest reliability and agreement of coherence variables calculated from muscular activity measured during treadmill walking in healthy subjects.

As several factors can influence the coherence spectra, we determined the reliability and agreement of the area of coherence and peak coherence for different conditions and processing settings. First, we determined the effect of walking speed. In more fundamental studies addressing cortical involvement during normal walking, healthy subjects generally walk at their preferred walking speed. Stroke survivors and spinal cord injury subjects often have a lower preferred walking speed. Therefore, we assessed the reliability during normal walking and slow walking. Second, as the discussion about the necessity of rectification is still unresolved, we will assess the reliability of coherence variables derived both from rectified and non-rectified EMG. Third, we will determine the effect of high-pass filtering with high cutoff frequencies. Finally, we will investigate how the variability of the coherence variables depends on the number of segments used to calculate the coherence spectra

2.2 Methods

Subjects

Ten healthy volunteers (nine male; age range 18 - 25 years) with no history of neurological conditions participated in this study. Nine subjects were right leg dominant. Leg domi-

nancy was determined using a combination of three tasks (leading leg when stepping up a platform, leg used to step out when pushed from behind, preferred leg to kick a ball) (de Ruiter et al., 2010).

Ethics statement

This study was approved by the Local Ethical Committee of the Medisch Spectrum Twente, Enschede, the Netherlands. Subjects signed informed consent in accordance with the *Declaration of Helsinki*.

Experimental design

The subjects participated in three experimental sessions separated by at least 1 week. These sessions were part of a double-blinded, crossover study to assess the effects of transcranial Direct Current Stimulation (tDCS). In each session subjects first performed baseline measurements before tDCS was applied. We use these baseline measurements to assess the test-retest reliability and agreement. Note that if tDCS would have any effects, they are relatively short lasting, less than 150 minutes. Carryover of effects to the baseline measurements of the subsequent session can therefore be excluded (Nitsche and Paulus, 2008).

Experimental procedures

In each of the sessions, subjects walked on the treadmill during baseline measurements for 3 minutes at 2.5km/h and for 2 minutes at 5km/h. These durations were chosen such that at least 100 complete gait cycles were obtained for each walking speed. Before recording started in each of the blocks, subjects were given time to get used to walking on the treadmill. The order of the walking speeds was randomized across subjects and sessions.

To obtain an indication of the variability of the coherence variables within one measurement session and to investigate the influence of the number of segments included in the coherence analysis on the coherence variables, three subjects (#1, #5 and #10) participated in additional session(s). The coherence variables obtained from these subjects in the regular sessions were not at the extremes of the ranges obtained from the complete subject population in the regular sessions. Here, these subjects walked longer on the treadmill: 10min blocks at 2.5 and at 5km/h. Two of three subjects participated in one additional session, the third subject participated in two additional sessions. These were performed on separated days to allow investigation of the reproducibility of the coherence variables for longer trials as well.

Recordings

Subjects walked on a split-belt instrumented treadmill (Y-mill, Forcelink, Culemborg, the Netherlands). EMG signals were recorded via disposable Ag-AgCl electrodes (1cm^2 recording area, type H93SG, Tyco Healthcare/Kendall, Mansfield, MA, USA) placed in a bipolar configuration over the right and left proximal and distal part of the m. tibialis anterior (TA). The two electrode pairs on the TA were separated by at least 10cm to avoid cross-talk and detection of activity from the same or overlapping motor unit territories (Hansen et al.,

2005; Roy et al., 1995). Electrode locations were referenced to anatomical landmarks to enable duplication of placements for subsequent testing. One pair was applied just lateral and distal of the tuberositas tibiae and the other 1cm from the distal end of the muscle belly. EMG Signals were sampled at 2048Hz using compact measurement equipment (Porti, TMS International, Oldenzaal, The Netherlands) and sent to a computer for visual on-line display and later off-line analysis. Ground reaction forces underneath each foot were recorded with a sampling frequency of 1000Hz using force sensors embedded in the treadmill.

Data analysis

Intramuscular coherence analysis

Recorded signals were processed off-line using MATLAB 7.11 (the MathWorks Inc., Natick, MA, USA). EMG was processed using one of three combinations of filtering and rectification to investigate the effect of these processing steps on the coherence spectra and the derived variables. First, EMG was band-pass filtered at $10-500$Hz and left non-rectified (NR). Second, after band-pass filtering ($10-500$Hz) the signals were rectified (HP10-R). Third, a high cutoff frequency of 100Hz was used in the band-pass filter ($100-500$Hz) and subsequently the data were rectified (HP100-R). All filters were fourth-order Butterworth filters with zero-lag.

The subsequent analysis (data segmentation and frequency analysis) was the same regardless of the previous EMG processing done. We used the measured vertical ground reaction forces below each belt to detect heel strike and toe off for every single step. These gait events were used to segment the EMG activity. TA is active during the complete swing phase, which lasts from approximately $60\%-100\%$ of the gait cycle (where 0 and 100% indicate heel strike of the concerned leg). As the timing of this muscle's burst is similar across the walking speeds used in this study (den Otter et al., 2004), we selected for every step the segment between 60% and 100% of the gait cycle. Although the TA activity extends into the stance phase, we did not use this data to exclude any possible heel strike artefacts from the analysis (Petersen et al., 2010). From each regular walking session, 100 segments were used to calculate the coherence.

Each segment was multiplied with a Hann window and padded with zeros to a length of 2048 samples (1s), resulting in a frequency resolution of 1Hz. All segments were transformed to the frequency domain using the fast Fourier transform. The power spectral density (Φ_{xx}) and cross spectral density (Φ_{xy}) were calculated as

$$\Phi_{xx}(f) = \frac{1}{N}\sum_{i=1}^{N} \bar{X}_i(f) \cdot X_i(f) \tag{2.1}$$

and

$$\Phi_{xy}(f) = \frac{1}{N}\sum_{i=1}^{N} \bar{X}_i(f) \cdot Y_i(f) \tag{2.2}$$

where $X_i(f)$ and $Y_i(f)$ are the Fourier coefficients at frequency f estimated from the i^{th} data segment of the proximal TA and distal TA respectively, N is the total number of segments and the bar indicates the complex conjugate. The (magnitude squared) coherence,

Coh_{xy} was calculated between signals using

$$\text{Coh}_{xy}(f) = \frac{|\Phi_{xy}(f)|^2}{\Phi_{xx}(f)\Phi_{xy}(f)} \tag{2.3}$$

Intramuscular coherence was calculated using the power spectra from and the cross spectra between the proximal TA and the distal TA. Coherence is a spectral measure between zero and one for the linear association between two signals. Zero indicates no linear relation, one indicates perfect, noise free, linear relation between the signals at that frequency (Priestley, 1983). The analysis steps above (zero-padding, calculation of spectral densities and coherence spectra) were performed using the Fieldtrip Toolbox for Matlab (Oostenveld et al., 2011). Intramuscular coherence is defined to be significantly larger than zero at a certain frequency when it exceeded a confidence limit (CL) with a probability of 95% ($\alpha = 0.05$). We determined the CL as:

$$CL = 1 - \alpha^{\frac{1}{N-1}} \tag{2.4}$$

where α is the desired significance level (Rosenberg et al., 1989). In addition, the cumulant density function, i.e. inverse Fourier transform of the coherence spectrum, was calculated as a time domain measure of association between EMG signals.

We calculated the coherence spectra and cumulant density function for every subject, for every session, for every speed for the dominant leg using each of the three differently processed EMG signals (NR, HP10-R and HP100-R). This resulted in a set of three coherence spectra per subject for every combination of walking speed and processing settings.

Similarity between these coherence spectra was quantified by calculating the correlation coefficient between all possible pairs of coherence spectra of these sets for the beta frequency band of $15-35$Hz. The individual correlation coefficients were averaged across subjects to obtain a single value for every combination of walking speed and processing settings.

Coherence variables

We extracted two variables from the coherence spectra. First, the area of coherence (Coh_{area}) was defined as the area between the coherence spectrum and the CL in the beta frequency band ($15-35$Hz) (see figure 2.1). Second, the peak coherence (Coh_{peak}) was defined as the maximum coherence within this frequency band and was expressed as the height above the CL (see 2.1).

Reliability and agreement

We estimated the reliability by calculation of the intraclass correlation coefficient (ICC) using a two-way random effects analysis of variance (ANOVA) (Portney and Watkins, 2009). This was done to separate the observed total variance of the variables into variance between subjects (MS_S), variance between trials/sessions (MS_T) and error variance (MS_E). We calculated ICC(2, 1) as

$$\text{ICC}(2,1) = \frac{MS_S - MS_E}{MS_S - (k-1)MS_E + \frac{k(MS_T - MS_E}{n}} \tag{2.5}$$

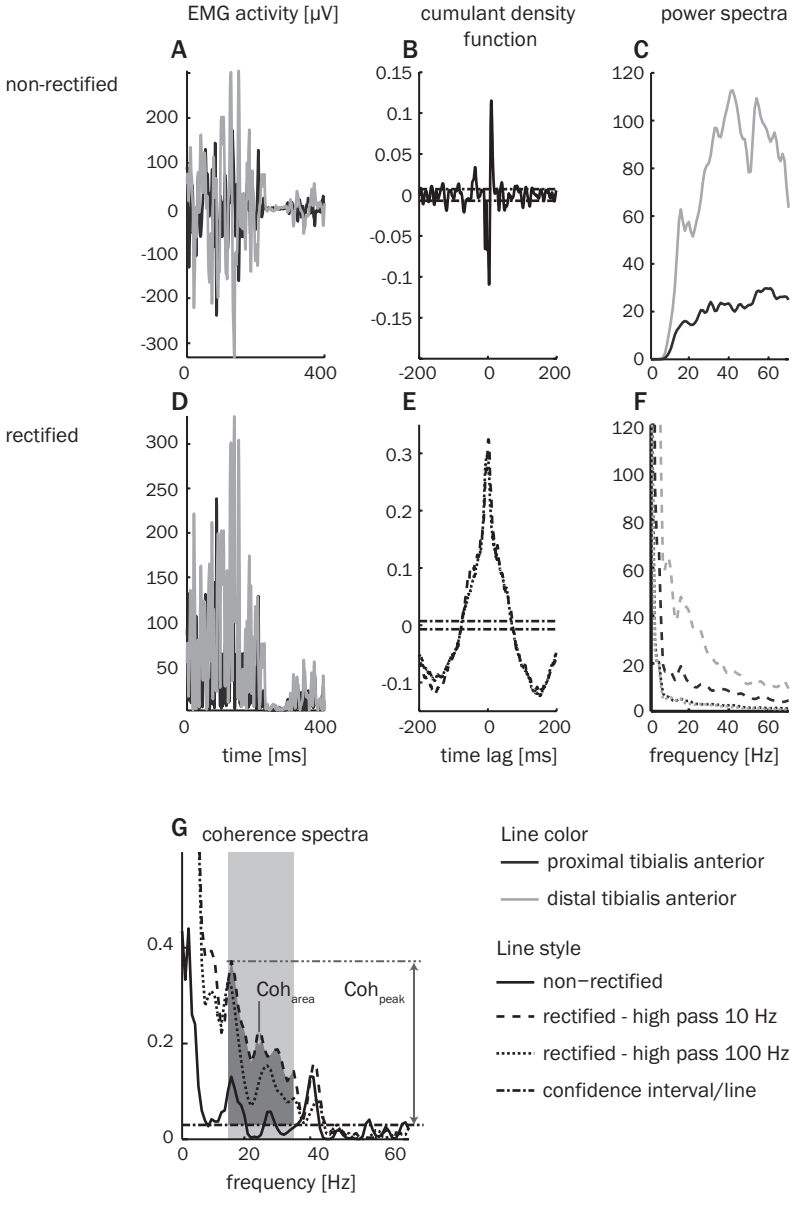

Figure 2.1: Rectifying and filtering of EMG signals has a large effect on power and coherence spectra. Representative data for a single subject (Subject #2) showing the effect of rectifying and filtering on the EMG activity (A, D), cumulant density function (B, E), power spectrum (C, F) and coherence spectrum (G).

where k is the number of sessions and n is the number of subjects. The ICC can range from zero to one, where ICC > 0.75 is generally considered to indicate a good reliability, an ICC between 0.4 and 0.75 indicates moderate reliability and an ICC below 0.4 indicates poor reliability.

The agreement was estimated using two measures. First, we determined the Standard Error of Measurement (SEM). The SEM expresses how repeated measures of a subject on the same test tend to be distributed around the "true" value, assuming that there are no systematic errors.

$$\text{SEM} = \sqrt{MS_E} \tag{2.6}$$

Second, we determined the Smallest Real Difference (SRD) (de Vet et al., 2006; Beckerman et al., 2001) also known as the Minimal Detectable Change (MDC). The SRD represents the smallest change necessary to exceed the measurement error of two repeated measures at a specified confidence interval (CI) (Wagner et al., 2008) and was calculated for the 95% CI as:

$$\text{SRD} = 1.96 \cdot \sqrt{2} \cdot \text{SEM} \tag{2.7}$$

where $\sqrt{2}$ is used to account for the combined variance of two measurements.

The three variables, ICC, SEM and SRD, were calculated using all subjects' individual Coh_{area} and Coh_{peak} values for every combination of speed (slow, normal) and processing settings (NR, HP10-R and HP100-R) using IBM SPSS statistics 20.0. The SRD was expressed in absolute values as well as a percentage of the average variable value for that specific combination.

Within trials variation of coherence variables

We used the data from the extra sessions to investigate the within trial variation in coherence variables. The 10min trials consisted of at least 400 segments. First we investigated how the coherence variables varied within these trials by calculating Coh_{area} and Coh_{peak} each consecutive subset of 100 segments. Second we investigate the effect of the number of segments used to calculate the coherence spectra and variables. The total number of segments was randomly divided into subsets consisting of 25, 50, 75, 100, 150, 200, 300 or 400 segments and the coherence spectra and variables were calculated for each of these subsets.

2.3 Results

All subjects showed significant intramuscular coherence in all sessions for all speeds and for all processing procedures (figure 2.2). One subject was suspected to show cross talk between the two EMG signals (high intramuscular coherence, of about 0.3 over the complete frequency range of interest and a narrow peak in the cumulant density function of the rectified EMG (Halliday et al., 2003)) and was left out of further analysis.

Unless specifically stated otherwise, the presented results are being obtained from rectified EMG (HP10-R). The results for the other settings will be discussed in relation to the HP10-R results.

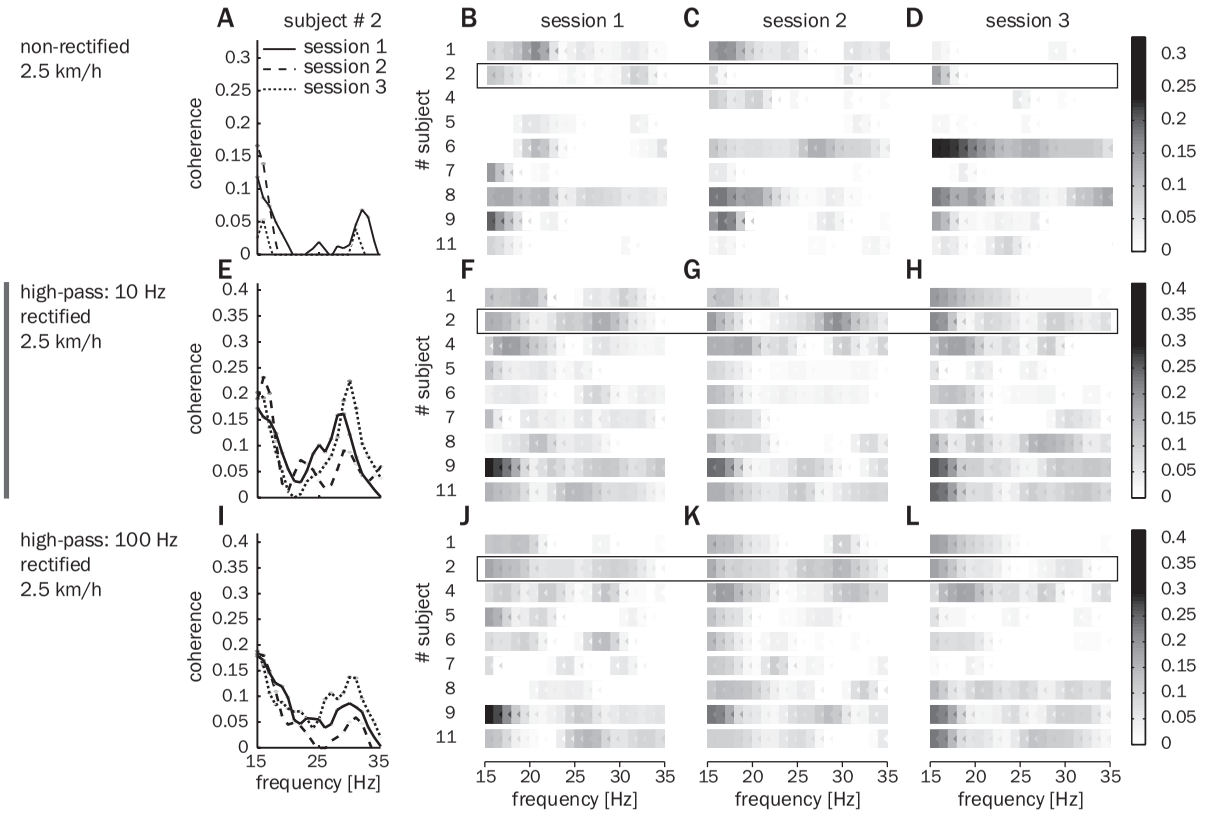

Figure 2.2: Coherence spectra are most consistent between sessions when estimated using rectified EMG signals. The most left graphs (A,E,I) depict the coherence spectra within the 15 – 35Hz frequency range for the three different sessions for a subject #2. The other graphs show the presence and magnitude of the coherence for all subjects. Here the coherence magnitude is indicated in a gray scale, where a darker rectangle indicates a higher coherence. Each gray scale graph is a different combination of session and processing settings. For easy comparison with the other processing settings, HP10-R is depicted in the middle row. The confidence limit was subtracted from all coherence values.

Table 2.1: The across subject average correlations ($\mu \pm$ std) between coherence spectra from different sessions.

Speed (km/h)	Proc.	Correlation
2.5	NR	0.30 ± 0.38
	HP10-R	0.56 ± 0.23
	HP100-R	0.48 ± 0.30
5.0	NR	0.02 ± 0.14
	HP10-R	0.48 ± 0.17
	HP100-R	0.55 ± 0.21

Coherence related measures determined from rectified signals show moderate reliability

During slow walking most subjects showed significant intramuscular coherence for more frequency bins within the 15 – 35Hz range when rectified EMGs (HP10-R) were used for computation (see figure 2.2 E-H). Between sessions, the number of frequency bins, the location of these bins and the magnitude of coherence within these bins were quite consistent. This was reflected in marginally strong cross correlations between a subject's coherence spectra from different sessions, 0.56 ± 0.23 (see table 2.1).

There was considerable within-subject variability for both coherence variables (see filled black squares in figure 2.3). The ICC was at the border for good reliability for both measures: 0.76 for Coh_{area} and 0.72 for the Coh_{peak} (see table 2.2). The SRD values amounted to approximately 66% of the average value. For normal walking the correlations between coherence spectra tended to be lower, 0.48 ± 0.17 (see table 2.1). Furthermore, the ICC was only fair (see table 2.2) and the SRD was approximately as large as the average variable value.

Coherence related measures determined from non-rectified signals show fair reliability

Using non-rectified signals for estimating the coherence resulted in clearly different power and coherence spectra compared to the spectra estimated from rectified signals (see figure 2.1). Not only the magnitude of the coherence changed, but also the number and location of the peaks (see figure 2.2 A-D vs. 2.2 E-H and figure 2.1). The coherence spectra from the non-rectified signals showed less similarity between sessions. This was reflected in smaller and weak correlations between subject's coherence spectra (see table 2.1).

The smaller similarity was also reflected in more within-subject variability in Coh_{area} and Coh_{peak} and in the measures for reliability and agreement (see figure 2.3, table 2.2). The ICC for both coherence variables was low (< 0.44) for both speed conditions and the SRD were high ($> 176\%$ of the across subject variable average; see table 2.2).

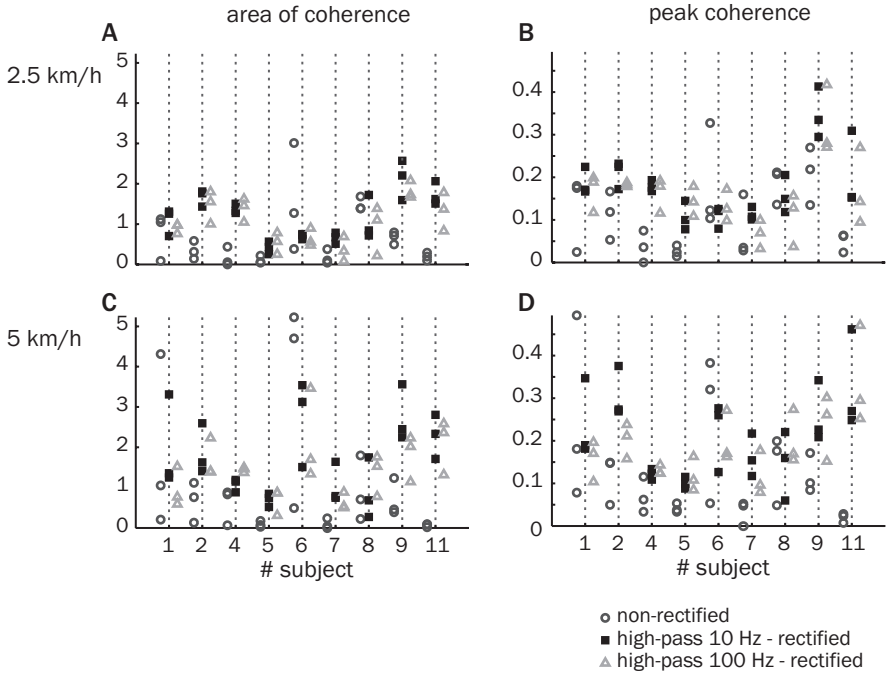

Figure 2.3: Coherence variables show considerable within-subject variability for HP10-R and even larger for different processing settings. Effect of processing settings on within and between subject variation in the area of coherence (A, C) and peak coherence (B, D) for slow (A, B) and normal (C, D) walking speeds. Each marker indicates the variable value of a single session. The different marker styles and colors depict different processing steps.

Table 2.2: Reliability and agreement of the coherence-related measures and the coherence spectra. Intra class correlation (ICC(2,1)), standard error of the mean (SEM) and smallest real difference (SRD) and the SRD expressed as percentage of the mean value (% SRD) are shown for the area of coherence (C_{area}) and peak coherence (C_{peak}) for two different walking speeds (2.5 and 5.0km/h) and different processing settings: non-rectified (NR), high-pass filtered with a cutoff frequency of 10 Hz and rectified (HP10-R) and high-pass filtered with a cutoff frequency of 100Hz and rectified (HP100-R).

Speed (km/h)	Proc.	ICC(2,1)		SEM		SRD		%SRD	
		C_{area}	C_{peak}	C_{area}	C_{peak}	C_{area}	C_{peak}	C_{area}	C_{peak}
2.5	NR	0.47	0.41	0.54	0.07	1.48	0.20	245	176
	HP10-R	0.76	0.72	0.30	0.04	0.83	0.12	69	66
	HP100-R	0.60	0.57	0.37	0.06	1.03	0.16	100	98
5.0	NR	0.33	0.28	1.26	0.11	3.49	0.29	372	252
	HP10-R	0.47	0.48	0.75	0.07	2.08	0.20	122	94
	HP100-R	0.38	0.48	0.61	0.06	1.68	0.18	118	94

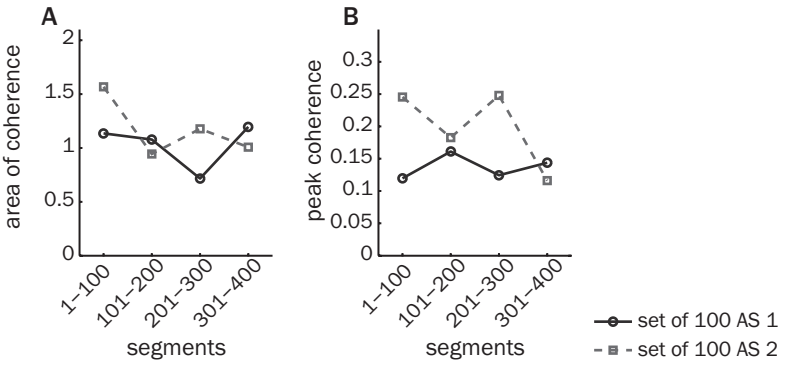

Figure 2.4: Coherence variables show within-session variation, which is about equal to observed between-session variation. Variation of area of coherence (A) and peak coherence (B) within a single 10min walking trail at 2.5km/h for subject #1 for the HP10-R processing. The values were calculated for consecutive subsets of 100 segments. The 10min walking trail was performed in two additional sessions (AS) each indicated with a different line/marker style.

High-pass filtering with high cutoff frequency does not further improve the reliability

Although high-pass filtering with a 100Hz cutoff frequency (HP100-R) reduces the power of the signals considerably (see figure 2.1), the magnitude of the coherence and its distribution across the different frequencies were quite similar to the coherence when filtering with a cutoff frequency of 10Hz (HP10-R)(figure 2.2 I-L vs. 2.2 E-H). Still, the ICC for Coh_{area} and Coh_{peak} are lower (fair to moderate) and the SRD was about 94% of the average variable value (table 2.2).

Within-session variation in coherence variables is close to between-session variation

To better understand the origin of the variability of coherence variables, we evaluated the within-session variation of these variables in the additional 10min walking sessions performed by three subjects. Coh_{area} and Coh_{peak}, as calculated from consecutive subsets of 100 segments show considerable variability within a single session (see figure 2.4). The observed variation was about equal in magnitude as the observed between-session variation for this subject (#1) in the three regular sessions as shown in figure 2.3 A and B and between extra session 1 and 2 (see figure 2.4).

This was a consistent finding for the slow as well as for the normal walking speed, for the other processing settings and for all three subjects that participated in these extra sessions (not depicted).

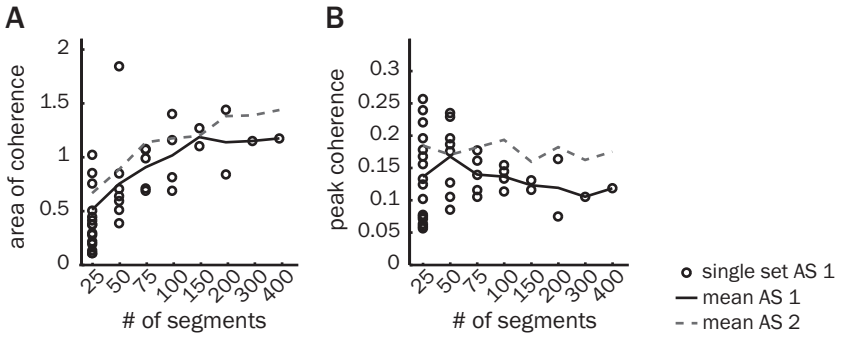

Figure 2.5: Area of coherence increases with number of segments used to calculate the coherence spectrum. Influence of number of segments on the area of coherence (A) and peak coherence (B) for HP10-R. Data of subject #1 for the slow walking condition were used. Each marker indicates the value calculated from a subset containing the specified number of segments. These subsets were randomly taken from a total of 421 (additional session 1, AS1) or 418 (additional session 2, AS2) segments. The solid line indicates the mean value as a function of the number of segments for AS1. The dashed line shows the mean for AS2. The separate values for AS2 are not shown.

Number of segments influences the mean value of area of coherence but not peak coherence

There was a large variability when few (25 or 50) segments were used to calculate the coherence variables. This variability tended to decrease with an increasing number of segments. Yet, a fair comparison is hampered as the number of available subsets also decreases with the number of segments. Strikingly, even when using 200 segments, the within-session difference between calculated Coh_{area} values can be as large as about 50% of the mean value (figure 2.5).

To determine the effect of the number of segments on the mean value of the coherence variables we calculated the mean for each number of segments. The mean Coh_{area} increased with the number of segments for all processing conditions, whereas Coh_{peak} did not show a clear trend (see figure 2.5, black solid lines). Similar trends for the variability and mean value were observed in the other subjects, for normal walking and also for the other processing settings.

The observed between-(extra)session variability is in line with the variability in the regular sessions. Using a larger number of segments to calculate the coherence values did not seem to influence the between-session variation. When using 400 segments the Coh_{area} differed about 22% in the second session compared to the first session (see figure 2.5 A bold vs. dashed line) and the Coh_{peak} differed 46% (see figure 2.5 B). For other processing settings and walking speed the differences were as large or larger, for non-rectified signals the increase in Coh_{area} was as high as 70%.

2.4 Discussion

In this study, we quantified the test-retest reliability and agreement of variables derived from intramuscular coherence during walking. Intramuscular coherence is a measure of the common input to different parts of the same muscle and is applied as a measure of the corticospinal drive (Grosse et al., 2003, 2002; Brown et al., 1999). We found that the reliability and agreement of intramuscular coherence variables depends on signal processing settings (EMG high-pass filtering and rectification) and experimental condition (walking speed). Reliability and agreement were best for slow walking and using rectified signals that were high-pass filtered with 10Hz. For this combination the reliability was on the limit of good for Coh_{area} (ICC = 0.76) and Coh_{peak} (ICC = 0.72), but the agreement was still low given the smallest real difference of ±66% of the average variable values, indicating that a difference between two measurements should at least be this 66% to be considered as a real difference. For other conditions and/or signal processing settings the reliability was fair to poor and the smallest real difference was larger than 94%. Finally, we demonstrated that the intramuscular coherence values were influenced by the number of segments included in the analysis and can show considerable within-subject variation even within a single session.

There was no clear and consistent difference between the reliability and agreement of the variables derived from the coherence spectra: Coh_{area} and Coh_{peak}. Both variables also show the same dependence on signal processing steps. Therefore, we cannot generally recommend using one variable over the other or specify in which conditions to use a certain variable.

Only one other study addressed the reproducibility of coherence variables measuring corticospinal drive (Pohja et al., 2005). However they used EEG-EMG coherence and quantified the peak value during isometric contractions of the hand muscles. They showed that there was no significant correlation between the peak values from different sessions. Despite the fact that the correlation they used only quantifies the strength of linear association between the two measures and does not provide direct information about reliability or agreement, the lack of correlation does indicate that the reproducibility was poor. So far, coherence related variables, being derived from EMG-EMG or EEG-EMG coherence, have shown poor reproducibility. Therefore, when these variables are used in intervention studies to assess neuroplasticity, their results should be interpreted with great caution. Still, the reproducibility of coherence variables has only been investigated for few muscles and tasks. The variables might be more reproducible for other combinations.

A limitation of this study is that we studied healthy individuals, and we do not know how the observations generalize to patients with motor deficits resulting from stroke or spinal cord injury. Different studies have shown that intramuscular coherence in these patients is lower than in healthy subjects (Barthélemy et al., 2010; Hansen et al., 2005; Bo Nielsen et al., 2008). Lower coherences, however, do not necessarily impact the reproducibility of coherence variables. Future reproducibility studies in these patients are therefore warranted.

The observed standard error of measurement was rather large for both intramuscular coherence variables, indicating that repeated measures of single subjects showed considerable variation around his/her "actual" score. These variations could at least partly be ascribed to errors in the measurement, but it might as well be that the underlying process

is variable. This would imply that there is no "actual" score. It is well known that there are step-to-step fluctuations in gait and these fluctuations are not just a consequence of random noise in the system. In fact, Hausdorff et al. (1995); Hausdorff (2007) have shown that step-to-step fluctuations are related to fluctuations that occur hundreds of strides earlier. The neural circuits in the CNS responsible for these long-term fluctuations make the process time variant and as such variable. How much of the variation in the repeated measures can be ascribed to measurement error or variation in the underlying process is not known. The source of variability between measurements is not of that much importance for the reproducibility of the measure as all sources of variability negatively influence the reproducibility. However for the validity of coherence variables as a measure of corticospinal drive the source of variability is of importance. When the underlying process generating the common oscillatory drive to the muscles shows considerable variation, there is no "actual" intramuscular coherence and the validity of intramuscular coherence is affected.

Measures of EMG-EMG coherence can be vulnerable for cross-talk. Cross-talk compromises the validity of intramuscular coherence as a measure of common oscillatory drive to different motor unit territories. To prevent cross-talk the target muscle should be large, allowing large inter-electrode distances, and have restricted motor unit territories, which the TA muscle has. Hansen et al. (2005) showed that significant intramuscular coherence was restricted to specific frequency bands ($\pm 12-32$Hz) and was small (< 0.05) during isometric contractions when the electrode pairs were positioned 10cm from each other, whereas with two pairs of electrodes closer together there was large significant coherence (> 0.2) over a wide frequency range ($0-500$Hz). The coherence spectra with 10cm inter-electrode distances were similar to those obtained earlier from needle recordings of pairs of individual motor units in the same muscle (Farmer et al., 1993), providing strong evidence that this electrode configuration indeed records activity from different motor unit territories. Furthermore, Roy and colleagues showed that the cat TA motor unit territories did not span the entire length of the muscle and had cross-sectional areas tapered along the proximodistal axis (Roy et al., 1995). This makes it unlikely that electrodes located at both ends of the muscle belly will pick up activity of the same motor unit. Nevertheless, data recording and analysis needs to be done with great caution to prevent occurrence of cross-talk and/or detect it (Barthélemy et al., 2010; Hansen et al., 2005). All our subjects but one, who was excluded, showed significant coherence only in specific frequency bands of the spectrum and had a small and relatively broad central peak in the cumulant density function in all three sessions. Therefore, it is unlikely that cross-talk contributed to their coherence spectra and has influenced the reproducibility of the intramuscular coherence variables.

Effect of processing settings and walking condition

The area of coherence showed a clear and gradual increase with the number of segments used to calculate the intramuscular coherence spectrum (figure 2.5 A). Therefore the number of segments should be held constant between different measurements to make a fair comparison possible. Care should be taken when comparing the area of coherence from studies or conditions with different amounts of segments available and/or used in the analysis. Especially when the area of coherence is used to assess the effect of rehabilitation

interventions, there is a considerable chance that individuals are able to walk for a longer time post compared to pre intervention (Norton and Gorassini, 2006). The larger number of available segments for analysis would introduce a bias towards finding an increase in the area of coherence.

The reliability and agreements were determined from variables calculated using 100 segments. Possibly reliability and agreement would have been higher when more segments were used. This number was chosen, as our experience is that mildly affected stroke survivors or spinal cord injury subjects can walk 100 steps without signs of fatigue. The number of segments used in previous studies that investigated EMG-EMG coherence in neurological subjects varied from $70-72$ (Norton and Gorassini, 2006) to $200-270$ segments (Bo Nielsen et al., 2008). Our results from the additional sessions showed that also when using larger number of segments ($200-400$), there is still a considerable within-session and between-session variation in intramuscular coherence variables that is almost as large as the variation seen when using 100 segments. For instance, differences between Coh_{area} calculated from two sets of 200 segments (recorded in one trial) could amount to 50% of the average value. As a consequence, we do not expect large improvements in agreement and reliability when using more segments.

There is an ongoing debate on the question which EMG processing steps, i.e. rectification and filtering, are necessary in EEG-EMG and EMG-EMG coherence analysis (Farina et al., 2013; McClelland et al., 2012b; Stegeman et al., 2010; Halliday and Farmer, 2010; Neto and Christou, 2010; Yao et al., 2007; Myers et al., 2003; Boonstra and Breakspear, 2012; Ward et al., 2013). Whether EMG rectification aids or impairs the detection of common drive and whether it can be detected at all, depends on many factors including the nature of the common drive (e.g. amplitude modulation or frequency modulation) (Stegeman et al., 2010; Boonstra and Breakspear, 2012), the number of active motor units or force production (Farina et al., 2013; Ward et al., 2013; Negro and Farina, 2011) and the amount of common drive that motor units receive (Stegeman et al., 2010). The complex interplay between all these factors cannot be controlled in experimental conditions and it is therefore difficult to determine which EMG processing setting results in the most valid quantification of corticospinal drive. However, a recent study of Ward et al. (2013) provides strong evidence that rectification is a necessary preprocessing step to estimate coherence values. By using simultaneous recording of paired single motor units and surface EMG they demonstrated that rectified EMG could account for a larger part of the motor unit synchronization due to common oscillatory drive than non-rectified EMG. Our results are also in favor of rectification. We observed that rectification resulted in a shift of the power spectrum to the lower frequencies and an increase in the coherence in the beta band as reflected in an increase of the coherence variables, which was in accordance with recent work (Boonstra and Breakspear, 2012). This increase of the coherence variables was accompanied by an increase in their reliability and agreement.

High-pass filtering with 100Hz had no consistent influence on the intramuscular coherence variables compared to high-pass filtering with 10 Hz. This was in contrast with results from Boonstra and Breakspear (2012) who showed that high-pass filtering with cut-off frequencies > 100Hz increased intermuscular coherence between bilateral leg muscles during quiet stance. We also showed that high-pass filtering resulted in a decrease of the reliability and agreement of the coherence variables. This shows that effects on reliability and agreement are not always in line with the effects on the magnitude of the coherence

variables.

Previous studies did not show a clear effect of walking speed on EMG-EMG (Hansen et al., 2005; den Otter et al., 2004) or EEG-EMG (Petersen et al., 2012) coherence. In accordance with these studies we also observed no influence of walking speed on the coherence variables. The reliability and agreement of the variables was higher when subjects walked at slow speed, irrespective of the performed processing, showing again that the reproducibility does not necessarily depend on the magnitude of the coherence variables.

Most EMG-EMG and EEG-EMG lower limb coherence studies estimate the coherence in a dynamic situation like walking and only few during static contractions. Assessing coherence during dynamic movements is attractive as it quantifies (recovery of) the cortical involvement in that movement. However, as indicated earlier, there is considerable variability in the execution of these movements, which is detrimental for the coherence. Therefore, a better-controlled task like isometric force production might be more appropriate. Only one study quantified EMG-EMG coherence during walking and isometric force production (Norton and Gorassini, 2006) but the reported data do not allow a quantitative comparison. For EEG-EMG coherence, Gwin and Ferris (2012) recently showed that the maximal coherence in the beta band did not significantly differ between a dynamic isotonic contraction and a static isometric contraction. Still, as stated earlier, from the (lack of) effects on the magnitude of the coherence variables, the effect on their reproducibility cannot be inferred. Future studies should address the reproducibility of EMG-EMG coherence variables in static conditions.

2.5 Conclusion

Our study demonstrates the importance of determining the reproducibility of coherence variables. These variables are rapidly growing in interest as a measure of corticospinal drive to investigate the neuroplasticity of the CNS. The reproducibility of these variables is largely unknown. We focused on a subclass of coherence, being intramuscular coherence during walking. Our findings indicate that the reliability of intramuscular coherence variables obtained during walking was on the limit of good only under specific conditions and processing of EMG data (slow walking, using rectified signals). Still, their use in interventions studies is hampered by the low agreement. These results cannot be generalized to other muscles and tasks. Reproducibility should be separately assessed for other circumstances before being used in an intervention study.

2

Chapter 3

Phase to face: Pitfalls in time delay estimation from coherency phase

Prelude: Alfred C. Schouten and **S. Floor Campfens** 'Directional coherence disentangles causality within the sensorimotor loop, but cannot open the loop.' Letter to the editor *Journal of Physiology*, 590(Pt 10):2523-2529, 2012. Author reply: 2531-2533

S. Floor Campfens, Herman van der Kooij and Alfred C. Schouten. *Journal of Computational Neuroscience*: 37(1): 1-8, 2014

ABSTRACT

Coherency phase is often interpreted as a time delay reflecting a transmission delay between spatially separated neural populations. However, time delays estimated from corticomuscular coherency are conflicting and often shorter than expected physiologically. Recent work suggests that corticomuscular coherence is influenced by afferent sensory feedback and bidirectional interactions.

We investigated how bidirectional interaction affects time delay estimated from coherency, using a feedback model of the corticomuscular system. We also evaluated the effect of bidirectional interaction on two popular directed connectivity measures: directed transfer function (DTF) and partial directed coherence (PDC).

The model is able to reproduce the range of time delays found experimentally from coherency phase by varying the strengths of the efferent and afferent pathways and the recording of sensory feedback in the cortical signal. Both coherency phase and DTF phase were affected by sensory feedback, resulting in an underestimation of the transmission delay. Coherency phase was altered by the recording of sensory feedback in the cortical signals and both measures were affected by the presence of a closed loop feedback system.

Only PDC phase led to the correct estimation of efferent transmission delay in all simulated model configurations. Coherency and DTF phase should not be used to estimate transmission delays in neural networks as the estimated time delays are meaningless in the presence of sensory feedback and closed feedback loops.

Prelude

Letter to the editor. Comment on Witham et al. (2011)

More and more studies indicate that corticomuscular coherence in the beta band (15 – 30Hz), which expresses the functional coupling between the cortex and the muscles, originates from the interaction within the sensorimotor loop (e.g. Witham et al., 2011). The phase of the corticomuscular coherence expresses the relative time-frequency relationship and is often explained as to result from the efferent delay between the cortex and the muscles. In a recent issue of the Journal of Physiology Witham and co-workers (Witham et al., 2011) demonstrated that the slope of the phase of corticomuscular coherence is less negative than would be expected of a pure efferent pathways and even becomes positive in some subjects (negative slopes indicate that the muscle lags the brain). This is a clear indication of a bidirectional coupling between EEG and EMG; in other words: the signals are part of a closed loop system. However, the authors also use the phase of the directional coherence to assess the delays in the efferent and afferent pathways, which will give erroneous results in a closed loop system, like the sensorimotor loop.

The causality of signals within a closed loop is difficult to assess. For example, in the sensorimotor loop it is not obvious whether cortical activity leads muscle activity - suggesting an efferent pathway -, or cortical activity lags muscle activity - suggesting an afferent pathway -. In the sensorimotor loop EEG and EMG signals will contain a combination of afferent and efferent influences.

As the authors demonstrate directional coherence provides a good measure to disentangle the causal relationships of the signals within the sensorimotor loop. With directional coherence multivariate autoregressive (MVAR) modelling is used to uncover causality. MVAR modelling is a common technique, which disentangles the recorded signals at a certain time instant as a weighted sum of the signals' previous values and (unknown) external noise sources, which enter the model just before the signals, see figure 3.1. The directed coherence is calculated using the directional transfer function $H_{ij}(f)$ (e.g. Witham et al., 2011, Eq. 3). The directional transfer function $H_{ij}(f)$ is calculated, which represents: *"the causal influence of signal j on signal i"*. Although this is a widely accepted expression, it is a simplified expression. The precise expression would be that the direction transfer function represents the causal influence of external noise source j on signal i (Kaminski and Blinowska, 1991). In other words the directional transfer function expresses how much signal i depends on the unknown external noise source which enters the model just before signal j.

The simplification on what directional transfer function represents has a tremendous effect on the understanding of the phase of the directional coherence. In Witham et al. (2011), the authors assume that the phase of the directional coherence represents the relative delay between signal i and signal j. With this assumption the slope of the phase would represent the delays in the open loop transfer functions, i.e. the relative delay of the efferent (EEG to EMG: $H_{efferent}$) and afferent (EMG to EEG: $H_{afferent}$) pathways. However the directional transfer function is a closed loop transfer functions between noise source i and signal j. In that sense directional transfer functions allow to disentangle the causality within a closed loop, but the phase of the directional coherence presents the relative delay between the signal within the sensorimotor loop (EEG and EMG) and the unknown

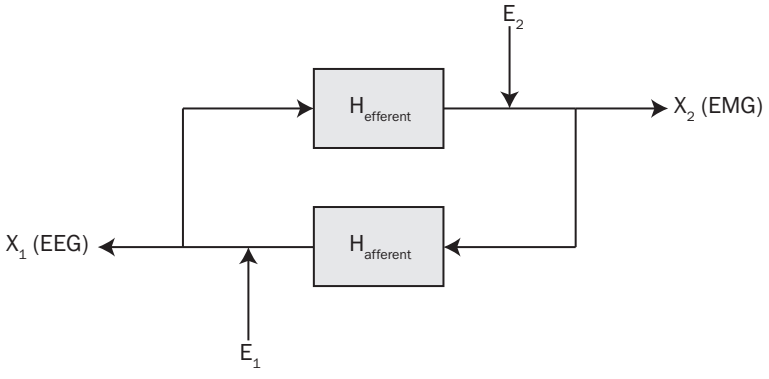

Figure 3.1: Schematic representation of the sensorimotor loop as a closed loop system

external noise sources ϵ (i.e. the cortical and afferent drive). This effect contributes to the observation of Witham and co-workers that the delays measured by using the directed coherence were often larger than would be expected the known conduction delays from the cortex to muscle assesses with stimulation and peripheral nerve stimulation.

In conclusion, the technique based on multivariate AR modeling - like directional coherence - decomposes signals within a closed loop as a weighted combination of external sources and the signals' past, and allows disentangling the causality. The phase of the directional coherence, however, describes the relative delay between the signals and the unknown external sources, and is not a direct measure of the phase of the inferred open loop transfer function, like the efferent and afferent pathways. New techniques which are able to assess the open loop transfer functions are highly desirable. The application of controlled external perturbations could be a promising way (Campfens et al., 2011).

Author reply: Witham and Baker (2012)

3.1 Introduction

Correlation analysis between signals, e.g. coherence, is widely used in neuroscience to detect connectivity between spatially separated populations of neurons (Varela et al., 2001; Horwitz, 2003; Fries, 2005; Stam and van Straaten, 2012). The (magnitude squared) coherence, a frequency domain measure of correlation, varies between zero (no correlation) and one (linear, noise free correlation) (Pintelon and Schoukens, 2001). Coherence is the magnitude squared of the (complex) coherency where coherency phase describes the relative timing between the two signals as a function of frequency (Halliday et al., 1995). The coherency phase is often used to indicate which signal is leading and to get an estimate of the transmission delay (Mima et al., 2000; Tallon-Baudry et al., 2001; Riddle et al., 2004; Nolte et al., 2004; Witham et al., 2007).

Corticomuscular coherence (CMC) in the beta band demonstrates connectivity between the cortex (activity recorded with EEG and MEG) and the spinal motor neurons (activity recorded with EMG). Typically a proportional phase-frequency relation is found, suggesting a transmission delay, which is estimated from the slope of the phase-frequency relation (Brown et al., 1998; Mima et al., 2000; Gross et al., 2000; Grosse et al., 2003; Riddle and Baker, 2005; Baker et al., 2006; Williams et al., 2009; Petersen et al., 2012). This estimated time delay can be compared with the delay of for example a motor evoked potential. Some studies found good agreement between these different methods to estimate the efferent transmission delay (Gross et al., 2000; Petersen et al., 2012). Others report shorter (Brown et al., 1998; Grosse et al., 2003; Riddle and Baker, 2005) or non-meaningful, i.e. zero (Halliday et al., 1998; Riddle and Baker, 2005), time delays based on phase analysis.

Over the last decade, evidence is accumulating that CMC is affected by the properties of the efferent and afferent pathways and that there is a bidirectional connectivity between cortical and peripheral activity in the corticomuscular system (Pohja and Salenius, 2003; Riddle and Baker, 2005; Williams et al., 2009; Witham et al., 2011). The bidirectional connectivity might underlie the low agreement between transmission delays that are estimated from coherency phase (Williams et al., 2009; Witham et al., 2011; Schouten and Campfens, 2012). One scenario for the bidirectional connectivity is the presence of a closed loop feedback system where the ongoing motor activity is modulated by the sensory feedback signals. Another scenario would be that sensory feedback signals are present in the recorded cortical activity, possibly due to afferent projections to the motor cortex or due to volume conduction.

Here, we investigated how the complex coherency phase and estimated time delay are affected by bidirectional connectivity due to the presence of a closed feedback loop, sensory feedback in the recorded cortical signal, or both. We also estimated time delays based on the two most popular directed connectivity measures based on Granger causality: the Directed Transfer Function (DTF, Kaminski and Blinowska, 1991) and Partial Directed Coherence (PDC, Baccalá and Sameshima, 2001).

3.2 Methods

We estimated time delays from the phase of connectivity measures (coherency, DTF and PDC) using model simulations of the corticomuscular system.

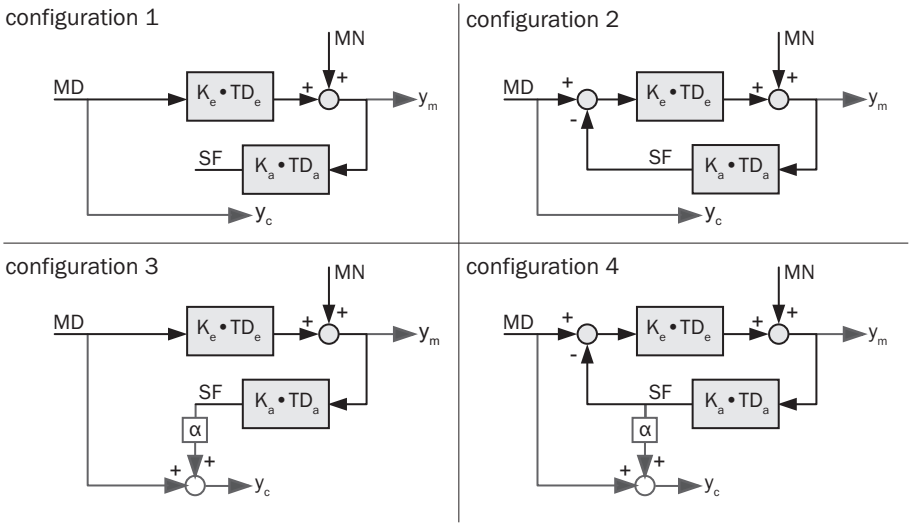

Figure 3.2: Overview of the four configurations of the corticomuscular system model. The efferent and afferent pathways are modeled as neural gains (K_E and K_A) and neural time delays (TD_E and TD_A). The model receives two inputs: a motor drive (MD) and motor noise (MN). The two output signal represent muscle activity (y_m) and cortical activity (y_c). In configurations 2 and 4 (right column) the system forms a closed feedback loop where the sensory feedback modulates the motor activity (input of the efferent pathway). In configurations 3 and 4 sensory feedback (SF) is recorded in cortical signal. The magnitude of SF in the cortical signal is determined by α.

Model of corticomuscular system

The corticomuscular system (figure 3.2) was modeled as a feedback system with two inputs: cortical motor drive (MD) and motor noise (MN). The efferent and afferent pathways were both modeled as a variable gains (K) and fixed time delays (TD). The values for the time delays were taken from literature where the response to external stimulation is taken as an estimate of transmission delay. The efferent delay was set at 18ms based on motor evoked potentials at the wrist (Rothwell et al., 1991). The afferent, proprioceptive, delay was set at 25ms based on sensory evoked potentials (Abbruzzese et al., 1985).

Two settings for the cortical signal and two different structures for the corticomuscular system were combined, resulting in four model configurations (see figure 3.2). In the first two configurations the cortical signal reflects the motor drive only (upper row in figure 3.2). In configurations 3 and 4 sensory feedback is present in the cortical signal, where the amount of the sensory feedback signal is varied with α. In the one system structure (configurations 1 and 3, left column in figure 3.2) the sensory feedback signal does not contribute to the motor activity. In the other system structure (configurations 2 and 4, right column in figure 3.2) the sensory feedback signal is fed back and modulates the ongoing motor activity resulting in a closed loop feedback system.

Model simulations

The model is implemented in Matlab as a discrete state space system. Input signals of the model (MD and MN) were two independent normally distributed white noise signals. For each of the model configurations, the model was simulated for 200s at 1kHz. The model simulations provided the cortical and muscle signal (y_c and y_m respectively) which were used for further analysis.

We investigated the effect of the relative afferent contribution by varying the strength of the afferent pathway (K_A) between 0.1 and 0.8 while the strength of the efferent pathway was kept constant($K_E = 1$). For all combinations of K_E and K_A the total loop gain is smaller than one assuring the model always satisfies the Nyquist stability criterion. The time delays of the efferent and afferent pathway were fixed in all simulations. Furthermore, to investigate the effect of the signal power we made three combinations of input signal variances and α:

- $\sigma^2_{\mathrm{MD}} = 1, \sigma^2_{\mathrm{MN}} = 0.5, \alpha = 0.25$;
- $\sigma^2_{\mathrm{MD}} = 0.5, \sigma^2_{\mathrm{MN}} = 1, \alpha = 0.25$ and
- $\sigma^2_{\mathrm{MD}} = 0.5, \sigma^2_{\mathrm{MN}} = 1, \alpha = 1$.

Coherency

Coherency was calculated following the standard procedures (Rosenberg et al., 1989; Halliday et al., 1995). Signals were segmented in 200 non-overlapping epochs of 1s and transformed to the frequency domain using the fast Fourier transform. Power spectral density ($\Phi_{y_c y_c}$ and $\Phi_{y_m y_m}$) and cross spectral density ($\Phi_{y_c y_m}$) were calculated using

$$\Phi_{y_c y_c}(f) = \frac{1}{N} \sum_{k=1}^{N} Y^*_{c,k}(f) \cdot Y_{c,k}(f) \tag{3.1}$$

and

$$\Phi_{y_c y_m}(f) = \frac{1}{N} \sum_{k=1}^{N} Y^*_{c,k}(f) \cdot Y_{m,k}(f) \tag{3.2}$$

where $Y_{c,k}(f)$ and $Y_{m,k}(f)$ are the Fourier coefficients at frequency f calculated from the k^{th} segment of y_c and y_m, respectively. The asterisk indicates the complex conjugate and N is the total number of segments (200). The complex valued coherency ($C_{y_c y_m}$) between the cortical and muscle signal was calculated according to:

$$C_{y_c y_m}(f) = \frac{\Phi_{y_c y_m}(f)}{\sqrt{\Phi_{y_c y_c}(f)\Phi_{y_m y_m}(f)}}. \tag{3.3}$$

We only evaluate coherency phase and not magnitude, as the latter is a measure of the amount of additional independent noise in the signals which is not related to the dynamics between y_c and y_m.

Directed connectivity

Both DTF and PDC are based on a multi-variate auto regressive (MVAR) model of the data.

An MVAR model of the form

$$\begin{bmatrix} y_c(n) \\ y_m(n) \end{bmatrix} = \sum_{r=1}^{p} \mathbf{A}_r \begin{bmatrix} y_c(n-r) \\ y_m(n-r) \end{bmatrix} + \begin{bmatrix} \varepsilon_1(n) \\ \varepsilon_2(n) \end{bmatrix} \tag{3.4}$$

was fitted to the segmented signals using the freely available ARfit package (Schneider and Neumaier, 2001). The 2-by-2 matrix $\mathbf{A}_r$ contains the coefficients that predict the current sample (n) of y_c and y_m from the r^{th} past sample of y_c and y_m. The model order, p, determines how many past samples are included in the prediction of the current sample and was chosen based on the final prediction error criterion (Akaike, 1971). The prediction error ε is minimized in the fitting of the coefficients of $\mathbf{A}_r$ of the MVAR model.

Transformation of the MVAR model to the frequency domain yields

$$\begin{bmatrix} Y_c(f) \\ Y_m(f) \end{bmatrix} = \mathbf{H}(f) \begin{bmatrix} E_1(f) \\ E_2(f) \end{bmatrix}, \tag{3.5}$$

where $\mathbf{H}(f)$ is the 2-by-2 *transfer function matrix* of the MVAR model. The transfer function matrix is calculated from the Fourier transform of $\mathbf{A}_r$ according to:

$$\mathbf{H}(f) = \left(\mathbf{I} - \sum_{r=1}^{p} \mathbf{A}_r e^{-i2\pi\Delta t f} \right)^{-1}, \tag{3.6}$$

where i is the imaginary unit and Δt is the sample time.

The directed transfer function (DTF) is calculated from the MVAR transfer function matrix $\mathbf{H}(f)$, normalizing each element $H_{i,j}(f)$ to the relevant row of $\mathbf{H}(f)$ (Kaminski and Blinowska, 1991):

$$DTF_{ij} = \frac{|H_{ij}(f)|^2}{\sum_{m=1}^{2} |H_{im}(f)|^2}. \tag{3.7}$$

Similar to how the coherency phase is determined by the phase of $\Phi_{y_c y_m}(f)$, the phase of the DTF is determined by the phase of $H_{i,j}(f)$. The phase of $H_{2,1}$ was used to estimate the time delay between y_c and y_m.

Partial directed coherence (PDC) is calculated directly from the Fourier transform of the matrices $\mathbf{A}_r$:

$$\overline{\mathbf{A}}(f) = \mathbf{I} - \sum_{r=1}^{p} \mathbf{A}_r e^{-i2\pi\Delta t f}. \tag{3.8}$$

In the calculation of the PDC, each element of $\overline{A}_{i,j}(f)$ in normalized to the relevant column of $\overline{\mathbf{A}}(f)$ (Baccalá and Sameshima, 2001; Florin et al., 2010a):

$$PDC_{ij}(f) = \frac{\overline{A}_{ij}(f)}{\sqrt{\sum_{m=1}^{2} |\overline{A}_{mj}|^2}}. \tag{3.9}$$

The phase of $\overline{A}_{2,1}$ was used to estimate the time delay between y_c and y_m.

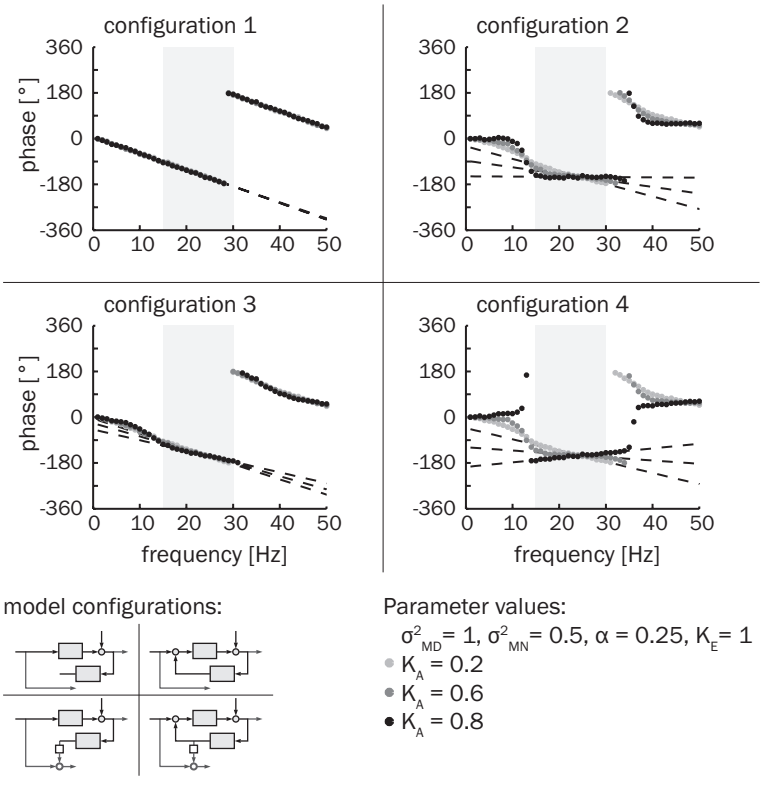

Figure 3.3: Coherency phase for the four model configurations and different values of K_A. Dashed lines are the straight lines fitted through the phases in the beta band (grey area), the slope of this line is the estimated time delay.

Time delay estimation

In experimental studies from literature, the time delay is estimated from the phase slope on frequencies where significant connectivity was found, typically the beta band (15 – 30Hz). For the simulations, time delays between the cortical and muscle signal were calculated by fitting a straight line onto the phases of coherency, DTF and PDC in the beta band (15 – 30Hz) (Mima et al., 2001a). A negative phase slope indicated that the cortical signal was leading the muscle signal. The slope was divided by −360° to transform the units from °/Hz (unit of the slope) to s (unit of time delay). Note that with this definition a positive value for the time delay indicated that y_c leads y_m.

3.3 Results

Coherency phase and time delay

When the corticomuscular system was modeled with an efferent pathway only (configuration 1) the coherency phase was proportionally related to frequency (figure 3.3), as expected. Both when sensory feedback was recorded in the cortical signal (configurations 3 and 4) and when the system formed a closed feedback loop (configurations 2 and 4) the phase had a very different relation with frequency. In these configurations the coherency phase showed fluctuations around the proportional phase frequency relation. The amplitude of the fluctuations increased when K_A was increased (figure 3.3). These fluctuations resulted in a reduced slope of the coherency phase in the beta band and the fitted line has a non-zero intercept, i.e. does not indicate zero degrees at $f = 0$. In configuration 4, increasing the value of K_A even led to a positive slope of the coherency phase in the beta band. Due to the fluctuations in the phase, the slope of the phase-frequency relation is not the same in different frequency bands.

The total transmission delay in the system ($TD_E + TD_A$) determines the period of the fluctuation, i.e. the frequency at which the fluctuating phase crosses the line corresponding to the efferent transmission delay for the second time. The transmission delays of the efferent and afferent pathway add to a total transmission delay of 43ms resulting in a period of the fluctuation of approximately 23Hz. As a result of this fluctuation-period, the phase frequency relation in the beta band can be described by a straight line with non-zero intercept and a slope suggesting a shorter time delay than the efferent transmission delay, similar to what is reported from experiments.

In figure 3.4 the estimated time delay is shown as a function of K_A for the three combinations of σ^2_{MD}, σ^2_{MN} and α. When sensory feedback was not recorded in the cortical signal and not fed back to the motor activity (configuration 1) the estimated time delay always equaled the efferent transmission delay. When the system formed a closed feedback loop (configuration 2) the estimated time delay decreased with increasing K_A but was not dependent on σ^2_{MD} and σ^2_{MN}. Additional simulations (not shown) indicated that in this configuration the estimated time delay was determined by the total loop gain ($K_E \cdot K_A$) and not by the relative strengths of the pathways.

When sensory feedback was recorded in the cortical signal (configurations 3 and 4) the estimated time delay was affected by the total loop gain, the relative strengths of the pathways, the variances of the input signals and the contribution of the sensory feedback to the cortical signal. In these configurations the estimated time delay could even become negative for the largest values of K_A. The decrease of the estimated time delay with increasing K_A was even steeper when the variance of MN (σ^2_{MN}) increased relative the variance of MD (σ^2_{MD}) and when the contribution of SF to y_c (α) increased. By manipulating the values of K_A, σ^2_{MN}, σ^2_{MD} and α the estimated time delay can vary between the actual efferent and afferent transmission delays (not all combinations are shown). The estimated time delay in configuration 4 can be seen as a combination of the estimated time delays in configuration 2 and configuration 3 as there is the added effect of the closed loop feedback system (configuration 2) and the recording of sensory feedback in the cortical signal (configuration 3).

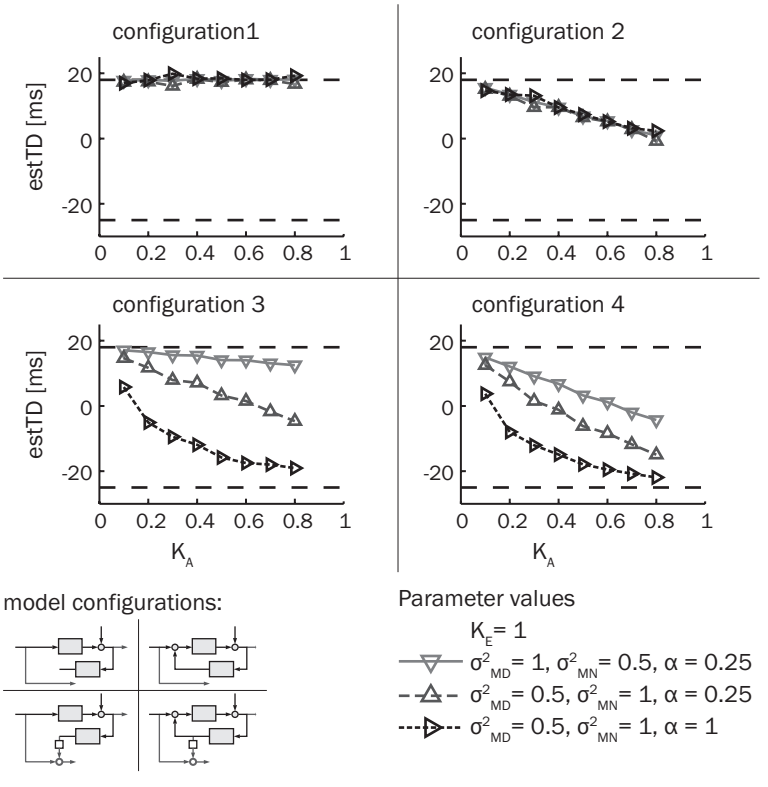

Figure 3.4: Time delays estimated from coherency phase as a function of K_A for three combinations of input signal variances and α. Dashed lines indicate transmission delays of efferent pathway (18ms) and afferent pathway (−25ms)

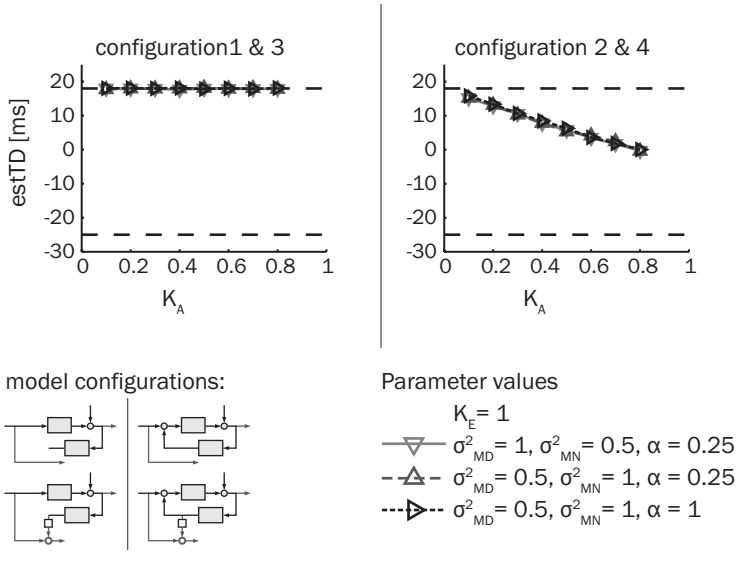

Figure 3.5: Time delays estimated from DTF phase ($y_c \rightarrow y_m$) as a function of K_A for three combinations of input signal variances and α. Model configuration 1 and 3 and model configurations 2 and 4 gave the same time delay estimates. Dashed lines indicate transmission delays of efferent pathway (18ms) and afferent pathway (−25ms)

Directed connectivity time delay

The recording of the sensory feedback signal in the cortical signal did not influence the time delay estimated from DTF phase. However, a closed feedback loop configuration induced the same fluctuations in the phase frequency relation as were seen in the coherency phase. This again led to estimated time delays shorter than the efferent transmission delay (figure 3.5). Similar to what was seen when estimating the time delay from coherency phase in configuration 2, the estimated time delay decreased with increasing K_A but was not affected by the variances of the input signals nor the the contribution of sensory feedback to the cortical signal.

The phase of PDC was proportional to frequency in all simulations and time delays estimated from PDC phase always equaled the efferent transmission delay (figure 3.6). There was no effect of the input signal variance nor of the contribution of sensory feedback to the cortical signal.

3.4 Discussion

In various fields of neuroscience, the coherency phase is interpreted in terms of a time delay between two signals and is used to disentangle the structure of functional networks between populations of neurons (Tallon-Baudry et al., 2001; Weiss and Mueller, 2003; Riddle et al., 2004; Witham et al., 2007; Nolte et al., 2008; Williams et al., 2009). In the corticomuscular system, smaller than expected time delays are found between cortical (EEG

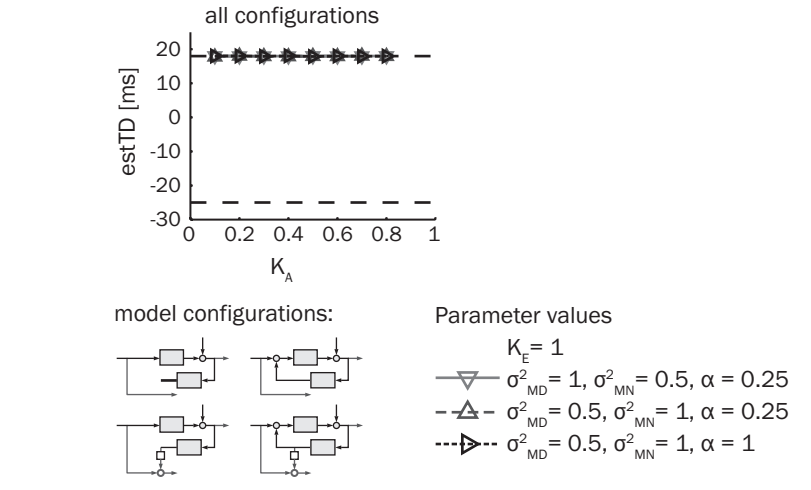

Figure 3.6: Time delays estimated from PDC phase ($y_c \rightarrow y_m$) as a function of K_A for three combinations of input signal variances and α. All model configurations gave the same time delay estimates. Dashed lines indicate transmission delays of efferent pathway (18ms) and afferent pathway (−25ms)

or MEG) and muscle (EMG) signals (Halliday et al., 1998; Brown et al., 1998; Grosse et al., 2003; Riddle and Baker, 2005). Although it is generally accepted that CMC arises due to bidirectional connectivity (Baker, 2007), the effect of sensory feedback on CMC phase or directed connectivity measures has not been thoroughly investigated. We used a model representing the corticomuscular system to investigate how time delays estimated from coherency, DTF and PDC phase are affected by a closed feedback loop and the recording of sensory feedback in the cortical signal.

When transmission delays can be estimated reliably from connectivity measures this could provide information about which pathways, i.e. direct oligosynaptic pathways or indirect polysynaptic pathways, are actually in use during a task (Lindemann et al., 2001). This is opposed to using external stimuli to elicit responses which provide structural information about the which pathways are available between different parts of the (central) nervous system.

An important outcome of our simulations is that in a closed feedback loop without the recording of sensory feedback in the cortical signal (model configuration 2), the estimated time delays based on coherency were shorter than the transmission delay of the efferent pathway. This means that even when no bidirectional connectivity is detected because sensory feedback is not recorded, time delays estimated from coherency phase are potentially meaningless estimates of the neural transmission delay. When sensory feedback was recorded in the cortical signal, resulting in a bidirectional connectivity between cortical and muscle signal, a wide range of time delays was estimated from coherency phase depending on the model configuration, strength of the efferent and afferent pathways, the variances of the input signals and the magnitude of the sensory feedback in the cortical signal. The different time delay estimates result from the fluctuations in the

phase frequency relation. With the physiologically realistic values for the efferent and afferent transmission delays, the fluctuations in the coherency phase cannot be seen in the beta band. The range of estimated positive and negative time delays based on the beta band was similar to the range of time delays reported from experiments in literature from CMC phase (Halliday et al., 1998; Brown et al., 1998; Gross et al., 2000; Grosse et al., 2003; Riddle and Baker, 2005; Petersen et al., 2012). When estimating time delays based on different frequency bands, an even wider range of estimated time delays would have been obtained. However, in experimental studies, significant coherence is generally not found outside the beta band. Recent studies showed that there is a bidirectional relation between the EEG/MEG and the EMG and that there are indeed sensory components in the EEG measured over the motor cortex (Witham et al., 2011; Jain et al., 2013). The complex interplay between the different structures in the corticomuscular system, essentially makes it impossible to estimate transmission delays based on coherency phase in the corticomuscular system.

There are multiple techniques and measures available that include directionality in the estimation of connectivity which may identify properties of individual pathways in case of bidirectional connectivity. We included two measures based on Granger causality (Granger, 1969) and a MVAR model of the data: the directed transfer function and partial directed coherence (Baccalá and Sameshima, 2001; Kaminski and Blinowska, 1991). Here we used these techniques to investigate a model representing corticomuscular connectivity. When the activity of multiple cortical areas can be directly measured by local field potentials or can be reliably reconstructed from scalp recordings, fitting of higher order MVAR models allows the study of connectivity between multiple cortical areas (Astolfi et al., 2007; Porcaro et al., 2013). However, care should be taken to avoid computational difficulties or the detection of spurious interaction due to common sources and volume conduction (Haufe et al., 2013). Recently, directed coherence, which is similar to DTF (Baker et al., 2006), has been used assess directionality and pathway properties in the corticomuscular system (Witham et al., 2011). The results of Witham et al. (2011) confirmed the bidirectional connectivity between cortex and periphery during motor control.

In the bivariate case, DTF and PDC give the same results on the connectivity pattern, as long as $\overline{\mathbf{A}}(f)$ (equation 3.8) is invertible (Baccalá and Sameshima, 2001). In a MVAR model $\overline{\mathbf{A}}(f)$ can become ill-conditioned when signals have a common source, for example as a result of volume conduction between EEG channels. In addition to this computational disadvantage of the DTF, our results show that DTF and PDC are not equally suited to estimate transmission delays. Only the time delays estimated from PDC phase equaled the afferent transmission delay. The DTF phase resulted in estimated time delays shorter that the efferent transmission delays when the model formed a closed loop feedback system. The DTF represents the transfer function from the external noise sources to the recorded signals, in a closed loop feedback system these transfer functions include the dynamics of the entire loop (Schouten and Campfens, 2012).

Partial directed coherence is directly based on the parameters of the MVAR model, describing the relation between past samples of the recorded signals and the current sample. In this way, the dynamics of individual pathways can be captured. In our simulations, correct identification of the MVAR model was aided by the simple model structure, absence of measurement noise, white noise characteristics of the input signals (Ljung, 1999) and no preprocessing of the recorded cortical and muscle activity (Florin et al., 2010a). The dy-

namics of the pathways were solely determined by the transmission delays and therefore the resulting PDC phase had a proportional relation with frequency. This allowed correct estimation of the time delay even in a narrow frequency band. When a neural pathway contains more dynamics than a transmission delay alone, these dynamics will be seen in the PDC phase and affect the estimated time delay (Lindemann et al., 2001).

Clearly, the simulation model is a simplification of the complex physiology underlying motor control. However, the evaluated techniques implicitly assume such a simple system underlies the recorded signals. If techniques fail to reliably estimate transmission delays in our idealized simulations, these techniques will certainly fail when the true system is even more complex. We therefore advice against the use of coherence phase and DTF phase to estimate time delays when a closed feedback loop could underlie the recorded signals.

Partial Directed Coherence phase resulted in the correct estimation of transmission delays in our simple simulation model. Whether a time delay estimated based on PDC phase will equal the transmission delay in experimental data will depend on many factors. As stated before, all dynamics of the pathways will affect the PDC phase and estimated time delay. Furthermore, the efferent and afferent pathway can most likely not be characterized by a single time delay while there are multiple nested feedback loops present in the motor control system. Because these nested feedback loops cannot be observed from non-invasive recordings of cortical activity and muscle activity, the time delays that are estimated based on PDC phase will represent a lumped time delay.

Chapter 4

Quantifying connectivity in motor control using coherence measures and joint position perturbations

S. Floor Campfens, Alfred C. Schouten, Michel J.A.M. van Putten and Herman van der Kooij. *Experimental Brain Research* 228(2): 141-153, 2013

ABSTRACT

The applicability of corticomuscular coherence (CMC) as a connectivity measure is limited since only 40 – 50% of the healthy population presents significant CMC. In this study, we applied continuous joint position perturbations to obtain a more reliable measure of connectivity in motor control. We evaluated the coherence between joint position perturbations and EEG (position-cortical coherence, PCC) and CMC. Healthy subjects performed two isotonic force tasks against the handle of a wrist manipulator. The baseline task was isometric; in the perturbed task, the handle moved continuously with small amplitude. The position perturbation signal covered frequencies between 5 and 29Hz. In the perturbed task, all subjects had significant PCC and 86% of the subjects had significant CMC, on both stimulus and non-stimulus frequencies. In the baseline task, CMC was present in only 45% of the subjects, mostly on beta-band frequencies. The position perturbations during an isotonic force task elicited PCC in all subjects and elicited CMC in most subjects on both stimulus and non-stimulus frequencies. Perturbed CMC possibly arises by two separate processes: an intrinsic process, similar to the process in an unperturbed task, involving both efferent and afferent pathways; and a process related to the excitation of the afferent and efferent pathways by the perturbation. These processes cannot be separated. PCC, however, reflects connectivity via the afferent pathways only. As PCC was present in all healthy subjects, we propose this coherence as a reliable measure for connectivity in motor control via the afferent pathways.

4.1 Introduction

The control of movement involves numerous interactions between various parts of the central nervous system (CNS), including multiple cortical areas, the basal ganglia, cerebellum, brainstem and the spinal cord. Interactions between these areas are quantified by various measures of correlation between recorded activity from the different structures. Widely applied measures of correlation are coherence and phase synchronization between pairs of EEG or MEG channels to quantify cortico-cortical connectivity (Varela et al., 2001) and study the formation of functional networks within the brain (Stam and van Straaten, 2012).

A frequently applied measure of connectivity in motor control is the coherence between cortical activity and muscle activity: corticomuscular coherence (CMC) (Conway et al., 1995; Mima et al., 2000; Baker, 2007; Halliday et al., 1998). Due to the large distance between the recording sites, there is no effect of volume conduction which may impede the detection of connectivity between neural populations close together (Fries, 2005). Corticomuscular coherence is generally found in the beta band ($15-30$Hz) and indicates synchronization between neural oscillations in the cortex and the spinal cord, although the physiological processes generating CMC are not fully understood. Since muscle activity, as well as cortical activity, is measured inside a closed-loop system, ordinary CMC arises via both efferent and afferent pathways. This bidirectional nature of CMC is widely accepted, and the descending motor contribution as well as the ascending sensory contribution to CMC has been studied (Witham et al., 2011; Mima et al., 2001a; Riddle and Baker, 2005; Pohja and Salenius, 2003). In addition, a recent study using invasive recordings in monkey showed that it is likely that coherent oscillation in the motor control system arises within the closed loop and is not the result of a single oscillatory motor drive (Williams et al., 2009). Although the contribution of both pathways can be shown using directed coherence or similar techniques (Gourévitch et al., 2006; Kaminski and Blinowska, 1991), separate properties of the pathways cannot be determined (Schouten and Campfens, 2012).

Corticomuscular coherence is not an epiphenomenon and has been shown to have a functional role in motor control. Corticomuscular coherence varies with different aspects of motor control such as attention (Kristeva-Feige et al., 2002; Johnson et al., 2011), performance (Kristeva et al., 2007), exerted force (Witte et al., 2007; Mima et al., 1999), fatigue (Yang et al., 2009, 2010), type of the task (Masakado and Nielsen, 2008; Baker et al., 1997), experience with the task (Perez et al., 2006; Mendez-Balbuena et al., 2011) and activity preceding the task (Riddle and Baker, 2006; Omlor et al., 2007).

Corticomuscular coherence has also been measured in a clinical setting to study movement disorders such as various types of tremor (van der Meer et al., 2010; Grosse et al., 2003; van Rootselaar et al., 2006), including the tremor present in Parkinson's disease (Florin et al., 2010b; Amtage et al., 2009). In addition, CMC has been proposed as an attractive measure of connectivity in motor control after stroke (Braun et al., 2007; Fang et al., 2009; Meng et al., 2009; Yao and Dewald, 2006). In stroke patients, some studies reported reduced CMC magnitude in the affected hemisphere when compared to the unaffected hemisphere (Mima et al., 2001b) or compared to healthy controls (Fang et al., 2009). However, Braun et al. (2007) found no difference in CMC magnitudes but instead reported increased dispersion of CMC in the affected hemisphere compared to the unaffected hemisphere in well-recovered stroke patients. Although the experimental evidence

is limited, Braun et al. (2007) hypothesized a relation between CMC magnitude and motor function in well-recovered stroke patients, where high CMC indicates better motor function. If such relation exists, CMC may be used to monitor the cortical contribution to the recovery of patients after stroke.

A potential limitation for the clinical applicability of CMC as a measure for connectivity in motor control is the large inter-individual variation in CMC that is normally obtained from a static, isometric force task. Only 40 – 50% of healthy subjects express significant CMC during such a static task, and the strength and bandwidth of CMC vary between individuals (Mima et al., 2000; Mendez-Balbuena et al., 2011; Ushiyama et al., 2011). With such large inter-individual differences within a healthy population, the absence of CMC does not necessarily indicate abnormal connectivity. This results in a limited general applicability of CMC during a static task to derive conclusions about the presence or strength of the efferent and afferent pathways in individual subjects or patients. To serve as an individual measure for connectivity in motor control, interventions that could reduce inter-individual difference in CMC or additional measures are needed. Recently, it was demonstrated that transient electrical or mechanical peripheral perturbations during a static task increase and even elicit CMC in healthy subjects (McClelland et al., 2012a). Subjects without pre-stimulus CMC did show CMC 400ms after the stimulus. The authors concluded that relevant sensory input could play a crucial role in modulating and revealing CMC.

In this study, we aim to obtain a reliable measure for connectivity in motor control that is present in all healthy subjects by applying continuous mechanical joint position perturbations during an isotonic force task. We investigated two measures: coherence between the position perturbation signal and EEG (position-cortical coherence, PCC) and CMC. Since the perturbation signal is measured outside the physiological feedback loop, PCC represents uni-directional causality: cortical activity is evoked by the applied perturbation, and cortical activity does not influence the perturbation. Position-cortical coherence is therefore a measure for the response evoked by the perturbation and reflects activity of the ascending sensory pathways only. Oscillatory input has been applied in the visual and auditory system to evoke a cortical response: a steady-state evoked potential (Herrmann, 2001). We expect that the position perturbation will elicit PCC and CMC at the stimulus frequencies via the same afferent pathways. Possibly the position perturbation affects CMC on the non-stimulus frequencies as well due to an interaction between responses to the perturbation and the intrinsic process leading to CMC in a baseline task. Part of this work was presented in abstract form (Campfens et al., 2011).

4.2 Methods

Twenty-two healthy volunteers participated in this study (nine women, mean age 27 years, age range 23-35, four subjects were left-hand dominant). The dominant hand was determined using the Dutch handedness questionnaire (van Strien, 1992). All measurements were conducted in accordance with the Declaration of Helsinki and were approved by the Medical Ethics Review Committee of the Medisch Spectrum Twente (Enschede, the Netherlands). All subjects gave signed informed consent before participating.

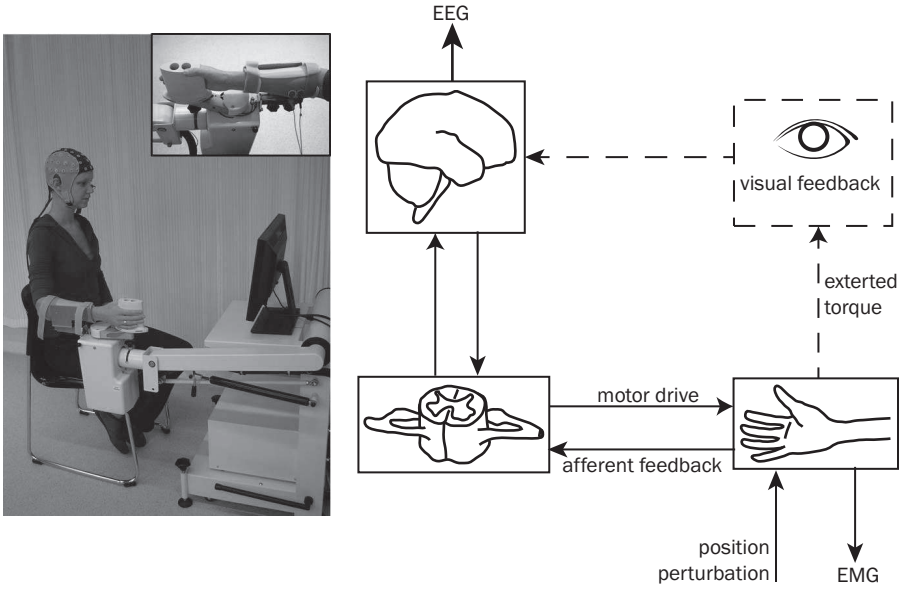

Figure 4.1: Overview of the experimental setup (left) and scheme of all signals (right). The subject holds the lever of the WM, and the lower arm is strapped in an arm rest using Velcro straps. To support the subject, visual feedback of the target torque and the exerted torque (2Hz low-pass filtered with third-order Butterworth filter) are provided on the display in front of the subject. EEG is measured using a head cap (64 channels), EOG is measured to monitor eye blinks and bipolar EMG is measured from the flexor carpi radialis (FCR) and extensor carpi radialis (ECR). During the position perturbations, the handle of the WM continuously moves around the neutral position with a small amplitude. As the subject has no influence on the position of the handle, coherence between position perturbation and EEG represents a uni-directional relation via the afferent sensory pathways while CMC represents connectivity involving activity via both the efferent and the afferent pathways

Experimental setup

Subjects were seated next to a wrist manipulator (Moog Inc., Nieuw-Vennep, the Netherlands), see Figure 4.1. The wrist manipulator (WM) is an actuated rotating device with a single degree of freedom that can exert flexion and extension perturbations to the wrist joint. The lower arm of the subject's dominant hand was strapped in an arm rest while the subject held the handle of the WM. The axis of rotation of the WM was aligned with the axis of rotation of the wrist. The neutral angle is defined as when the handle keeps the thumb in line with the lower arm, resulting in a slight extension of the wrist. The lever of the WM is equipped with a force transducer to measure the torques exerted by the subject. Due to the high stiffness of the WM, the subject has no influence on the angular position of the handle.

EEG was measured from 64 electrodes on the scalp, placed according to the 5% electrode system (Oostenveld and Praamstra, 2001) using a standard EEG cap with Ag/AgCl electrodes (WaveGuard cap by ANT, Enschede, the Netherlands). Electrode impedances

were below 5kOhm. EMG was measured from the m.flexor carpi radialis (EMG_{FCR}) and the m.extensor carpi radialis (EMG_{ECR}) using bipolar Ag/AgCl electrode pairs placed on the muscle belly (diameter: 1cm, inter-electrode distance: 2cm). To monitor eye blinks, the vertical electrooculogram (EOG) was measured from the left eye. All physiological signals were sampled at 2048Hz (refa system by TMSi, Oldenzaal, the Netherlands). The angle of the WM and torque on the lever were synchronously recorded on a separate system (porti system by TMSi, Oldenzaal, the Netherlands) at 2048Hz.

Protocol

Subjects exerted a constant wrist flexion torque to the handle of the WM, while the WM either kept the neutral angle or imposed a continuous position perturbation. Subjects received visual feedback of the exerted and target torque via a display. Subjects were instructed to keep the exerted torque within a block of 1.8 ± 0.27Nm. For the visualization, the exerted torque was filtered online (third-order low-pass Butterworth, 2Hz) to remove the stimulus frequencies. The target torque of 1.8Nm is comparable with 15% of maximum voluntary contraction torque for an average subject. The constant neutral angle served as a baseline task, similar to the standard procedure to measure CMC. During the position perturbations, the handle moved continuously with small amplitude around the neutral angle. For each of the two tasks - baseline and perturbed - five trials of 55s were recorded. The baseline trials were performed first. Ten subjects performed a second set of five baseline trials to assess a possible carryover effect of the perturbation on baseline CMC. Between trials, subjects were given sufficient rest time to prevent fatigue.

The position perturbation signal (Figure 4.2) consisted of a sum of sine waves (5, 9, 13, 17, 21, 25 and 29Hz), and the phases of the sine waves were optimized such that the perturbation contained maximal power (Pintelon and Schoukens, 2001). The perturbation signal had a period of 1s, and peak-to-peak amplitude was 0.03rad (1.7°). The power of the sine waves decreased with frequency, giving the perturbation a flat velocity spectrum. Since we expect the neuromuscular system to have non-linear responses, the perturbation signal was designed to reveal non-linear responses (Pintelon and Schoukens, 2001): possible responses at even and odd higher harmonics of the stimulus frequencies appear at non-stimulus frequencies. Since the perturbation signal contains multiple frequencies, non-linearity could also result in power at higher harmonics of combinations of stimulus frequencies, including both positive and negative frequency components. These higher harmonics at frequency combinations also do not coincide with the stimulus frequencies. The beta band was included in the position perturbation signal because this frequency band is involved in oscillatory coupling in an unperturbed task; we expected that including beta-band frequencies increases the chance of eliciting PCC and CMC by a perturbation.

Data analysis

Recorded signals were visually inspected and processed off-line using MATLAB 7.11 (the MathWorks, Inc., Natick, MA, USA). Raw EEG and EOG signals were band-pass filtered ($2-70$Hz), and the EEG was transformed to a nearest neighbor Laplacian derivation. EMG was band-pass filtered ($2-500$Hz). The filters were fourth-order Butterworth filters applied

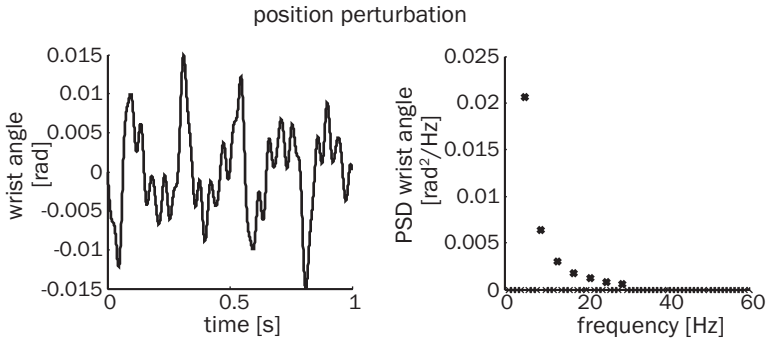

Figure 4.2: Time series (left) and Power Spectral Density (PSD, right) of the position perturbation

with zero lag. All signals were inspected visually.

Power spectral density

All signals were segmented in 1s segments (2048 samples) - the period of the perturbation - with 75% overlap between segments; the use of overlapping segments decreases the bias and variance of the coherence estimates (Bortel and Sovka, 2007; Carter, 1987). The EOG was used to remove segments containing eye blinks. Segments where the average exerted torque deviated more than 10% from the target force were removed as well. The 50-Hz component (power line artefact) was removed from each segment using the discrete Fourier transform (algorithm taken from Fieldtrip Toolbox for MATLAB; Oostenveld et al., 2011). To exclude the possibility of movement artefacts in the EMG signal, frequency components below 75Hz were filtered from the EMG using an ideal high-pass filter: EMG was transformed to the frequency domain using the fast Fourier transform (FFT), frequencies below 75Hz are set to zero, and the resulting signal is transformed back to the time domain using the inverse FFT. After this high-pass filtering, the EMG was rectified. The use of high-pass filtering prior to rectifying EMG is shown to be suitable for coherence analysis by Boonstra and Breakspear (2012).

All segments were transformed to the frequency domain using the FFT. The power spectral density (PSD, Φ_{xx}) and cross-spectral density (CSD, Φ_{xy}) were estimated per task for every individual subject using

$$\Phi_{xx}(f) = \frac{1}{N}\sum_{i=1}^{N} X_i^*(f)\cdot X_i(f) \tag{4.1}$$

and

$$\Phi_{xy}(f) = \frac{1}{N}\sum_{i=1}^{N} X_i^*(f)\cdot Y_i(f) \tag{4.2}$$

respectively, where $X_i(f)$ and $Y_i(f)$ are the Fourier coefficients at frequency f estimated from the i^{th} data segment. The asterisk indicates the complex conjugate, and N is the total number of segments.

The power spectra of the EEG and EMG signals in the baseline and the perturbed task were compared, considering stimulus and non-stimulus frequencies separately. The non-stimulus power of the EEG (NSP_{EEG}) was defined as the integral of the log-transformed PSD over non-stimulus frequencies between 1 and 60Hz. The non-stimulus power of the rectified EMG signals ($NSP_{EMG-FCR}$ and $NSP_{EMG-ECR}$) included the power on non-stimulus frequencies between 1 and 200Hz. The stimulus power of EEG and rectified EMG (SP_{EEG}, $SP_{EMG-FCR}$ and $SP_{EMG-ECR}$) was the log-transformed power summed over the stimulus frequencies. All power measures were compared between the baseline and perturbed task; statistical significance was evaluated using paired Student's t tests with $\alpha = 0.05$.

Coherence

The (magnitude squared) coherence ($C_{xy}(f)$) was calculated between signals according to

$$C_{xy}(f) = \frac{|\Phi_{xy}(f)|^2}{\Phi_{xx}(f)\Phi_{xy}(f)} \tag{4.3}$$

The CMC was expressed as coherence between EEG channels and EMG_{FCR} and was calculated per task for every subject. Coherences between the position perturbation and EEG/EMG_{FCR} (PCC and position-musculo coherence, PMC) were only evaluated at stimulus frequencies.

Significance of coherence values was determined using the approximation of the confidence limit (CL) by Bortel and Sovka (2007). They provided an approximation for the number of degrees of freedom for the probability density function and CL formula of the magnitude squared coherence for overlapping segments. The confidence level was set to 0.95 ($\alpha = 0.05$). To limit false positives, a subject was considered to have CMC for a task if CMC was largest at electrodes over the contralateral motor cortex.

Subjects were divided in two groups based on the presence of CMC in the baseline task. The *baseline CMC+* group had significant CMC in the baseline task, and the *baseline CMC-* group did not have significant CMC in the baseline task. For subjects in the baseline CMC+ group, the electrode at the contralateral side with the highest CMC was used for single channel analysis. In the baseline CMC- group, C3 (right-handed subject) or C4 (left-handed subject) was used for single channel analysis. An exception was made if the signal quality at C3 (C4 for left-handed subjects) was poor; in such cases, C1 (C2 for left-handed subjects) was used. For single channel analysis of CMC in the perturbed task, the same electrode was used as in the baseline task. Mean significant CMC amplitude between 1 and 60 Hz was calculated by taking the averaged CMC over the bins where the CMC exceeded CL. In the baseline tasks, this typically only includes frequencies in the beta band. In addition, topoplots of the total significant CMC and PCC visualized the spatial distribution of coherence over the scalp.

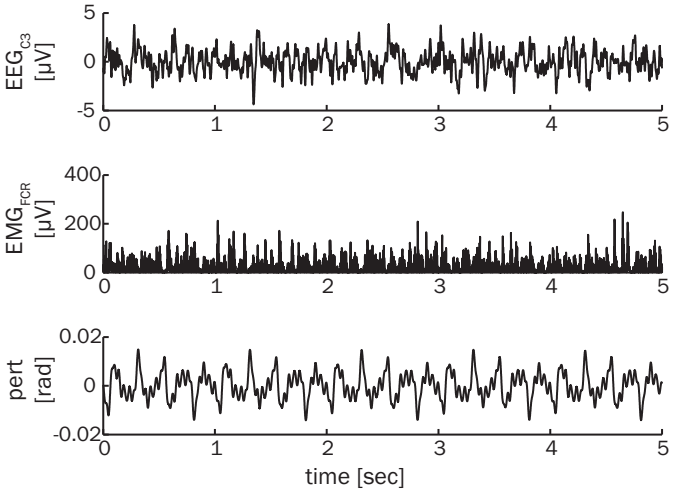

Figure 4.3: Example of time series in the perturbed task of a representative subject (S08). Upper row EEG at electrode C3. Middle row high-pass filtered (cutoff: 75Hz) and rectified EMG_{FCR}. Bottom row position perturbation signal

4.3 Results

Power spectral density

Examples of time series recorded in the perturbed task of a representative subject are presented in figure 4.3. The PSDs of the EEG were similar in the baseline and perturbed task (figure 4.4). No significant difference of EEG power was detected between the baseline and perturbed task both on stimulus and on non-stimulus frequencies ($SP_{EEG}: p = 0.28; NSP_{EEG}: p = 0.46$). In the perturbed task, the PSD of the EMG_{FCR} showed maxima at the stimulus frequencies. A significant difference in EMG_{FCR} power was present both on stimulus and on non-stimulus frequencies ($SP_{EMG-FCR}: p < 0.001; NSP_{EMG-FCR}: p < 0.01$). The power of the EMG_{FCR} on the stimulus and non-stimulus frequencies increased by 12 and 4%, respectively. A significant difference was also present in the power of the EMG_{ECR} on both stimulus and non-stimulus frequencies ($SP_{EMG-ECR}: p < 0.001; NSP_{EMG-ECR}: p < 0.01$). The power of the EMG_{ECR} on the stimulus and non-stimulus frequencies increased by 32 and 28%, respectively.

Coherence at contralateral motor cortex

Typical PCC and CMC spectra for the baseline and the perturbed task are presented in figure 4.5; these examples show the significant PCC and the increased CMC in the perturbed task. The CMC spectra in the perturbed task have more sharp peaks compared to the baseline CMC spectra. The peaks in the CMC spectra mostly coincide with higher PCC, although CMC peaks are also found at non-stimulus frequencies. Figures 4.6 and 4.7

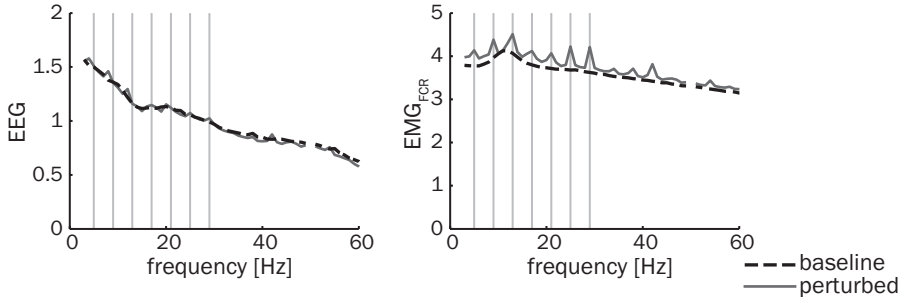

Figure 4.4: Grand average log-transformed PSD of EEG (left) and EMG_{FCR} (right) in both tasks. Gray vertical lines indicate stimulus frequencies. No statistical difference was detected in EEG power, EMG_{FCR} power changed significantly at stimulus and at non-stimulus frequencies

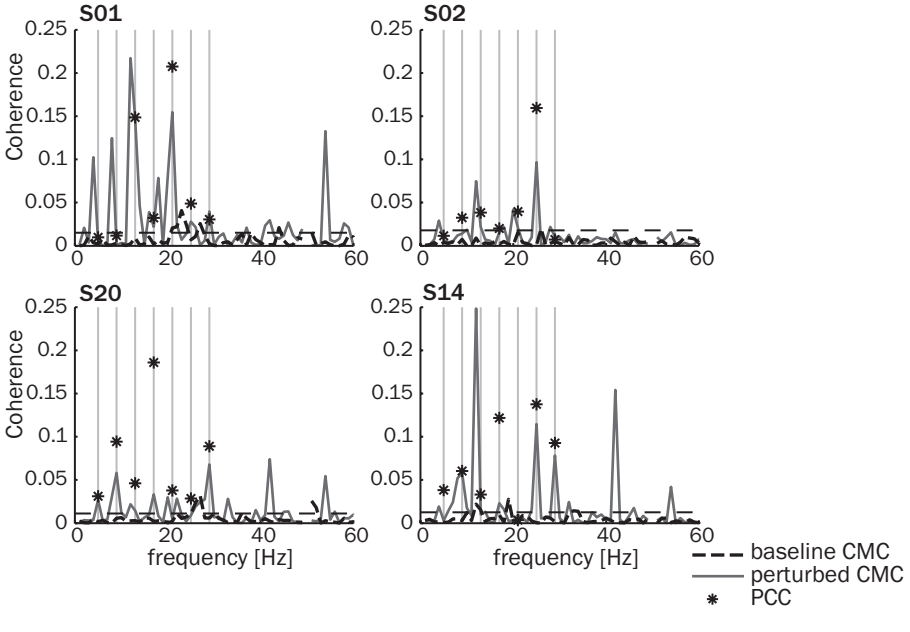

Figure 4.5: Individual CMC and PCC spectra of four representative subjects from the group baseline CMC+ (S01, S14 and S20) and baseline CMC- (S02). Dashed horizontal lines indicate the CL. Gray vertical lines indicate the stimulus frequencies

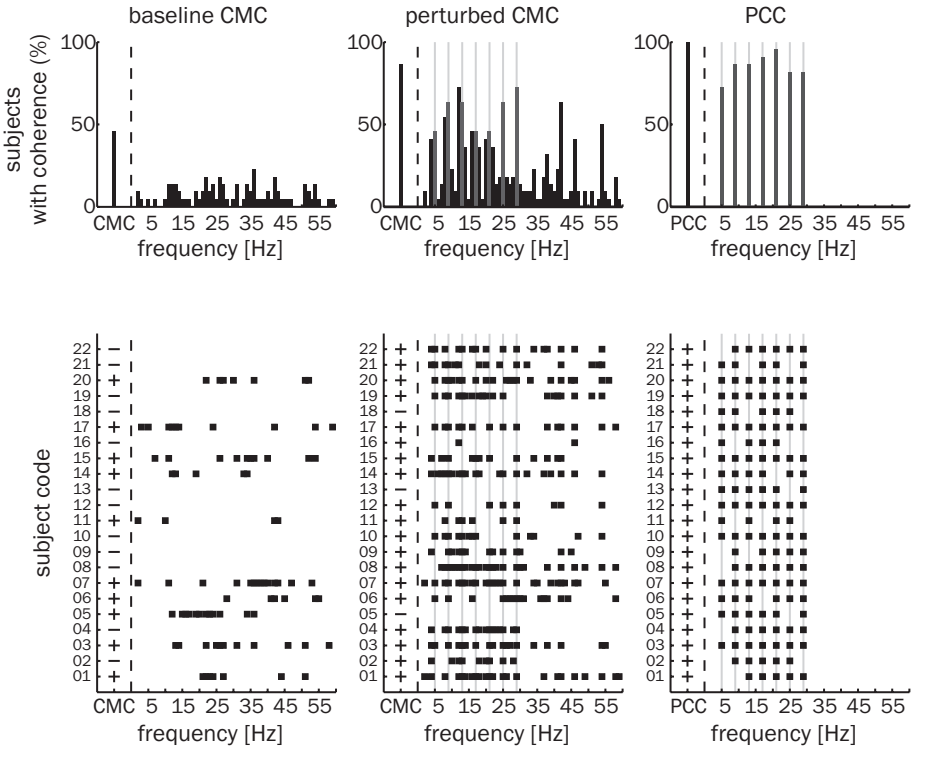

Figure 4.6: Overview of CMC and PCC in the baseline and perturbed task in all subjects. From left to right baseline task CMC, perturbed task CMC and PCC. Upper row percentage of subjects with CMC per frequency. Lower row CMC presence in the individual subjects. On the vertical axis, the subject code, a '+' in the first column indicates CMC/PCC, a '-' indicates no CMC/PCC. The frequencies with CMC in the individual subjects are indicated by the dots. Gray vertical lines indicate the stimulus frequencies

summarize for all individual subjects the presence (figure 4.6) and amplitude (figure 4.7) of significant CMC and PCC. In the perturbed task, all subjects had significant PCC and more subjects had CMC compared to the baseline task. In general, the perturbation resulted in PCC and CMC in the baseline CMC- group and even increased CMC in the baseline CMC+ group.

In the baseline task, ten out of twenty-two subjects (45%) had significant CMC between EEG at the contralateral motor cortex and EMG_{FCR}, mostly in the beta band. In seven subjects, the maximal CMC was at electrode C3, in two subjects (S11 and S14) at electrode C2 and in one subject (S20) at electrode FC3. Subjects in the baseline CMC+ group had significant CMC on frequencies ranging from 11 to 41Hz. The number of frequencies on which a subject in the CMC+ group had significant CMC always exceeded the number which would be expected from a false positive (expected from a false positive is $2-3$ significant frequencies in the range of $1-60$Hz and with $\alpha = 0.05$). Twelve subjects did not have CMC in the baseline task.

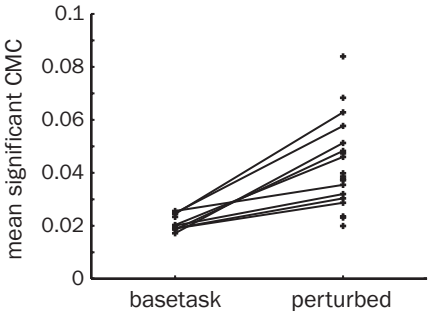

Figure 4.7: Mean significant CMC amplitude over all frequencies under 60Hz, for all subjects with CMC in the baseline or perturbed task. Each subject is represented as a cross, lines indicate the subjects presenting CMC in both tasks

In the perturbed task, all subjects had significant PCC and nineteen of twenty-two subjects (86%) had significant CMC. From the three subjects without CMC in the perturbed task, two subjects came from the baseline CMC- group. The three subjects without significant CMC in the perturbed task did have PCC. One subject had significant CMC in the baseline task, and not in the perturbed task. In all nine subjects with significant CMC in both tasks, CMC amplitude was higher in the perturbed task (figure 4.7).

The presence of PCC was very similar to the CMC at the stimulus frequencies: if significant CMC was found at a stimulus frequency, the PCC was also significant at that frequency in nearly all subjects. Only three subjects had significant CMC but no significant PCC at that frequency (S09 at 13Hz, S11 at 29Hz and S22 at 5Hz). Seventeen subjects had significant PCC at frequencies where the CMC did not exceed the CL.

The PMC was significant at almost all stimulus frequencies in all subjects. The PMC was high compared to CMC and PCC and could be as high as 0.8 in some subjects.

Four of the ten subjects that performed the second baseline task after the perturbed task had significant CMC in the first baseline task. Two of these subjects had significant CMC in the second baseline task as well and in the same frequency band. One subject had no significant CMC in the first baseline task but did show significant CMC in the second baseline task.

There was a large variability in the frequencies at which individual subjects had significant CMC in the perturbed task. Almost all subjects with significant CMC in the perturbed task had significant CMC on at least one stimulus frequency. Only one subject (S16) had no significant CMC on the stimulus frequencies, although this subject had significant PCC on four stimulus frequencies. Of the stimulus frequencies, significant PCC or CMC was found at 5Hz in the fewest number of subjects. Significant CMC at 29Hz was present in the highest number of subjects. Significant PCC was found most often on 21Hz.

Significant CMC was found on non-stimulus frequencies in all subjects with CMC in the perturbed task; especially, the number of subjects with significant CMC at 12 and 42Hz is noticeably higher than on other non-stimulus frequencies.

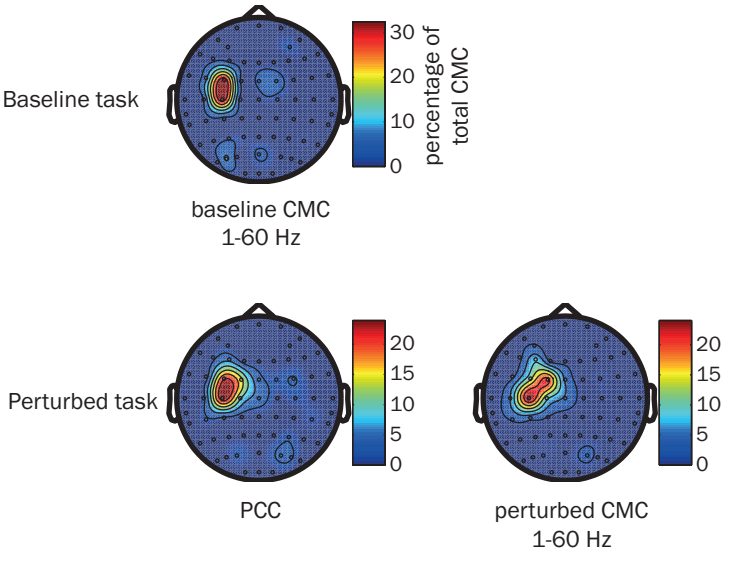

Figure 4.8: Topoplots of the CMC and PCC expressed as percentage of the total coherence over all electrodes of a representative subject (S07). Top row baseline task. Significant CMC summed over all frequencies between 1 and 60Hz. Bottom row perturbed task. Left plot shows significant PCC over all stimulus frequencies. Right plot shows the significant CMC over all frequencies between 1 and 60Hz

Localization of coherence

Both in the baseline and in the perturbed task, no significant coherence was found at the ipsilateral motor cortex. Topoplots indicated that significant PCC and CMC were generally present on multiple electrodes in the perturbed task (figure 4.8), including the electrode(s) where CMC was present in the baseline task (baseline CMC+ group). The electrode where maximal coherence occurred in the perturbed task was not necessarily the electrode where maximal CMC was present in the baseline task.

4.4 Discussion

In this study, we investigated the use of angular joint position perturbations and coherence measures as a novel tool to reliably quantify connectivity in motor control. Corticomuscular coherence is a correlation measure that reflects activity via both descending and ascending pathways. Contrary, coherence between position perturbation and EEG (PCC) is introduced as a uni-directional correlation measure reflecting activity via the ascending afferent pathways. Small wrist perturbations induced PCC in all subjects. These perturbations increased the number of subjects presenting CMC and the amplitude of CMC, on both stimulus and non-stimulus frequencies, but did not evoke significant CMC in all subjects.

In the isometric, isotonic motor task without perturbations, ten out of twenty-two subjects (45%) had significant CMC, mostly on beta-band frequencies. This is in line with other studies, reporting significant CMC during isotonic, isometric motor tasks in 40−50% of healthy subjects (Ushiyama et al., 2011; Mima et al., 2000; Mendez-Balbuena et al., 2011). The second baseline task performed by ten subjects showed that even within a subject, the presence of CMC is variable; in one subject, CMC appeared in the second baseline task and in two subjects significant CMC disappeared. The low number of healthy subjects presenting significant CMC in a static motor tasks and the within-subject variation limits the clinical applicability of CMC as a measure of connectivity in motor control.

Mechanical perturbations elicit coherence

The addition of small continuous position perturbations during an isotonic force task had a large effect on CMC. In the perturbed task, all subjects had significant PCC and nineteen of twenty-two subjects (86%) had significant CMC. In subjects with significant CMC in both tasks, the CMC was higher in the perturbed task with an average increase of 109% of the mean significant CMC amplitude.

Our results may appear different from the results in van der Meer et al. (2010) who used a similar approach applying position perturbations to the wrist to investigate intermuscular drive in dystonia patients and healthy controls during an isotonic force task. In this study, no CMC was elicited in the healthy controls when position perturbations were applied. However, van der Meer et al. (2010) applied perturbations up to 12Hz while we applied a perturbation also including frequencies in the beta band. Williams and Baker (2009b) showed that Renshaw cell recurrent inhibition reduces oscillatory coupling at frequencies under approximately 10 Hz which may explain why van der Meer et al. (2010) found no CMC. We argue, therefore, that to elicit CMC using a continuous perturbation, the perturbation signal should contain frequencies in the beta band.

Possible confounding factors

Significant PCC or CMC in the perturbed task could have resulted from artefacts caused by the WM. However, in the EMG signal, possible (movement) artefacts were removed by high-pass filtering and rectification. In the EEG, such artefacts would be distributed over the whole scalp and be accompanied by an increase in EEG power. Significant PCC and CMC were predominantly localized over the contralateral motor cortex, as expected (Conway et al., 1995), and the EEG power was not significantly different between baseline and perturbed task. Therefore, we rule out the possibility of artefacts as a cause for the significant PCC and CMC in the perturbed task.

In comparison with the baseline task, the power of the EMG signals increased on stimulus and on non-stimulus frequencies, with clear maxima at stimulus frequencies and some higher harmonics. By itself, an increase in power is not sufficient to explain the increased presence of CMC in the perturbed task as coherence is normalized by signal power. Coherence is primarily a measure for phase synchronization between two signals as phase synchronization is a necessary condition for significant coherence (Bruns, 2004). Only if the increased signal power reduces the relative amount of measurement noise, the increased signal power could improve SNR and increase coherence. The PCC is indepen-

dent from changes in EMG power. The absence of changes in EEG power at the stimulus frequencies indicates that PCC indeed arose from phase locking of ongoing cortical oscillations to the perturbation.

Origin of coherence at stimulus and non-stimulus frequencies

Corticomuscular coherence indicates significant phase synchronization between EEG and EMG but does not show how this synchronization arises. In general, coherence can arise due to multiple processes: a uni-directional relation between two signals (open loop system), a bidirectional relation (closed-loop system) or a common drive to two signals. Although the coherence between EEG and EMG has been studied for over 15 years, the process generating CMC during an isometric, isotonic remains poorly understood. Currently, it is widely accepted that in an unperturbed task, this CMC involves activity via both the descending efferent and the ascending afferent pathways connecting cortical and spinal neurons forming a closed-loop system with unknown inputs.

In the perturbed task, a position perturbation was added to the closed-loop neuromuscular system which elicited significant CMC on both stimulus and non-stimulus frequencies. The perturbation acts as an external excitation of the neuromuscular system, primarily exciting muscle spindles and Golgi tendon organs. Via the spinal reflex loop, the perturbation elicits a response in the EMG. In addition, an EEG response to the perturbation is elicited via afferent sensory pathways, this is quantified by PCC and represents a process similar to how steady-state evoked potentials are evoked in the visual or auditory system (Herrmann, 2001). A transcortical reflex loop provides a second pathway that can elicit an EMG response. With the perturbation as a common input signal driving the EEG and EMG, CMC is also induced. If significant CMC at a stimulus frequency was observed, this was almost always accompanied by significant PCC. This suggests that the common drive of the position perturbation is indeed the main contributor to CMC at the stimulus frequencies. PCC and CMC at the stimulus frequencies both represent activity of the same ascending afferent pathways; in addition, CMC at the stimulus frequencies can contain contributions from the descending efferent pathways due to transcortical reflexes. Note that the coherence due to a common drive to EEG and EMG represents a different process than the process due to which CMC arises in the unperturbed task, but still involves both the efferent and the afferent pathways.

In our study, EEG activity was evoked by sensory input by an external perturbation. Evidence exists that also in non-perturbed conditions EEG activity has a large sensory component. Recently, Jain et al. (2013) found similar averaged EEG waveforms in active and passive pedalling tasks. This suggests that afferent sensory input is a large contributor to the EEG during an active task. Witham et al. (2011) applied directed coherence (Granger causality) analysis and showed that both efferent and afferent pathways contribute to unperturbed CMC. It was also found that the contribution of both pathways varies considerably between subjects.

Recently,McClelland et al. (2012a) showed that CMC during a isometric task can even be modulated by sensory input. After a sudden mechanical perturbation, the CMC was initially decreased for 400ms and reappeared with a larger amplitude after the initial reflexive activation. Even subjects without significant CMC in the pre-stimulus period showed significant CMC in the post-stimulus rebound period, resulting in 100% of the

subjects showing significant CMC post-stimulus. Possibly the rebound response found by McClelland et al. (2012a) contributes to the response to the continuous perturbation although we were not able to elicit significant CMC in all subjects.

In the perturbed task, significant CMC was found on several non-stimulus frequencies as well; the likelihood of finding significant CMC at some harmonics of the stimulus frequencies (8, 12 and 42Hz) was even comparable to the likelihood of finding CMC at the stimulus frequencies: more than 50% of the subjects had CMC on at least one of these frequencies. The CMC at non-stimulus frequencies may represent CMC generated by the same intrinsic mechanisms as in an unperturbed task. However, as the neuromuscular system is highly non-linear, CMC at these frequencies may also be a sign of non-linear responses to the perturbation. In a recent study, Langdon et al. (2011) presented such non-linear responses of the somatosensory system. Neural oscillations, recorded using EEG, phase locked to a single frequency vibrotactile stimulation, not only on the frequency of the stimulation but also on higher harmonics: $n:m$ phase locking. The phase locking was not accompanied by power changes at stimulated frequencies. The responses we found at specific non-stimulus frequencies suggest that the phase locked oscillations described by Langdon et al. (2011) may also occur in an active motor task. Using a linear analysis technique, such as coherence, it is not possible to separate these non-linear responses to the perturbation from the intrinsic mechanisms generating unperturbed beta-band CMC. Possibly, these processes can be separated using granger causality (Florin et al., 2011), multi-frequency phase locking measures, or by using multiple position perturbations with different frequency contents. However, such analysis is outside the scope of the current study. Our aim was to obtain a reliable measure of connectivity in motor control with less variability between healthy subjects. We present PCC as an attractive measure connectivity via the afferent pathways present in all healthy subjects. Significant CMC is also induced by the position perturbation in most subjects and represents connectivity involving both the efferent and the afferent pathways arising by two simultaneous processes.

Corticomuscular coherence in an unperturbed task is modulated by various factors, which may also influence CMC in the perturbed task. Attention toward the task is known to influence CMC amplitude (Kristeva-Feige et al., 2002; Johnson et al., 2011). The experiment was set up to limit the necessity of behavioral changes in the perturbed task: subjects perceived the tasks as easy, the tasks did not require a high level of precision, and for the visual feedback, the exerted torque was low-pass filtered. However, the sensation of the position perturbation may have had an alerting effect, increasing attention toward the task and contributing to the found increase in CMC.

Another possible contributing factor to the CMC amplitude in the perturbed task is the increased co-contraction, indicated by the increased EMG power in that task. Co-contraction may lead to increased CMC levels when the co-contraction results from an increased cortical motor drive, thus raising the signal-to-noise ratio in the EMG. However, Mima et al. (1999) found no change in CMC magnitude with weak to moderate (up to 60% MVC) contraction levels such as the contraction levels in our baseline and perturbed task. Furthermore, the peaks at the stimulus frequencies in the EMG power spectral densities suggest that the co-contraction originates at least partly from the spinal reflex loops (Matthews, 1993) and not from an increased cortical motor drive.

As a final note, the use of an external excitation to quantify connectivity via afferent sensory pathways is not uncommon in research and clinical practice. The response to

electrical stimulation of the median nerve at the wrist is widely used in clinical practice. Also, the response evoked by muscle stretch has been studied (Abbruzzese et al., 1985; MacKinnon et al., 2000; Seiss et al., 2002). MacKinnon et al. (2000) and Seiss et al. (2002) compared the location of sources generating the evoked potentials elicited electrically and by muscle stretch. Both studies reported that the response evoked by muscle stretch originated from sources in the motor cortex, while the electrically elicited evoked potentials originated from the sensory cortex. The muscle stretch evoked potential may therefore provide additional information about sensorimotor function compared to the electrically evoked potential which only represents sensory function. PCC may be viewed as a frequency domain equivalent of the muscle stretch evoked potential.

4.5 Conclusion

A limitation of CMC as a measure for connectivity during an isometric motor task is the absence of significant CMC in over 50% of the healthy population. The aim of this study was to develop a reliable measure of connectivity in motor control. Using an isotonic motor task with an added position perturbation, that excites the beta band, we elicited significant PCC in all subjects, while significant CMC was elicited in 86% of the subjects. PCC is a reliable measure for connectivity via the afferent pathways that was present in all healthy subjects.

Chapter 5

Poor motor function is associated with reduced sensory pathway integrity after stroke

S. Floor Campfens, Sarah B. Zandvliet, Carel G.M. Meskers, Alfred C. Schouten, Michel J.A.M. van Putten and Herman van der Kooij. *Submitted*

ABSTRACT

The possibility to regain motor function after stroke depends on the intactness of motor and sensory pathways. In this study, we evaluated afferent sensory pathway integrity after stroke with the coherence between cortical activity and a position perturbation (position-cortical coherence, PCC). Eleven subacute and two chronic stroke survivors participated in this study. Subjects performed a motor task with the affected and non-affected arm while continuous wrist position perturbations were applied. Cortical activity was measured using EEG. Position-cortical coherence (PCC) was calculated between position perturbation and EEG at the contralateral and ipsilateral sensorimotor area. Presence of PCC was quantified as the number of frequencies where PCC is larger than zero across the sensorimotor area.

All subjects showed significant contralateral PCC in affected and non-affected wrist tasks. Subacute stroke subjects with poor motor function had a reduced presence of contralateral PCC compared to subacute subjects with good motor function in the affected wrist tasks. Amplitude of significant PCC did not differ between subacute subjects with good and poor motor function.

Our results show that poor motor function is associated with reduced integrity of the sensory pathways in subacute stroke subjects. Position-cortical coherence provides an objective measure of sensory pathway integrity after stroke and may provide additional insight in mechanisms of recovery of motor function after stroke.

5.1 Introduction

Stroke is a leading cause of adult-onset disability in the western world. Rehabilitation after stroke has a strong emphasis on reducing motor impairment to improve the quality of life (Kwakkel et al., 2004). Within rehabilitation practice sensory impairment does not receive as much attention as motor impairment does, although it is known that sensory impairment is common after stroke (Connell et al., 2008) and related to motor impairment (Schabrun and Hillier, 2009).

The relation between sensory and motor impairment is unsurprising because motor control requires bidirectional interaction between cortex and periphery (Scott, 2004; Baker, 2007). Sensory feedback via the afferent pathways is necessary to generate proper motor commands which reach the muscles via the efferent pathways. Invasive recordings in monkeys showed that both sensory and motor cortical neural populations synchronise their oscillatory activity to peripheral signals (Williams et al., 2009). This synchronisation is thought to play an important role in the transmission of information within closed loop motor control (Varela et al., 2001; Fries, 2005; Baker, 2007). Coherence between cortical activity and muscle activity, corticomuscular coherence (CMC) (Conway et al., 1995; Halliday et al., 1998; Mima et al., 2000), is used as a measure of cortical sensorimotor integration during a motor task and depends on the integrity of both efferent and afferent pathways (Mima et al., 2001a; Pohja and Salenius, 2003; Riddle and Baker, 2005; Witham et al., 2011).

As a measure of both efferent and afferent pathway integrity, changes in CMC cannot be related to changes in sensory or motor processes. In addition, measurement of CMC requires a measurable EMG signal and thus is only possible in subjects that are able to voluntarily generate muscle force. When studying sensory and motor function after stroke with CMC, no information can be obtained from individuals without voluntary muscle control. Finally, a large downside for the potential clinical application of CMC is that it cannot be detected in all cases: even healthy subjects, with normal voluntary motor control, do not all present CMC (Ushiyama et al., 2011; Mendez-Balbuena et al., 2011; Campfens et al., 2013). The inter-individual difference in the presence of CMC reflect physiological inter-individual differences in the strength of the oscillatory corticomuscular coupling and are not the result of technical aspects such as the (mis-) placement of EEG electrodes (Ushiyama et al., 2011).

We previously showed that adding a small continuous position perturbation during an isotonic force tasks elicits CMC and coherence between the position perturbation and the EEG (Campfens et al., 2013).The perturbation acts as an external excitation signal, which excites the proprioceptive system (primarily the Golgi tendon organs and muscle spindles). As a result the coherence between perturbation and EEG, i.e. the position-cortical coherence (PCC), represents unidirectional connectivity across the afferent sensory pathways.

The aim of this study is to show the value of PCC as a measure of sensory pathway integrity after stroke. Based on the association between sensory and motor impairment after stroke, we hypothesize that stroke survivors with poor motor function have a lower amount of PCC. We make a distinction between presence of PCC (i.e. the number of frequencies and electrodes where PCC in significantly larger than zero) and the mean amplitude of significant PCC in order to assess which is the most informative on sensory pathway integrity.

In addition, we introduce a lateralisation index of PCC to evaluate the distribution of PCC between the lesioned and non-lesioned hemisphere. While in normal subjects PCC was localised at the contra-SM (Campfens et al., 2013), it has been shown with fMRI and EEG that stroke survivors recruit additional, ipsilateral areas during movement (Ward, 2003; Serrien et al., 2004). We therefore hypothesize that stroke survivors present PCC in both hemispheres.

5.2 Methods

Thirteen first ever hemispheric stroke survivors participated in the study (three women). Details of the subjects are presented in table 5.1. Eleven subjects were in the subacute phase (within six months post stroke). Within the group of subjects in the subacute phase a distinction was made based on the motor function as scored by the Brunström Fugl-Meyer upper extremity (FM-UE) scale (Fugl-Meyer et al., 1975). Six subacute subjects had a FM-UE of 55 points or higher (the maximum possible FM-UE score is 66 points), these subjects were considered to have a good motor function (group: good subacute). The other five subaute subjects had considerably lower FM-UE scores, these subjects all scored less than 20 points en were considered to have poor motor function (group: poor subacute). Two subjects were in the chronic phase (more than six months post stroke). These subjects had low FM-UE scores (4 points and 6 points) and were considered to have a poor motor function (group: poor chronic). Sensory function of subjects was evaluated using the Erasmus modification of the Nottingham sensory assessment (EmNSA) scale (Stolk-Hornsveld et al., 2006). This scale evaluates different test items across multiple locations on the upper extremity. Test items are: light touch, pressure, pin prick, sharp-blunt discrimination and proprioception. When a subject scored less than the maximal score for a test item on more than one location on the upper extremity the test item is marked as reduced.

All measurements were conducted in accordance with the *Declaration of Helsinki* and were approved by the Medical Ethics review Committee of the Leiden University Medical Center (Leiden, the Netherlands). All participants gave signed informed consent before the measurements.

Experimental setup

Subjects were seated next to a wrist manipulator (Moog Inc., Nieuw-Vennep, the Netherlands), see figure 5.1. The wrist manipulator (WM) is an actuated rotating device with a single degree of freedom that can impose flexion and extension movements on the wrist. The lower arm of the subject was strapped in an arm rest while the subject held the handle of the WM. The axis of rotation of the WM was aligned with the axis of rotation of the wrist. The lever of the WM is equipped with a force transducer to measure the torques exerted by the subject.

EEG was measured using 64 scalp electrodes, placed according to the 5% electrode system (Oostenveld and Praamstra, 2001) using a standard EEG cap with Ag/AgCl electrodes (actively shielded headcap by TMSi, Oldenzaal, the Netherlands). Electrode impedances were below $20k\Omega$ and signal quality was monitored on line. EMG was measured from the

Table 5.1: Overview of subjects.

subject code	age	group	lesion	days since lesion	FM-UE	AS wrist	sensory function (EmNSA)	task affected arm (*)
CVA001	77	good subacute	MCA left	106	65	0	normal	active
CVA002	58	good subacute	MCA right	36	63	0	normal	active
CVA003	58	poor chronic	thal. right	265	4	1	normal	relax
CVA004	62	poor subacute	MCA right	27	17	1	normal	relax
CVA005	59	poor subacute	MCA right	21	15	1+ (flex)	normal	relax
CVA006	77	good subacute	MCA right	18	56	0	normal	active
CVA007	58	poor subacute	MCA right	11	19	0	reduced	relax
CVA008	35	good subacute	MCA right	22	63	0	normal	active
CVA009	54	good subacute	MCA left	60	65	0	normal	active
CVA010	46	poor subacute	MCA right	34	6	1+ (flex)	normal	relax
CVA011	72	good subacute	MCA right	13	65	0	normal	active
CVA018	59	poor chronic	MCA right	5465	6	3	reduced	relax
CVA019	67	poor subacute	MCA right	121	6	4 (flex)	reduced	relax

MCA: Middle Cerebral Artery. thal: thalamus. FM-UE: Brunnström Fugl-Meyer upper extremity score (maximum 66 points). AS: Ashworth scale. EmNSA: Erasmus modification of the Nottingham Sensory Assessment scale. (*) all subjects performed the active task with the unaffected arm

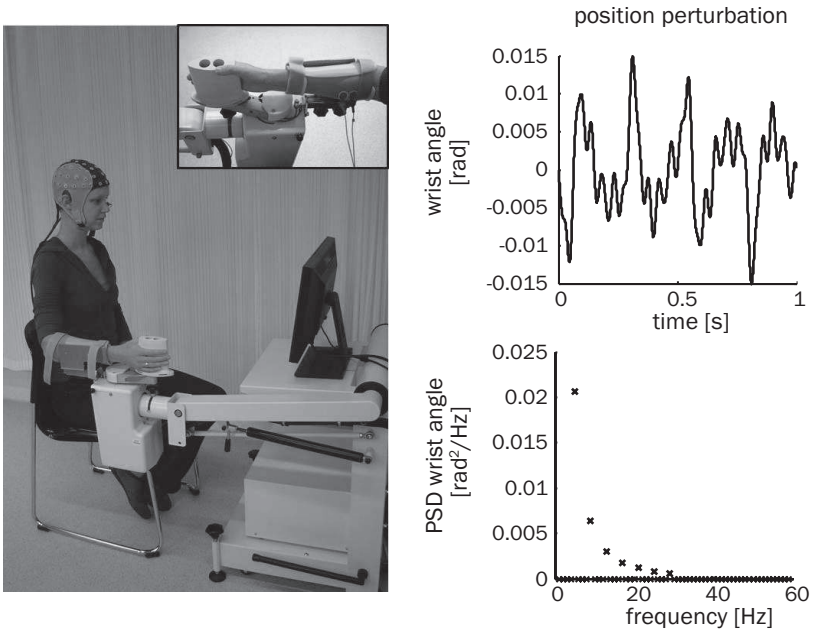

Figure 5.1: Overview of the experimental setup (left) and a 1s segment of the position perturbation (right). The subject holds the handle of the wrist manipulator (WM), and the lower arm is strapped in an arm rest using Velcro straps. To support the subject, visual feedback of exerted and target torque is provided on the display in front of the subject. The position perturbation is a sum of sines with a decreasing value of the power with frequency. PSD: power spectral density

flexor carpi radialis (EMG_{FCR}) using bipolar Ag/AgCl electrode pairs placed on the muscle belly. All physiological signals were sampled at 2048Hz (Refa system by TMSi, Oldenzaal, the Netherlands). The angle of the WM and the torque exerted on the lever were synchronously measured on a separate system at 2048Hz (Porti system by TMSi, Oldenzaal, the Netherlands) or via electrically isolated channels on the same amplifier as the physiological signals.

Protocol

Subjects performed a motor task with the affected arm and with the non-affected arm. In the active motor task subjects had to exert a constant wrist flexion torque against the handle of the WM, while the WM imposed a continuous wrist position perturbation. Subjects received visual feedback of the exerted and target torque via a display. Subjects were instructed to keep the exerted torque within a range of 1.8 ± 0.27Nm. For the visualisation, the exerted torque was filtered online (third order low-pass Butterworth, 2Hz to remove frequencies contained in the position perturbation.

All subjects performed the active motor task (active task) with the non-affected arm and attempted the active task with the affected arm. When a subject was unable to pro-

duce a steady wrist flexion torque, the subject held the handle of the WM without a wrist flexion contraction (relax task). Table 5.1 lists which task was performed with the affected arm for each subject. At least 8 trials of 40 seconds were performed at each side. The affected arm trials were performed first.

Six subjects (CVA005, CVA007, CVA008, CVA010, CVA011 and CVA019) were willing to perform both the active and relax task with the affected and/or non-affected arm to allow comparison between the active and relax task. Two subjects performed these extra trials in a separate measurement session. The subjects with poor motor function that performed the extra active motor tasks with the affected arm (CVA005, CVA007 and CVA019), performed the extra active task with a lower target torque. The target torque was set such that muscle activation was seen in the EMG signal. Even with a low target torque, these subjects were unable to maintain a stable contraction; during the trials subjects were motivated to keep attempting to exert torque and return to the target torque when the exerted torque decreased.

The position perturbation signal (figure 5.1, right side) consisted of a sum of sine waves (5, 9, 13, 17, 21, 25 and 29Hz). The perturbation signal had a period of 1s, and a peak-to-peak amplitude of 0.03rad (1.7°). The power of the sine waves decreased with frequency, giving the perturbation a flat velocity spectrum.

Data analysis

Recorded signals were processed off-line using MATLAB 2010b (the MathWorks, Inc., Natick, MA, USA). First, raw EEG signals were high pass filtered (1Hz, second order Butterworth filter applied with zero phase shift) to remove baseline drift. Channels containing artefacts due to bad electrode contact were removed from the common average reference. EEG signals were low pass filtered (70Hz, second order Butterworth applied with zero phase shift) and resampled to 1024Hz.

All signals were segmented in 1s segments (1024 samples) - the period of the perturbation - with 75% overlap between segments. Segments were visually inspected and segments that contained eye blinks or muscle activity were removed. The 50Hz component was removed from each segment using the discrete Fourier transform (algorithm taken from Fieldtrip Toolbox for MATLAB; Oostenveld et al., 2011). EEG data was then referenced to a nearest neighbor Laplacian derivation.

Subsequent coherence analysis was performed on EEG channels overlying the left and right sensorimotor areas (SM). The left SM consists of FC1, FC3, FC5, C1, C3, C5, CP1, CP3 and CP5, the right SM consists of the equivalent electrodes on the right hemisphere.

Estimation of PCC

All segments were transformed to the frequency domain using the fast Fourier transform. The power spectral density (PSD, $\Phi_{xx}(f)$) and cross spectral density (CSD, $\Phi_{xy}(f)$) were estimated using

$$\Phi_{xx}(f) = \frac{1}{N}\sum_{i=1}^{N} X_i^*(f) \cdot X_i(f) \tag{5.1}$$

and

$$\Phi_{xy}(f) = \frac{1}{N}\sum_{i=1}^{N} X_i^*(f) \cdot Y_i(f) \tag{5.2}$$

respectively, where $X_i(f)$ and $Y_i(f)$ are the Fourier coefficients at frequency f estimated from the i^{th} data segment. The asterisk indicates the complex conjugate, and N is the total number of segments.

EEG channels were excluded from coherence analysis when the mean power in the frequency band between 25 and 49Hz was larger than the mean power between 5 and 15Hz. Channels with this power distribution were presumed to reflect mostly EMG activity. This method for marking channels with EMG activity is based on the method applied by Severens et al. (2012) to select EEG and EMG components in a blind source separation method. Presence of EMG activity obscures the detection of PCC as it severely decreases signal to noise ratio.

The (magnitude squared) coherence ($C_{xy}(f)$) between signals was calculated according to:

$$C_{xy}(f) = \frac{|\Phi_{xy}(f)|^2}{\Phi_{xx}(f)\Phi_{yy}(f)}. \tag{5.3}$$

Position-cortical coherence (PCC) was calculated between the position perturbation signal and each EEG channel and was only evaluated at the frequencies contained in the perturbation signal. Significance of coherence values was determined using the approximation of the confidence limit (CL) by Bortel and Sovka (2007). The confidence level was set to 0.99 ($\alpha = 0.01$).

Presence of PCC across the sensorimotor area contralateral to the wrist perturbation (contra-SM) was evaluated by summing the number of frequencies where the PCC exceeds the 99% CI per electrode and summing across the contra-SM. This number was expressed as a percentage of the total number of frequency bins on the contra-SM (i.e. number of stimulus frequencies times the number of electrodes in the contra-SM). Amplitude of significant PCC was evaluated by the mean significant PCC over the contra-SM.

Lateralisation of PCC was quantified by the lateralisation index (L):

$$L = \log_{10}(PCC_{\text{contra-SM}}) - \log_{10}(PCC_{\text{ipsi-SM}}) \tag{5.4}$$

where $\text{PCC}_{\text{contra-SM}}$ and $\text{PCC}_{\text{ipsi-SM}}$ are the mean PCC amplitudes over all frequencies and all electrodes in the contra-SM and ipsilateral SM (ipsi-SM) respectively. Note that in the lateralisation index no distinction is made between presence and amplitude of significant PCC. When $L > 0$ the PCC is more lateralised towards the contra-SM. $L < 0$ indicates PCC is more lateralised towards the ipsi-SM.

The non-parametric Wilcoxon rank-sum test was used to compare presence and amplitude of significant PCC at the contra-SM and the lateralisation index between the good subacute and poor subacute subjects. Paired t-tests were used to compare contra-SM PCC and lateralisation index in response to affected wrist perturbation and non-affected wrist perturbation within one subject. Amplitude of significant PCC was $\log_{10}$ transformed prior to statistical analysis.

5.3 Results

All good subacute subjects had normal sensory function on all test items according to the EmNSA scale. In the poor subacute group, CVA007 had a reduced sensory function affected arm at the time of the first measurement session (11 days post stroke). CVA007 had a reduced tactile sensation in the hand and fingers and a reduced ability to discriminate between sharp and blunt tactile stimuli in the whole arm including hand and fingers. In addition, CVA0019 had a reduced sensory function in the affected arm: a reduced ability to discriminate between sharp and blunt stimuli across the whole arm including hand and fingers and a reduced proprioceptive sense in the fingers, wrist and elbow. In the poor chronic group CVA0018 had severely reduced sensory function in the affected arm: there was no sensation of any tactile stimuli across the whole arm including hand and fingers. She also had a reduced proprioceptive function across the arm and was unable to sense movement of the fingers, wrist and elbow.

In all eleven subjects, EEG on one or more electrodes in the left and right SM were excluded due to poor signal quality. In nine subjects this concerned one or more of the most temporal electrodes (FC5, FC6, C5, C6, CP5, CP6). In two subjects also electrodes other than the most temporal ones were excluded. For CVA006 electrodes FC3, C3 and CP3 were excluded in addition to the most temporal electrodes (FC5, FC6, C5, C6, CP5 and CP6). For CVA007 electrodes C3 and FC3 were excluded in addition to the most temporal electrodes (FC5, FC6, C5 and C6).

Presence and amplitude of significant PCC in the contralateral sensorimotor area.

All subjects presented significant PCC at the contra-SM on at least three stimulus frequencies in the affected wrist task and in the non-affected wrist task (see figure 5.2). Five of the six subjects in the good subacute group had significant contra-SM PCC during the affected wrist task on all stimulus frequencies, while none of the subjects in the poor subacute group had significant contra-SM PCC on all stimulus frequencies during the affected wrist task. The poor subacute subjects all presented significant PCC on the highest stimulus frequencies (17, 21, 25 and 19Hz) in the affected wrist task. In the poor chronic group, one of the subjects had contra-SM PCC on all stimulus frequencies during both the affected and non-affected wrist tasks. The other poor chronic subject, who also had severe sensory deficits, had significant PCC on only three stimulus frequencies in the affected wrist task and on five stimulus frequencies in the non-affected wrist task.

The presence of significant PCC at the contra-SM varied between affected and non-affected wrist tasks and between subjects (figure 5.3). Poor subacute subjects tended to have a lower presence of contra-SM PCC in the affected wrist task compared to the non-affected wrist task but the difference did not reach statistical significance. The difference in the presence of contra-SM PCC in the affected wrist tasks between poor and good subacute subjects was significant (Wilcoxon rank-sum test $p < 0.01$). The average difference between the subacute subject groups was 31%.

The poor chronic subject with severe sensory deficits (CVA018) showed significant PCC at the contra-SM both during the affected wrist task and the non-affected wrist task. During both tasks, the percentage of frequency bins with significant PCC at the contra-SM was

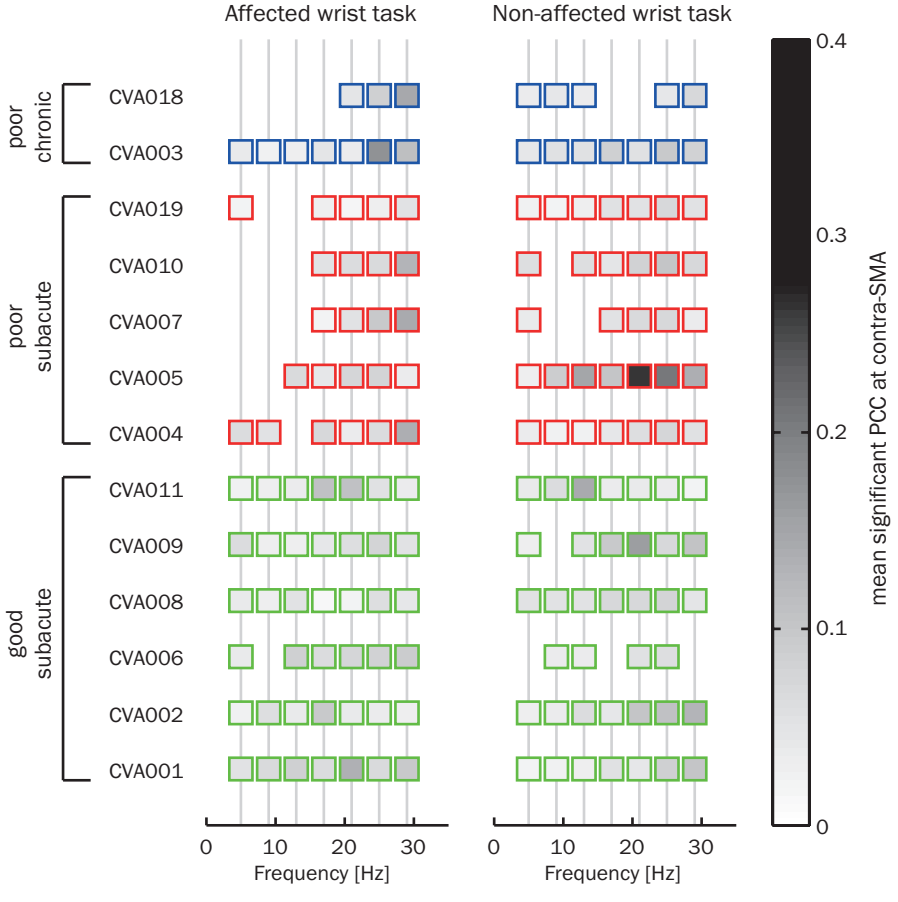

Figure 5.2: Mean significant PCC at the contra-SM per stimulus frequency. *Left*: affected wrist task, *right*: non-affected wrist task. Gray vertical lines indicate the stimulus frequencies, a square indicates that there was significant PCC at at least one electrode in the contra-SM.

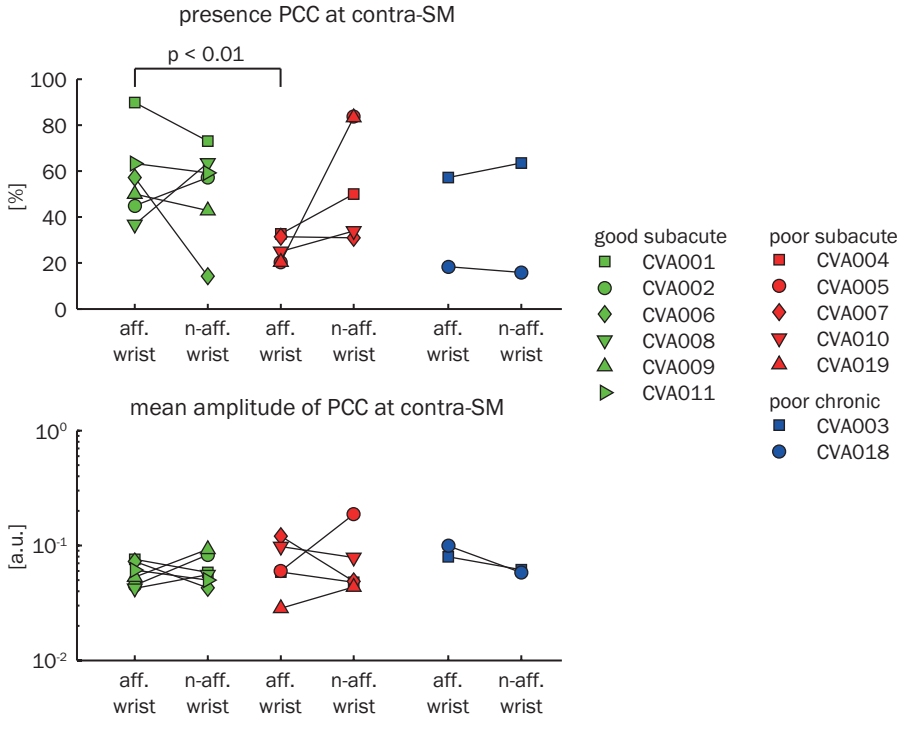

Figure 5.3: Presence and amplitude of significant PCC at the contra-SM in the affected wrist task (aff. wrist) and non-affected task (n-aff. wrist). *Upper panel*: presence of PCC expressed as a percentage of the total number of frequency bins on the contra-SM. *Lower panel*: mean significant PCC over the contra-SM and all stimulus frequencies in arbitrary units (a.u.).

low compared to the other subjects.

The mean significant amplitude of PCC on the contra-SM varied between subjects and between affected and non-affected wrist tasks (figure 5.3). There was no significant difference in mean PCC amplitude at contra-SM between good and poor subacute subjects, not in the affected wrist task and not in the non-affected wrist task. Neither was there a significant difference between affected and non-affected wrist task within subjects. In the poor chronic subjects, the mean significant amplitude of contra-SM PCC in the affected and non-affected wrist tasks was in the same range as in the subacute subjects.

Comparison of PCC in active and relaxed tasks

The difference in tasks performed with the affected wrist by the subacute subjects with poor function and those with good motor function (relax and active motor tasks respectively) could be a confounding factor. Therefore, five subacute subjects performed an extra active or relax task with the affected and/or non-affected wrist to enable comparison of the presence and mean significant amplitude of contra-SM PCC between the active and relax tasks. Results are summarized in figure 5.4. Presence of contra-SM PCC in the af-

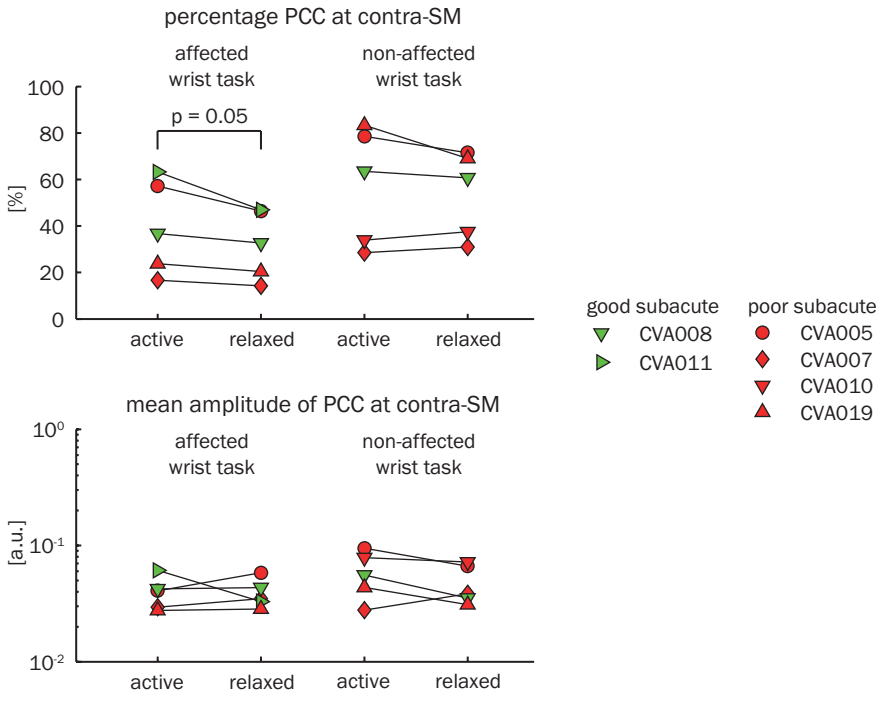

Figure 5.4: Comparison of presence and magnitude of significant PCC between an active and a relaxed task. *Upper panel*: presence of PCC expressed as a percentage of the total number of frequency bins across the contra-SM. *Lower panel*: mean significant PCC over the contra-SM in arbitrary units (a.u.). CVA010 performed both tasks only with the non-affected wrist, CVA011 performed both tasks only with the affected wrist.

fected wrist tasks tended to be lower in the relax task compared to the active task. This difference was on the limit of significance (paired t-test $p = 0.05$). The average difference in presence of contra-SM PCC was 7.4%. In the non-affected wrist tasks the difference was not significant. There were no significant differences in mean significant contra-SM PCC amplitude between active and relaxed tasks.

Lateralisation of PCC

In twelve subjects PCC was significantly larger than zero on at least one electrode on the ipsi-SM during both the affected and the non-affected wrist task. In the non-affected wrist task, the lateralisation index was larger than zero in all subacute subjects, showing that PCC was lateralised more towards the contra-SM (see figure 5.5).

In the poor subacute group the lateralisation index was significantly lower during the affected wrist task compared to the non-affected wrist task (paired t-test: $p = 0.03$). This indicates that in the poor subacute group, PCC is distributed more evenly between the lesioned and non-lesioned hemisphere during the affected wrist task while during the non-

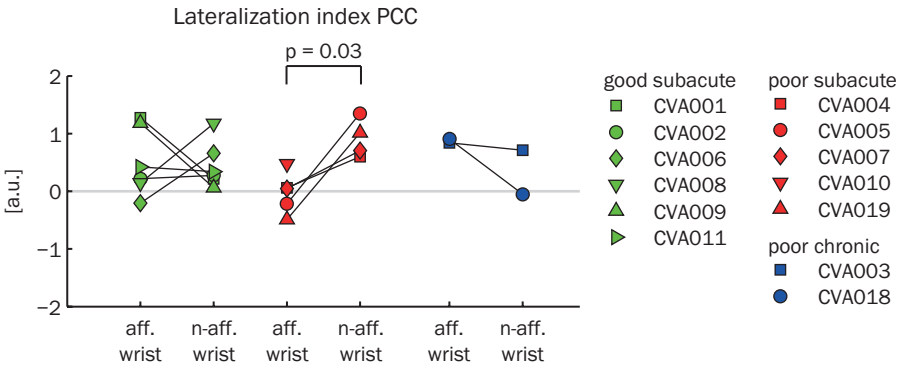

Figure 5.5: Lateralisation index for affected and non-affected wrist tasks (aff. wrist and n-aff. wrist respectively) in arbitrary units (a.u.). $L > 0$ indicates that PCC is more lateralised towards the contra-SM compared to the ipsi-SM. $L < 0$ indicates PCC is more lateralised towards the ipsi-SM.

affected wrist task PCC is more lateralised to the (non-lesioned) contra-SM.

Three subacute subjects (CVA006, CVA005 and CVA019) had a negative lateralisation index during the affected wrist task. This indicates that the PCC is more lateralised towards the ipsi-SM. In CVA018 (chronic stage) a negative lareralisation index was found during the non-affected wrist task.

5.4 Discussion

In this study, we evaluated position-cortical coherence (PCC) in eleven subacute and two chronic stroke subjects. Position-cortical coherence is the coherence between a joint position perturbation and the EEG during a motor task and is a measure of afferent pathway integrity (Campfens et al., 2013). All stroke subjects presented PCC at the contralateral sensorimotor area (contra-SM) during an affected and non-affected wrist angle perturbation. Presence of contra-SM PCC in during an affected wrist perturbation was lower in poor motor function subacute stroke subjects than in good motor function subacute stroke subjects. The presence of contra-SM PCC differed between subacute subjects with good and poor motor function, the amplitude of significant contra-SM PCC did not differ between these group. This implies that when contra-SM PCC is significantly larger than zero, the amplitude does not contain extra information. The reduced presence of PCC in the ipsi-lesional hemisphere of poor function subacute subjects shows that these subjects not only have poor functioning efferent motor pathways but a reduced integrity of their afferent sensory pathways as well. This agrees with the notion that motor control takes place in a closed loop where sensory feedback is crucial for generating proper motor commands.

From the reduced presence of PCC it can not directly be determined whether subacute subjects with poor motor function showed contra-SM PCC on less frequencies or on less electrodes. However, none of the subacute poor function subjects presented significant PCC on the lowest stimulus frequencies in the affected wrist task (figure 5.2). This indi-

cates that a reduced number of frequencies where PCC is present is the main contributing factor to the reduced presence of PCC in the poor function subacute subjects.

In the population of subacute stroke subjects included in this study, the subjects with good and poor motor function had very distinct ranges of FM-UE scores. Due to this sharp distinction we cannot correlate the PCC measures with the FM-UE score. In a larger population of stroke subjects, that exhibit a more continuous distribution of FM-UE scores, it would be possible to perform correlation analysis on presence of contra-SM PCC and motor function score to find out whether there is a continuous relation between motor function and afferent pathway integrity.

Contralateral SM PCC during affected wrist tasks was even found in subjects that had sensory deficits according to the EmNSA (Stolk-Hornsveld et al., 2006), even in the subject with very poor sensory function according to the EmNSA (CVA018). This chronic subject had no tactile sensation across the affected hand and arm and did not sense wrist angle. However, contra-SM PCC was detected when the affected wrist was perturbed. The presence of PCC in this subject shows that proprioceptive sensory feedback does arrive at the sensorimotor cortex, indicating that the afferent pathways are to some extend intact. However, apparently the arrival of sensory feedback at the cortex does not lead to a conscious sensation of the wrist angle. The subject is unable to reproduce the affected wrist angle with the healthy wrist, which is required for a normal score in the EmNSA. Clinical scaling of sensory function has been shown to be unreliable (Lincoln et al., 1991). Although progress has been made to obtain more reliable clinical scoring of sensory function (Stolk-Hornsveld et al., 2006), especially impairment of proprioception is often overlooked (Dukelow et al., 2010). Position-cortical coherence could serve as an objective measure of sensory pathway integrity that reveals whether there still is sensory information arriving at the cortex.

Subjects with poor motor function were not able to generate a steady wrist flexion torque, these subjects performed a relax task. Also during the relax tasks subjects showed significant contra-SM PCC. In the subjects that performed additional active and relax tasks for comparison, the presence of contra-SM PCC did not differ between active and relax tasks performed with the non-affected wrist. This implies that the cortical response to the position perturbation is similar during active and relax tasks. However, when performed with the affected wrist presence of PCC was 7% smaller during a relax task. This difference between active and relax tasks is not sufficient to explain the difference in presence of PCC found between the subjects with good and poor motor function (30%). Although the difference between active and relax tasks is small or absent, we advise to let subjects relax in future studies to avoid possible bias due to differences in ability to perform motor tasks.

The frequency dependent likelihood of finding significant contra-SM PCC during the affected wrist task in the poor function subacute group indicates that there is a frequency dependency of the signal to noise ratio in the ipsilesional EEG. Either the EEG contains more contributions of sources other than the position perturbation at the lowest stimulus frequencies (increased noise at lowest stimulus frequencies) or the contribution of the position perturbation to the EEG is higher at the highest stimulus frequencies (increased signal at the highest stimulus frequencies). The perturbation signal was designed such that it had a flat velocity spectrum. As a result the position/velocity sensitive muscle spindles were excited with decreasing/equal power at each frequency. Higher sensitivity of muscle spindles to higher velocities or excitation of Golgi tendon organs could still result

in a higher output of the sensory pathways at the higher stimulus frequencies, thus increasing the likelihood of finding PCC at these frequencies. An alternative explanation for an increased signal at the highest stimulus frequencies could be that these stimulus frequencies are transmitted more efficiently along the afferent pathways. The higher stimulus frequencies lie in the beta band ($15-30$Hz). During an isotonic and isometric motor task, coherence between EEG and EMG is typically found in the beta band, indicating that oscillations in this frequency band are already being transmitted along the afferent pathways.

Using the lateralization index of PCC we found that three of the eleven subacute subjects (two poor function, one good function) had PCC predominantly localized in the ipsi-SM during the affected wrist task. It is known from several studies that after stroke there can be a disbalance between the lesioned and the non-lesioned hemisphere. This results in abnormal activation of the ipsilateral sensorimotor cortex during motor tasks with the affected hand and is especially seen in stroke survivors with poor recovery of motor function (Ward, 2003; Serrien et al., 2004). During motor tasks with the affected side, the increased activity of the ipsilateral sensorimotor cortex is seen as a sign of increased motor output of the ipsilateral sensorimotor cortex. Our results in lateralisation of PCC indicate that sensory input from the affected wrist elicits response in the ipsilateral sensorimotor cortex and that this response can even be stronger than in the contralateral sensorimotor cortex. Increased activation of the ipsilateral sensorimotor cortex can thus also indicate increased sensory input to this area during an affected arm motor task. Further research is required to establish whether this relates to recovery of motor function.

About two-third of the stroke survivors with initial hemiplegia does not regain dexterity and remains impaired despite rehabilitation therapy (Kwakkel et al., 2003; Dobkin, 2005). The ability to extend the fingers and abduct the shoulder at 72 hours post stroke gives a strong indication of an individual's ability to recover motor function (Nijland et al., 2010). Nevertheless, 25% of the stroke survivors with an initial poor prognosis does regain dexterity. It is important to identify individuals in this so-called crossover group since they will most likely benefit most from early applied intensive rehabilitation training. So far, no techniques or measures have been found that enable the identification of individuals in this crossover group early after stroke. In a larger longitudinal study design it should be evaluated whether PCC, as an objective measure of sensory pathway integrity provides additional information that allows separation between the good prognosis, poor prognosis and crossover group.

5.5 Conclusion

This study shows that subacute and chronic stroke subjects present PCC, indicating that afferent sensory information arrives at the cortex. Position-cortical coherence can even be detected in subjects with very poor motor function, who are unable to generate voluntary force. In subacute subjects, presence of PCC on the sensorimotor area contralateral to the affected wrist is lower in poor function subjects compared to good function subjects. This shows that afferent pathways integrity and sensorimotor integration are affected in stroke survivors with poor motor function. In addition, in subacute subject with poor motor function PCC is distributed more evenly between the lesioned and non-lesioned hemi-

sphere during affected wrist perturbations that during non-affected wrist perturbations. Position-cortical coherence provides an objective measure of sensory pathway integrity after stroke and may provide additional insight in mechanisms of recovery of motor function after stroke.

5

Chapter 6

Stretch evoked potentials in normal subjects and after stroke: a potential marker for proprioceptive sensory function

S. Floor Campfens, Carel G.M. Meskers, Alfred C. Schouten, Michel J.A.M. van Putten and Herman van der Kooij. *Submitted*

ABSTRACT

Sensory feedback is of vital importance in motor control, yet rarely assessed in diseases with impaired motor function like stroke. Muscle stretch evoked potentials (StrEPs) may serve as a measure of cortical sensorimotor activation in response to proprioceptive input. The aim of this study was 1) to determine early and late features of the StrEP and 2) to explore whether StrEP waveform and features can be measured after stroke.

Consistency of StrEP waveforms and features was evaluated in 22 normal subjects. StrEP features and similarity between hemispheres were evaluated in eight subacute stroke subjects.

StrEPs of normal subjects had a consistent shape across conditions and sessions (mean cross correlation waveforms > 0.75). Stroke subjects showed heterogeneous StrEP waveforms. Stroke subjects presented a normal early peak (40ms after movement onset) but later peaks had abnormal amplitudes and latencies. No significant differences between stroke subjects with good and poor motor function were found ($p > 0.14$).

With the consistent responses of normal subjects the StrEP meets a prerequisite for potential clinical value. Recording of StrEPs is feasible even in subacute stroke survivors with poor motor function. How StrEP features relate to clinical phenotypes and recovery needs further investigation.

6.1 Introduction

Stroke is a leading cause of adult-onset disability in the western world. Rehabilitation after stroke aims at reducing motor impairment via restitution - actual return of motor function - and compensation - the emergence of new movement patterns (Kwakkel et al., 2004). Although proprioception, stereognosis (i.e. the ability to recognize objects without visual input) and tactile sensation are commonly impaired after stroke (Connell et al., 2008), assessment and training of sensory modalities is generally not part of regular therapy. This is surprising given that voluntary motor control takes place in a closed loop where sensory feedback is essential (Scott, 2004). Indeed, there is evidence that training of sensory function reduces impairment after stroke (Schabrun and Hillier, 2009).

Integrity of the sensory pathways can be assessed by measuring the cortical response, by means of electroencephalography (EEG) or magnetoencephalography (MEG), to an external stimulus. The electrically elicited somatosensory evoked potential (SSEP) is used in clinical practice to evaluate whether sensory input is processed by the brain, for example in comatose patients or patients unable to communicate (van Putten, 2012). The early peaks of an evoked potential (within the first 30 or 40ms after the stimulus in case of the median nerve SSEP) represent the arrival of sensory information at the cortex, indicating the integrity of the afferent sensory pathways. Later peaks are associated with processing of the sensory input (Desmedt and Tomberg, 1989; Josiassen et al., 1990).

Abnormal SSEP waveforms were found in patients after stroke, indicating the presence of sensory deficits (Tsumoto et al., 1973). Presence, latency and amplitude of the early peaks of the SSEP (N20 and N20-P25) were found to normalize during motor recovery after stroke (Kato et al., 1991; Al-Rawi et al., 2009). Some studies even found the early peaks of the SSEP to be of predictive value regarding motor recovery after stroke; absence of the SSEP early after stroke is associated with poor motor recovery (Feys et al., 2000; Tzvetanov and Rousseff, 2003).

Electrical stimulation of the median nerve provides a mixed artificial activation of sensory fibres, mainly related to tactile sensation (Allison et al., 1991), which does not necessarily reflect sensory feedback relevant for motor control. Real joint movement and muscle stretch also activate sensory fibers. This elicits a cortical response which can resemble sensory feedback and subsequent sensorimotor integration in movement control more closely, with a large contribution of muscle spindle afferent feedback (Starr et al., 1981; Abbruzzese et al., 1985; MacKinnon et al., 2000; Seiss et al., 2002; Mima et al., 1996). It was shown that such a muscle stretch evoked potential (StrEP) has a different shape and involves activation of other cortical areas compared to the electrical SSEP (MacKinnon et al., 2000; Seiss et al., 2002). More specifically, the sources generating the first peaks of the StrEP are positioned a few centimetres anterior of the sources of the first peak (N20) of the electrical SSEP. Authors concluded that the StrEP is generated, at least in part, by the primary motor cortex (MacKinnon et al., 2000; Seiss et al., 2002), while the electrical SSEP is generated by the primary sensory cortex (Allison et al., 1991).

Prevalence of proprioceptive deficits was found to exceed that of tactile deficits after stroke (Connell et al., 2008). Muscle stretch addresses the afferent volley involved in motor control, mainly proprioception, and activates cortical motor areas. Muscle stretch may therefore be an attractive way of assessing integration of sensory feedback in motor function during motor recovery after stroke. As most of the motor function recovery happens

within the first weeks after stroke (Kwakkel et al., 2004), assessing proprioceptive function objectively in the subacute phase can provide additional insight in the mechanisms of recovery of closed-loop motor control. However, before the potential clinical value of the StrEP can be established, invariant features of the StrEP need to be determined in a normal population. Furthermore, the feasibility of estimating StrEPs in the subacute phase after stroke should be demonstrated.

The aim of the current study is two-fold: first, we identify early and late components of the StrEP and their variability across stretch amplitudes and measurement sessions in a group of normal subjects. Consistent presence of the StrEP in normal subjects is a prerequisite for potential clinical value of the StrEP in patients; when the StrEP cannot be elicited consistently in normal subjects, absence or alteration of the StrEP cannot be related to pathology. Secondly, we explore StrEPs in a small group of subacute stroke survivors to evaluate whether the StrEPs and StrEP components can be measured in stroke survivors in the acute phase.

6.2 Methods

Subjects

Twenty-two healthy volunteers (nine women, mean age 27 years, age range 23-35, four subjects were left-hand dominant) participated in this study as normal subjects. The dominant hand was determined using the Dutch handedness questionnaire (van Strien, 1992).

Eight first ever hemispheric stroke patients participated in this study (one woman, mean age 57 years, age range 35-77). All stroke subjects were measured within 6 months post stroke (range 13 - 135 days post stroke). Stroke subject details are presented in table 6.1. Lesion location and class were determined based on clinical signs and CT images. In the Netherlands, the use of MRI imaging is not part of standard clinical care for this patient group. All stroke subjects had normal wrist proprioceptive function according to the Erasmus MC Modifications of the (revised) Nottingham Sensory Assessment (Stolk-Hornsveld et al., 2006). Within the group of stroke subjects a distinction was made between subjects with good and poor motor function based on the Brunström Fugl-Meyer (FM) upper extremity score (Fugl-Meyer et al., 1975). Five stroke subjects had a FM-UE of 63 points or higher (maximum FM-UE score is 66) these subjects were considered to have good motor function. The remaining three stroke subjects had considerably lower FM-UE scores. These subjects scored less than 30 points and were considered to have poor motor function.

All measurements were conducted in accordance with the *Declaration of Helsinki*. The measurements with the normal subjects were performed at the University of Twente and were approved by the Medical Ethics Review Committee of the Medisch Spectrum Twente (Enschede, the Netherlands). Measurements with the stroke subjects were performed at the Leiden University Medical Centre and were approved by the Medical Ethics Review Committee of the Leiden University Medical Centre (Leiden, the Netherlands). All subjects gave signed informed consent before the measurements.

Table 6.1: Overview of stroke subjects.

subject code	age	lesion	days since lesion	FM-UE	AS wrist	task
CVA001	77	MCA left, subcortical	106	65	0	active
CVA002	58	MCA right, subcortical	36	63	0	active
CVA005	59	MCA right, subcortical	135	26	1+ (flex)	relaxed
CVA007	58	MCA right, cortical	81	28	1+ (flex)	relaxed
CVA008	35	MCA right, cortical	22	63	0	relaxed
CVA009	54	MCA left, subcortical	60	65	0	relaxed
CVA010	46	MCA right, cortical	34	6	1+ (flex)	relaxed
CVA011	72	MCA right, cortical	13	65	0	relaxed

Lesion was determined based on CT-imaging and clinical signs. MCA: Middle Cerebral Artery. Motor function is evaluated using the Brunnström Fugl-Meyer test for the upper extremity (FM-UE, maximal score: 66) (Fugl-Meyer et al., 1975). Spasticity at the wrist is assessed using the modified Ashworth scale (AS) (Bohannon and Smith, 1987).

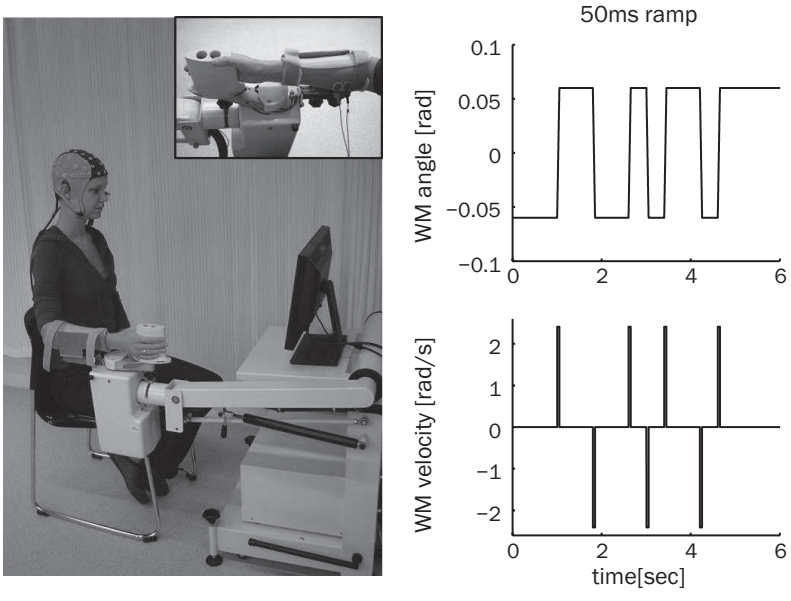

Figure 6.1: Left: overview of the experimental setup. The subject holds the lever of the WM and the lower arm is strapped in an arm rest using Velcro straps. To support the subject, visual feedback of the target torque and the exerted torque (2Hz low-pass filtered with third-order Butterworth filter) are provided on the display in front of the subject. EEG is measured using a head cap (64 channels), bipolar EMG is measured from the flexor carpi radialis (FCR). The handle of the WM moves according to a block shaped profile, imposing fast flexion and extension ramp movements on the wrist. Right: portion of the block shaped position perturbation signal with a 50ms stretch, position profile and velocity profile. During the transition between the two positions the handle has a constant velocity.

Experimental setup

Subjects were seated next to a wrist manipulator (Moog Inc., Nieuw-Vennep, the Netherlands), see figure 6.1. The wrist manipulator (WM) is an actuated rotating device with a single degree of freedom that can exert flexion and extension perturbations to the wrist joint. The lower arm of the subject was strapped in an arm rest while the subject held the handle of the WM. The axis of rotation of the WM was aligned with the axis of rotation of the wrist. The lever of the WM is equipped with a force transducer to measure the torques exerted by the subject.

EEG was measured using 64 scalp electrodes, placed according to the 5% electrode system (Oostenveld and Praamstra, 2001) using a standard EEG cap with Ag/AgCl electrodes (measurements at University of Twente (normal subjects): WaveGuard cap by ANT, Enschede, the Netherlands. Measurements at Leiden University Medical Centre (stroke subjects): actively shielded headcap by TMSi, Oldenzaal, the Netherlands). Electrode impedances were below 20kOhm and signal quality was monitored on line. The EEG was measured against common average reference. The electromyogram (EMG) was measured from the flexor carpi radialis (EMG_{FCR}) and the extensor carpi radialis (EMG_{ECR}) using

bipolar Ag/AgCl electrode pairs placed on the muscle belly. In the normal subjects, the vertical electro-oculogram (EOG) was measured to monitor eye blinks, in the stroke subjects the frontal EEG channels (Fp1, Fpz and Fp2) were used to detect eye blinks. All physiological signals were sampled at 2048Hz (Refa system by TMSi, Oldenzaal, the Netherlands). The angle of the WM and the torque exerted on the lever were synchronously measured on a separate system at 2048Hz (Porti system by TMSi, Oldenzaal, the Netherlands) or via optical isolation modules on the same amplifier as the physiological signal.

Protocol

Normal subjects

Normal subjects exerted a constant wrist flexion torque on the handle of the WM, while the WM imposed block shaped angular position perturbations. Visual feedback of the exerted and the target torque were presented via a display. Subjects were instructed to keep the exerted torque within a range of 1.8 ± 0.27Nm. Because the maximum torque the WM could deliver was limited for safety reasons, maximal voluntary contraction torque could not be determined per subject. All subjects reported that this target torque could easily be maintained. For the visualization the exerted torque was filtered on line (third order low pass Butterworth, 2Hz).

The block shaped angular position perturbations imposed alternating flexion and extension ramp-and-hold movements on the wrist. During the ramp movement the velocity of the WM was 2.4rad/s. The interval between ramp movements is chosen pseudo randomly to ensure an unpredictable perturbation for the subject and was an integer multiple of 400ms. Combinations of ramp amplitudes and task instructions resulted in three conditions:

1. active 50ms ramp: stretch duration of 50ms during the isotonic force task (amplitude = 0.12rad).

2. active 25ms ramp: stretch duration of 25ms during the isotonic force task (amplitude = 0.06rad).

3. relaxed 50ms ramp: stretch duration of 50ms without an active task, subjects held the handle of the WM without applying a force.

These conditions were part of a larger protocol which also included other types of tasks (Campfens et al., 2013). Subjects were given sufficient rest between parts of the protocol to prevent interference. To restrict the duration of the total protocol, not all subjects performed all tasks: all twenty-two normal subjects performed the two active conditions; ten normal subjects performed the relaxed condition as an additional task. Furthermore, nine subjects performed the protocol in a second measurement session. The two measurement sessions were separated by at least one week (range: 7-39 days, median: 16 days). For five subjects the second measurement included the relaxed 50ms ramp task.

In all conditions, five 60s trials were recorded with sufficient rest time to prevent fatigue. The order of the conditions was fixed and performed as indicated above. Subjects performed an active 50ms ramp trial to practice which was not included in the analysis.

Stroke subjects

Based on the experience from the normal subjects, the protocol for the stroke subjects was slightly adapted. First, the block shaped angular position perturbation was shortened and adapted. Some of the normal subjects indicated that the perturbation signal with the 50ms ramps felt aggressive due to the large amplitude of the stretch and the high repetition rate. The ramp velocity was not changed. The position perturbation used with the stroke subjects had a ramp duration of 30ms with a constant speed of 2.4rad/s (amplitude = 0.072rad). The minimal time between ramps was 500ms. The same angular position perturbation was used in the measurements of all stroke subjects. Second, all stroke subjects performed the task both with the wrist at the affected side and at the unaffected side. At each side, at least 8 trials of 30s were performed. The affected side was measured first to ensure that data was always collected from the affected side even when the complete protocol would be too long for the stroke subject to finish. Third and finally, after performing the measurements of the first two stroke subjects the task instruction was changed. The active tasks were challenging, also for the stroke subjects with good motor function. Two stroke subjects performed the active isotonic wrist flexion task, the other six stroke subjects were relaxed while they held the handle of the WM that moved according to the position perturbation. Table 6.1 indicates which stroke subjects performed the active and which the relaxed task. The same task was performed at the affected and the unaffected side.

Data analysis

Recorded signals were processed off-line using MATLAB 7.11 (the MathWorks, Inc., Natick, MA, USA). Recorded EEG and EMG was high pass filtered (1Hz, fourth order Butterworth filter applied with zero phase shift) to remove drift. EMG was rectified and subsequently low pass filtered (80Hz, fourth order Butterworth filter applied with zero phase shift). All signals were segmented into epochs time locked to the onset of movement of the WM: from 200ms before movement onset till 400ms post movement onset.

Segments were visually inspected and segments that contained eye blinks or muscle activity in the EEG were removed. Segments from relaxed task conditions were excluded when EMG activity was seen prior to movement onset. The mean EMG_{FCR} stretch response was calculated by averaging the EMG_{FCR} over all remaining extension movements.

EEG channels in remaining segments were further filtered using a low pass filter (70Hz, fourth order Butterworth filter applied in the forward direction) and the 50Hz component was removed from each segment using the discrete Fourier transform (Oostenveld et al., 2011). Finally, spatial selectivity of the EEG was enhanced by transforming to a nearest neighbor Laplacian derivation, i.e. each EEG channel was referenced to the mean of the four neighboring channels.

Before calculating the mean StrEP the baseline of each segment was corrected by subtracting the average potential in the 50ms before movement onset from the waveform. At each electrode the mean StrEP was obtained by averaging the baseline corrected waveforms over all segments. Note that the averaging includes both the flexion and the extension movements. This procedure enhances the signal to noise ration in the estimated StrEPs and has previously been applied (Seiss et al., 2002). We confirmed the similarity between StrEP waveforms elicited by flexion and extension movement in preliminary anal-

ysis (see figure 6.2). When the task was performed with the left hand, the EEG channels were mirrored around the midline such that in visualization the hemisphere contralateral to the movement is always the left side.

Two electrode positions were chosen for further evaluation of the StrEP waveform. The waveform at electrode C3 (C4 when the task was performed with the left wrist) was evaluated because in normal subjects, the early peak (within 60ms after movement onset) was largest at this location. This location is referred to as *contralateral motor cortex*. In addition, the waveform at the *vertex* (Cz) was evaluated because in normal subjects, the overall largest peak was measured at this location.

Comparison of StrEP waveforms

In the normal subjects, similarity of StrEP waveforms was evaluated by calculating the cross correlation coefficient ($0 < t < 400$ms) between conditions and sessions for both the contralateral motor cortex and the vertex.

In the stroke subjects, similarity between the affected and unaffected side was evaluated by the cross correlation coefficient between the StrEP waveforms elicited by affected side movement and unaffected side movement. A Wilcoxon rank-sum test was used to compare cross correlation coefficients between the stroke subjects with good motor function and with poor motor function ($\alpha = 0.05$).

Evaluation of StrEP features

Specific features of the StrEP (figure 6.2) were further assessed as follows. In the waveform at the contralateral motor cortex the presence, amplitude and latency of the early peak was determined. The early peak was considered present if the maximum positive deflection at the contralateral motor cortex in the interval between 10 and 60ms after movement onset exceeding the 99% confidence interval (CI): $EP_{C3}(t) - CI_{C3}(t) > 0$ using

$$CI_{C3}(t) = 2.6\frac{1}{\sqrt{n}}\sigma_{EP_{C3}}(t). \tag{6.1}$$

The standard deviation over repetitions of the averaged StrEP ($\sigma_{EP}(t)$) was divided by the square root of the number of segments (n) to obtain the standard error of the mean. This was multiplied by 2.6 to obtain the 99% CI. Only if the early peak was larger than the 99% CI, i.e. the peak was present, the early peak latency (t_1) and early peak amplitude (A_1) were determined.

As later peaks stretch over a longer time interval, we used the mean absolute amplitude in the late interval at the vertex instead of considering individual peaks. The amplitude of the late peaks (late mean amplitude, A_2) was determined as the mean absolute amplitude in the late interval ($60 < t < 300$ms). The latency of the late peaks (50% late amplitude latency, t_2) was determined as the latency at which the cumulative absolute amplitude was 50% of the total cumulative absolute amplitude in the late interval.

In the normal subjects, the effect of condition, i.e. on StrEP features, was assessed by linear mixed model analysis, as this technique is particularly suited for unbalanced datasets. For each StrEP feature, a model was fitted with the condition as a fixed effect factor and a variable intercept to allow inter-individual differences between the subjects. When a significant effect of the condition on the StrEP feature was found, estimated

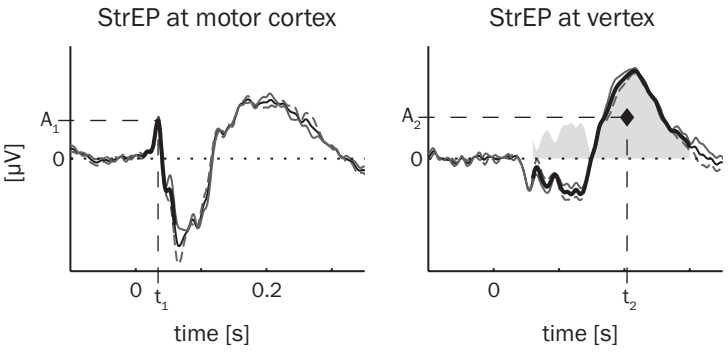

Figure 6.2: StrEP features. StrEP (solid black line) of a representative normal subject at the contralateral motor cortex (left) and vertex (right) in the active 50ms ramp condition. Grey lines are the StrEP of the extension (solid grey) and the flexion movements (dashed grey). The early peak latency (t_1) and early peak amplitude (A_1) are determined from the interval 10 to 60ms (thicker black line) in the evoked potential at the contralateral motor cortex. The late mean absolute amplitude (A_2) and 50% late amplitude latency (t_2) are determined from the interval between 60 and 300ms (thicker black line and absolute amplitude shaded) in the evoked potential at the vertex.

marginal means were used to test for differences between the active 50ms ramp and the relaxed 50ms ramp and between the active 50ms ramp and the active 25ms ramp. Bonferroni correction for multiple comparisons was applied. Linear mixed model analyses were performed with IBM SPSS Statistics version 20. Reliability of the StrEP features over the two sessions was evaluated using the intraclass correlation coefficient (ICC(2,1))

Absolute difference between the StrEP features of affected and unaffected hemisphere of stroke subjects with good motor function were compared to subjects with poor function using a Wilcoxon rank-sum test.

6.3 Results

Normal subjects

The extension movements elicited typical stretch responses in the FCR muscle in the normal subjects (see figure 6.3). Typically, in the active 25ms ramp condition, a single short latency response (within 50ms after movement onset) was elicited. In the active 50ms the short latency response had an amplitude similar to the active 25ms ramp condition. However, the longer ramp also elicited a longer latency response (between 50 and 150ms after movement onset). The relaxed 50ms ramp condition elicited a single short latency response with an amplitude that was considerably smaller than in the active conditions.

In normal subjects, fast wrist movement elicited consistent StrEPs in all conditions. The StrEPs were mainly localized over the contralateral sensorimotor area with the early peak (within the 60ms after movement onset) having the largest amplitude at electrode C3 (figure 6.4).

The active 50ms ramp and active 25ms ramp elicited StrEPs with a similar waveform

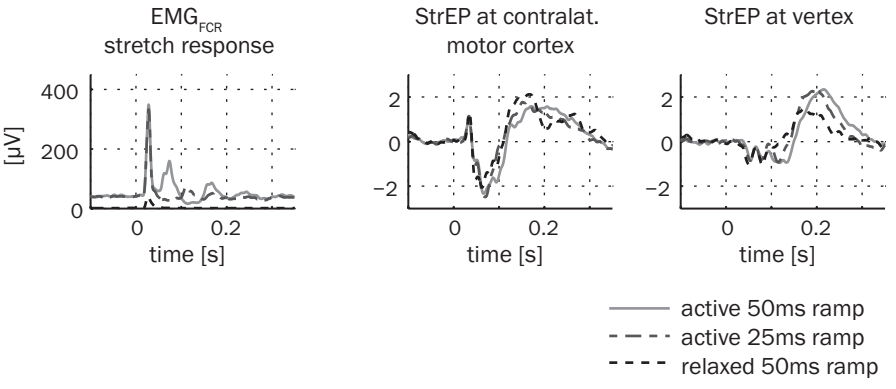

Figure 6.3: Stretch responses in the FCR muscle and StrEPs in a representative normal subject that performed the three task conditions. All traces are from the same measurement session. Cross correlation coefficients between active 50ms ramp and active 25ms ramp conditions: 0.93 at the contralateral motor cortex and 0.90 at the vertex. Cross correlation coefficients between the active and relaxed 50ms ramp conditions: 0.89 at the contralateral motor cortex and 0.74 at the vertex.

(see figure 6.3). The average cross correlation coefficient between the StrEPs in the active 50ms condition and the active 25ms ramp condition was 0.85 at the contralateral motor cortex and 0.92 at the vertex. Also in the active 50ms ramp condition and the relaxed 50ms ramp condition there were large similarities between StrEP waveforms, with an average cross correlation coefficient of 0.83 at the contralateral motor cortex and 0.76 at the vertex.

There was also a large similarity of the StrEP waveforms over sessions. The average cross correlation coefficient between the same conditions in the first and the second measurement session was 0.91 at the contralateral motor cortex and 0.93 at the vertex.

Variability of StrEP features

The active 25ms condition elicited a significant early peak in all subjects and both sessions. The active 50ms ramp condition also elicited a significant early peak in most subjects (21 out of 22 subjects in the first session and eight out of nine subjects in the second session). The relaxed 50ms ramp condition elicited a significant early peak in all normal subjects that performed this condition in the first measurement (ten subjects). However, in the second measurement session the relaxed 50ms ramp condition elicited a significant early peak in only two out of the five subjects that performed in task in the second session.

The averages of the StrEP features in the different conditions and sessions are listed in table 6.2. There was a significant effect of condition on the early peak amplitude ($F(2,48.364) = 8.341, p = 0.001$). The early peak amplitude was on average $0.29\mu V$ larger in the relaxed 50ms ramp condition than in the active 50ms ramp condition according to post hoc comparisons ($p < 0.001$). There was no effect of condition on the early peak latency ($F(2,49.193) = 0.69, p = 0.506$) and the effect of condition on the late mean amplitude was on the border of significance ($F(2,54.345) = 3.091, p = 0.054$. Finally, there was a significant effect of condition on the 50% late amplitude latency ($F(2,57.675) = 4.524, p = 0.015$).

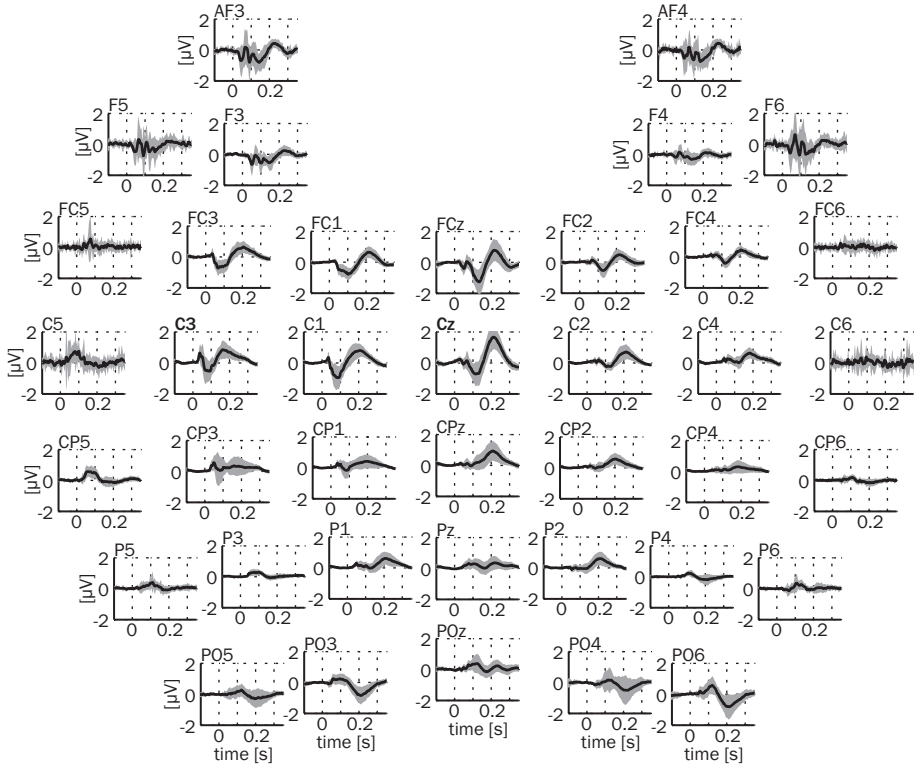

Figure 6.4: Grand average response over all normal subjects ($n = 22$) in active 50ms ramp condition. Black line indicates mean, grey fill is standard deviation over controls ($n = 22$). The responses of left handed subjects are mirrored across the mid line such that the hemisphere contralateral to the movement is always on the left side.

Table 6.2: Averages and standard deviations of the StrEP features in the different tasks and sessions in the normal subjects. S1: sessions 1, S2: session 2. A_1: early peak amplitude, A_2: late mean amplitude, t_1: early peak latency, t_2: 50% late amplitude latency. Not all normal subjects showed a significant early peak. n is the number of subjects on which the estimate of the average and standard deviation is based, between square brackets the number of normal subjects that performed the task.

	A_1 [μV]		A_2 [μV]	
	S1	S2	S1	S2
active 50ms ramp	0.86 ± 0.59 $n = 21[22]$	0.85 ± 0.58 $n = 8[9]$	0.85 ± 0.38 $n = 22[22]$	0.91 ± 0.47 $n = 9[9]$
active 25ms ramp	0.87 ± 0.64 $n = 22[22]$	0.89 ± 0.73 $n = 9[9]$	0.79 ± 0.40 $n = 22[22]$	0.80 ± 0.47 $n = 9[9]$
relaxed 50ms ramp	0.93 ± 0.72 $n = 10[10]$	2.03 ± 0.92 $n = 2[5]$	0.70 ± 0.52 $n = 10[10]$	0.83 ± 0.45 $n = 5[5]$
	t_1 [ms]		t_2 [ms]	
	S1	S2	S1	S2
active 50ms ramp	40 ± 6.6 $n = 21[22]$	38 ± 7.6 $n = 8[9]$	199 ± 13 $n = 22[22]$	200 ± 11 $n = 9[9]$
active 25ms ramp	40 ± 6.3 $n = 22[22]$	37 ± 7.4 $n = 9[9]$	194 ± 14 $n = 22[22]$	188 ± 19 $n = 9[9]$
relaxed 50ms ramp	39 ± 3.8 $n = 10[10]$	46 ± 6.6 $n = 2[5]$	184 ± 14 $n = 10[10]$	196 ± 13 $n = 5[5]$

The average 50% late amplitude latency was 11ms shorter in the relaxed 50ms ramp condition compared to the active 50ms ramp condition ($p = 0.017$).

Reliability of both StrEP features relating to amplitude was very good: early peak amplitude ICC = 0.94, late mean amplitude ICC = 0.85. The reliability of the StrEP features relating to time was good for the early peak latency ICC = 0.78. However, the reliability was poor for the 50% late amplitude latency: ICC = 0.29.

Stroke subjects

The EMG_{FCR} at the affected side of P11 was excluded because the signal contained large artefacts. The extension movements elicited stretch responses in the FCR muscles of the stroke subjects that performed the active task (CVA001 and CVA002, figure 6.5). Stretch responses of the affected side FCR muscle were also elicited in the stroke subjects with poor motor function (CVA005, CVA007 and CVA010), although these subjects were relaxed. These subjects also experienced some spasticity of the wrist as determined by the Ashworth scale (Bohannon and Smith, 1987) (table 6.1). The muscle stretch responses were clearly visible in the EMG and consisted of a short latency muscle stretch response (figure 6.5).

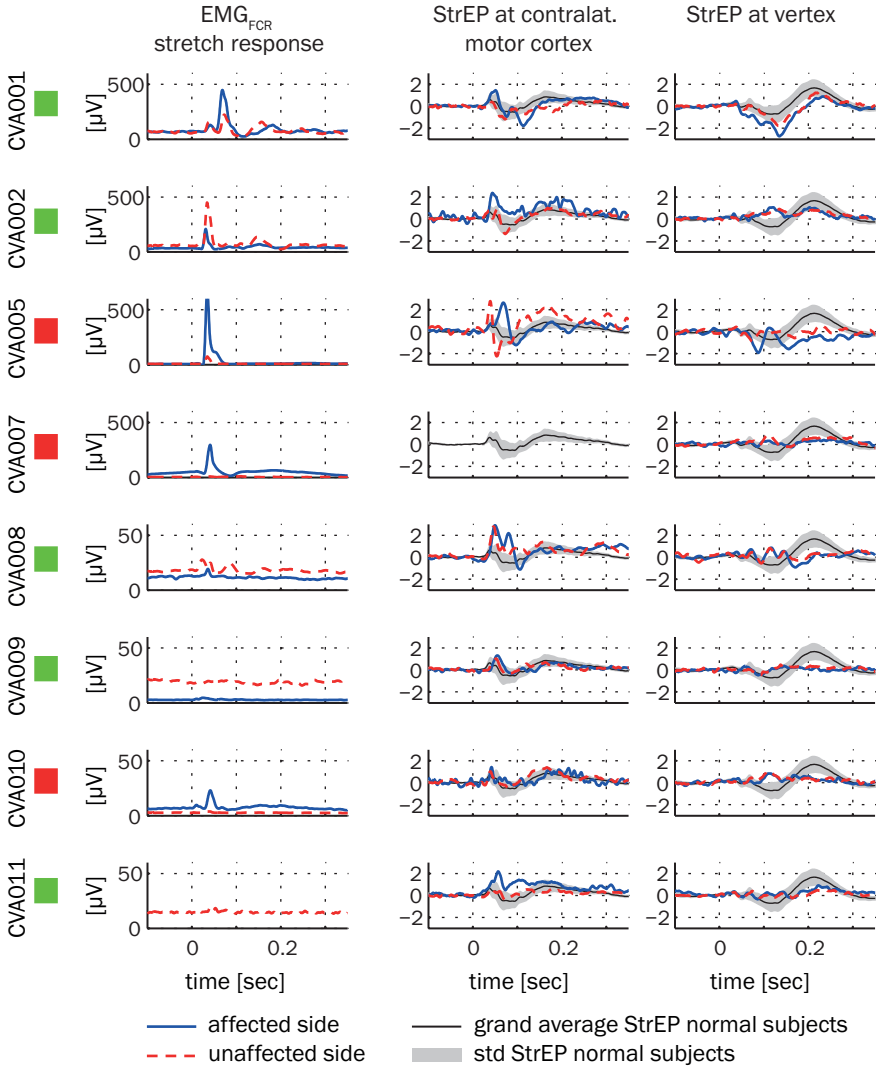

Figure 6.5: Individual FCR stretch responses and StrEPs of the stroke subjects. A green block indicates a subject with good motor function, a red block indicates poor motor function. Left column de muscle stretch response, middle column the response at the contralateral motor cortex (i.e. C3 or C4), right column the response at the vertex (Cz). As a reference the grand average StrEP and standard deviation (std) of the normal subjects in the active 50ms ramp condition is plotted. No contralateral motor cortex StrEPs are plotted for CVA007, this data was contaminated by continuous scalp muscle activity. Affected side EMG_{FCR} of CVA011 was excluded due to artefacts.

The quality of the EEG data recorded from the stroke subjects was poorer than in the normal subjects and more segments were rejected due to eye blinks or EMG artefacts. In the normal subjects on average 10% of the segments was rejected due to artefacts, in the stroke subjects on average 35% of the segments was rejected. Stroke subject CVA007 showed continuous muscle activity on channels C3 and C4 and on surrounding temporal electrodes, resulting in a very low signal-to-noise ratio, these channels were therefore excluded from analysis.

Figure 6.5 shows the individual StrEPs of the stroke subjects in response to affected and unaffected wrist movement. This figure shows that there is considerable inter-individual variation in StrEP waveforms and that the stroke subjects have different StrEP waveforms compared to the normal subjects, especially at the vertex. All stroke subjects presented a significant early peak at the contralateral motor cortex within the first 60ms after movement onset, both in the StrEP elicited by movement at the affected and by movement at the non-affected side. Especially in the later interval (between 60 and 300ms after movement onset) and at the vertex, the shape of the StrEP waveform in stroke subjects differs from the typical StrEP waveform of the normal subjects. In this interval, the normal subjects grand average StrEP at the vertex is characterized by a negative deflection followed by a larger positive deflection peaking around 200ms after movement onset. This large positive deflection was absent in most stroke subjects. Several stroke subjects (CVA002, CVA007, CVA008 and CVA010) showed a positive deflection around 100ms. Only CVA001 showed StrEPs which resembled the global shape of the StrEPs seen in normal subjects at both affected and non-affected side. Although this stroke subject had a good motor function, other subjects with good motor function did not necessarily present a close to normal StrEP waveform.

The early peak latency (t_1) of the StrEPs of the stroke subjects fell in the same range as seen in the normal subjects (figure 6.6). However, the early peak amplitude (A_1) exceeded the range found in normal subjects in three stroke subjects. CVA008 showed a high early peak amplitude on both sides, CVA002 and CVA005 had a high early peak amplitude at the affected and unaffected side respectively.

For all stroke subjects, the late mean amplitude (A_2) was low compared to the range of values found in the normal subjects (figure 6.6). In CVA009 the late mean amplitude on the affected side was below the range seen in normal subjects. In CVA011 the late mean amplitude on the unaffected side was below the range of normal subjects.

In the stroke subjects with good motor function there was a considerable similarity between the StrEP waveforms elicited at the affected and the unaffected side. In the stroke subjects with poor motor function, the similarity between affected and unaffected hemisphere tended to be lower (figure 6.7, left side). However, no statistical significant difference was found between the good and poor function stroke subjects (Wilcoxon rank-sum test: $p = 0.19$ at the contralateral motor cortex, $p = 0.14$ at the vertex).

The StrEP latency features (figure 6.7, right side) were similar at the affected and unaffected side (early peak latency ICC = 0.73, 50% late amplitude latency ICC = 0.84). The amplitude features showed a larger degree of variation between the affected and unaffected side (early peak amplitude ICC = 0.19, late mean amplitude: ICC = 0.53). There was no significant difference between stroke subjects with good and poor motor function in the absolute difference between StrEP features at the affected and the unaffected side (Wilcoxon rank-sum test: $p = 0.57$ for the early peak amplitude, $p = 0.19$ for the early peak

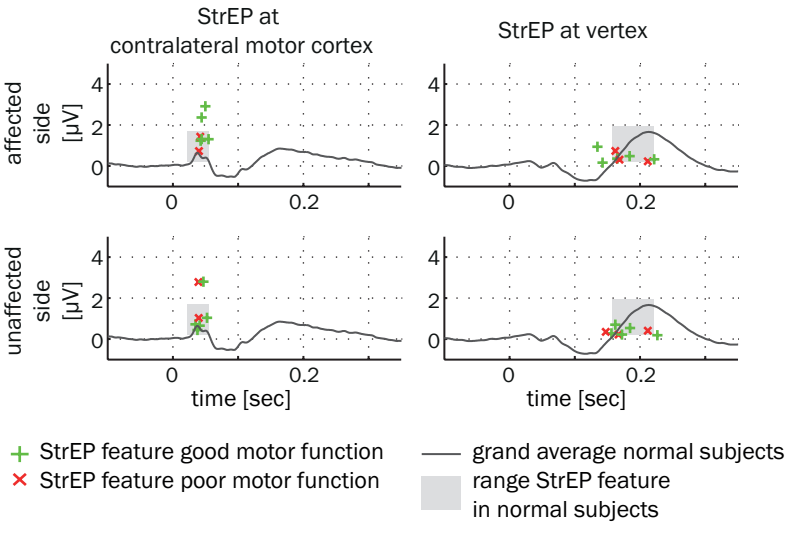

Figure 6.6: StrEP features in stroke subjects. Left: StrEP at the contralateral motor cortex with the early peak (t_1, A_1) indicated for individual stroke subjects and the range of t_1 and A_1 found in normal subjects over all conditions and sessions. Right: StrEP at the vertex with the late amplitude features (t_2, A_2) indicated for individual stroke subjects and the range of t_2 and A_2 found in normal subjects over all conditions and sessions.

latency, $p = 0.79$ for the late mean amplitude and $p = 0.46$ for 50% late amplitude latency).

6.4 Discussion

In this study we evaluated the cortical response to fast muscle stretch: the stretch evoked potential (StrEP). The StrEP waveform of normal subjects is characterized by an early peak within 60ms after movement onset over the contralateral primary motor cortex, and a complex of late peaks between 60 and 300ms after movement onset at the vertex. In stroke survivors the early peak was also present. However, they showed abnormal late peaks both in the StrEP elicited by affected and by unaffected wrist movement.

Consistent stretch evoked potentials in normal subjects

The 25ms and 50ms ramps elicited clear muscle stretch responses in the active conditions. The 25ms ramp only elicited a short latency response (within 50ms after movement onset) while the 50ms ramp elicited both a short and a long latency stretch response (between 50 and 150ms after movement onset), this result is consistent with previous experimental work using a similar experimental setup (Schuurmans et al., 2009). The short latency response is generally thought to be mediated by a monosynaptic reflex pathway. The origin of the long latency reflex is more complex, several pathways may contribute to this reflex including a transcortical pathway (MacKinnon et al., 2000; Spieser et al., 2010; Pruszynski and Scott, 2012)

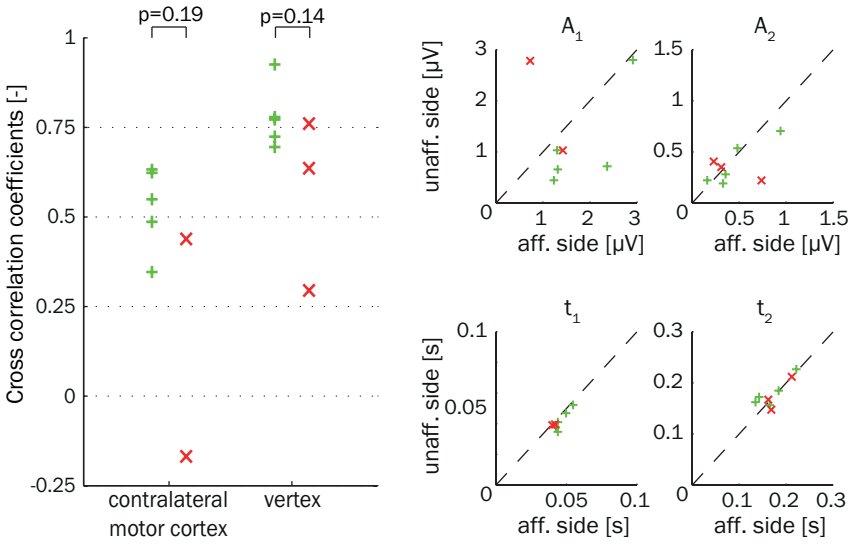

Figure 6.7: Left: cross correlation coefficients between StrEP waveforms elicited at the affected and the unaffected side in stroke subjects. Right: StrEP features measured at the affected (x-axes) and the unaffected side (y-axes). Dashed line indicates the line $y = x$. A green + indicates a subject with good motor function, a red × indicates a subject with poor motor function.

Although the muscle stretch response recorded by the EMG depends on the direction of joint movement, the StrEP is not. StrEP waveforms obtained from flexion and extension movements were very similar (figure 6.2). This suggests that the responses to flexion and extension movements are generated by nearly identical cortical populations. In addition, it suggests that the inputs, i.e. the trains of action potentials, these cortical populations receive from the afferent pathways are similar as well. A potential effect of direction on StrEP features has been lost by collapsing over movement direction. However, averaging over both flexion and extension movements doubles the number of available segments and substantially increases the signal to noise ratio of the StrEP (Seiss et al., 2002). As the signal to noise ratio of the EEG data from the stroke subjects could be very poor, averaging over flexion and extension movements allows including more segments without increasing the total recording time for the subjects.

Within a single subject the StrEP waveform was very similar over the two stretch amplitudes (mean cross correlation > 0.85) and also when comparing StrEPs during the active conditions (i.e. an isotonic wrist flexion task) and the relaxed conditions (mean cross correlation > 0.76). In all task conditions the StrEP waveform is characterized by an early peak at a latency of 40ms after movement onset, localised at the sensorimotor cortex contralateral to the wrist movement. In the later interval (between 60 and 300ms after movement onset) the StrEP has the largest amplitude at the vertex and is characterized by an initial negative deflection, followed by a positive deflection, peaking at around 200ms after movement onset (figure 6.3). The global StrEP waveform is in concordance with the waveforms elicited by muscle stretch in previous studies, although detailed comparison of latency and amplitude features is hampered by differences in the type of perturbations

applied, EEG derivation and data processing (Abbruzzese et al., 1985; MacKinnon et al., 2000; Seiss et al., 2002; Spieser et al., 2010).

The active 25ms ramp condition elicited a significant early peak in all normal subjects, while the 50ms conditions did not elicit this peak in some subjects. This suggests that shorter ramp movements may be more suitable for eliciting the early peak of the StrEP. It was previously reported that an early peak, between 30 and 50ms after movement onset was not consistently present after passive movement of at least 100ms of the index finger (Seiss et al., 2002). Despite the differences in elicited muscle stretch reflexes, the two ramp amplitudes did not result in significant difference between StrEP features (Abbruzzese et al., 1985). Only the duration of the ramp was different, task instruction and ramp velocity were equal in the active tasks. A model simulation study previously showed that also the monosynaptic Ia afferent pathway can explain the appearance of long latency responses in the muscle stretch reflexes as a function of stretch duration (Schuurmans et al., 2009).

StrEP features were sensitive to small changes in the StrEP waveform in the different task conditions: the initial peak amplitude was larger and the 50% late amplitude latency shorter in the relaxed compared to the active 50ms ramp condition. Previous studies obtained varying results on changes of StrEP features due to different task instructions. Abbruzzese et al. (Abbruzzese et al., 1985) showed covariation of long latency muscle responses and early StrEP amplitudes ($30-75$ms after wrist extension onset) with task instruction. Intention related modulation of early StrEP amplitudes (45ms after wrist extension onset) was also shown by Spieser et al. (Spieser et al., 2010). In contrast to these studies, MacKinnon et al. (MacKinnon et al., 2000) found that StrEPs elicited during tasks with different instruction were only different more than 135ms after wrist extension onset, which does not support a relation between a trans-cortical reflex loop and the StrEP.

While the results on modulation of StrEP features with task instruction are inconclusive, the electrically elicited SSEP is sensitive to differences in tasks. The earliest components of the SSEP are suppressed during active and passive movement, as compared to a resting condition (Abbruzzese et al., 1981; Starr and Cohen, 1985). This effect is known as 'gating' and represents the modulation of the sensitivity of the cortex to various sources of sensory information. However, in the StrEP paradigms the different task instructions do not lead to different, competing sources of sensory information and the modulation of StrEP features with task instruction could therefore represent a different mechanism.

An important aspect of the usefulness of the StrEP as a potential clinical measure for proprioceptive function after stroke is the reliability of the StrEP waveform and features over multiple sessions (Kottner et al., 2011). The similarity of StrEP waveforms between sessions was larger than the similarity between conditions in one session. When the early peak was consistently elicited over sessions, the StrEP amplitude features (early peak amplitude and late mean amplitude) showed a very good reliability, while both features related to latency had considerable poorer reliability. This indicates that the amplitude features are better suited to differentiate between subjects, because the variance between sessions is small compared to the variance between subjects.

Stretch evoked potentials after hemispheric stroke

The possibility to elicit StrEPs during a relaxed task similar to those during an active task opens the possibility to investigate processing of proprioceptive input also in stroke survivors that are not able to voluntarily generate force. Especially in this severely impaired patient group, prediction of the potential motor recovery is difficult (Prabhakaran et al., 2008). Given the importance of sensory feedback for voluntary motor control and motor learning, assessment of proprioceptive function and sensorimotor integration may aid in the prediction of the potential motor recovery. Such assessment is needed early after stroke, within four weeks post stroke, as recovery in this time window predicts the recovery of a patient after six months (Kwakkel et al., 2003). Monitoring recovery of sensorimotor function in these first weeks after stroke will potentially be most valuable and our results show that the StrEP can be elicited within this time frame in subjects with poor motor function.

Fast wrist movement elicited StrEPs both in stroke subjects with good motor function (FM > 60) and with poor motor function (FM < 30). Despite the large heterogeneity in subject characteristics and StrEP waveforms, all stroke subjects showed the early peak at the contralateral motor cortex within 60ms after movement onset. This peak most likely represents the arrival of afferent sensory information from the muscle spindles to the motor cortex (Mima et al., 1996; MacKinnon et al., 2000; Seiss et al., 2002). The presence of the early peak shows intact afferent pathways in all stroke subjects, which is in line with the clinical assessment of sensory function Nottingham sensory assessment scale.

While it is likely that the early peak of the StrEP indicates the arrival of afferent sensory information, the meaning of the late peaks is unknown but possibly indicates the processing of proprioceptive input from the muscle spindles by a cortical sensorimotor network. The large variety of StrEP waveforms in the stroke subjects then indicates changes of this sensorimotor network after stroke. While abnormal StrEP waveforms were also seen in stroke subjects with good motor function, changes in the sensorimotor network do not necessarily represent poor motor control. In subacute stroke survivors, StrEP waveform is altered but does not allow discrimination between good and poor motor function.

An unexpected results is that although stroke affects one hemisphere, the StrEP elicited by unaffected wrist movement was not necessary similar to the StrEPs of the normal subjects. Although the StrEP waveforms at the vertex and the contralateral motor cortex were abnormal both in subjects with good and poor motor function, stroke subjects with good motor function tended to have a larger similarity between StrEPs elicited at the affected and unaffected side. However, no significant difference was found in our small group of stroke subjects. A recent study (Graziadio et al., 2012) showed that in chronic stroke subjects, recovery is not associated with the absolute normality of beta band EEG power and corticomuscular coherence during muscle contraction but rather with the symmetry of these measures between the ipslesional and contralesional hemisphere. It may be more valuable to compare stroke subjects with themselves instead of healthy controls, as recovery may not result in a restoration of the pre-stroke activity pattern but rather with a new balance between both hemispheres. In our results, the cross correlation between StrEP waveforms seemed to be smaller in the stroke subjects with poor recovery but the difference did not reach statistical significance. Although we cannot confirm this from the current data set, it is expected that the StrEP, like the SSEP, in normal subjects exhibit a

large degree of similarity (Tecchio et al., 2000).

Study limitations and future directions

Quantitative comparison of StrEP features between normal and stroke subjects in this study is hampered due to non-matched characteristics of the two populations. Subject age can affect the expected latencies of evoked potential peaks due to decreased fibre conduction velocity (Allison et al., 1984). Within our study, such conduction velocity related effects would mainly result in increased initial peak amplitude latencies, an overall alteration of evoked potential waveform, like we saw in the stroke subjects, is not expected. One study evaluated age-related changes of evoked potentials induced by joint movement (Starr et al., 1981). In that study, cortical potentials induced by ankle flexion did not change as a function of age. However, with only ten subjects, their study population was relatively small. Despite the age difference between the normal and stroke subjects, we found that the stroke subjects all present the initial peak at latencies comparable to the normal, younger, subjects. We did see a large variety in StrEP waveforms in the late interval in the stroke subjects. Although we cannot rule out that age differences contributed to the observed abnormal StrEP waveforms in stroke subjects, age differences are not likely to be the sole explanation.

The difference in task instruction and perturbation characteristics also hampers the direct comparison between normal and stroke subjects. However, like the age differences, these changes in the protocol are not expected to fully explain the abnormal StrEP waveform seen in the stroke subjects. In the normal subjects, the shortening of the ramp duration increased the likelihood of eliciting a significant early peak. Although the StrEP features differed between the active and relaxed task, the correlation coefficients were high between StrEPs obtained in active and relaxed conditions (average cross correlations > 0.75) indicating that the global StrEP waveform did not change between conditions.

Further assessment of the relation between the StrEP and sensorimotor function after stroke requires data of a larger cohort of patients and matched controls, including patients with good and poor motor function and with good and poor sensory function. Future work should include the longitudinal assessment of StrEP and sensorimotor function in a large cohort of patients from the subacute till the chronic phase to monitor changes in cortical processing of sensory input in relation to recovery. As clinical assessment of sensory function is shown to be unreliable (Lincoln et al., 1991), proprioceptive function may be evaluated with objective and quantitative assessment of position sense by robotic devices (Dukelow et al., 2010). Eliciting StrEPs can easily be combined with such robotic assessment of position sense or with robotic rehabilitation training. Comparison of the StrEP with the electrically elicited SSEP in such a longitudinal study design should provide insight in how the cortical response to different types of sensory input is related to sensorimotor integration and recovery of motor function.

6.5 Conclusion

Measurement of cortical responses evoked by fast joint movement (StrEPs) potentially offers a method to objectively measure the integrity of the afferent sensory pathways associated with proprioceptive function and sensorimotor function. In normal subjects, StrEPs

have a very consistent waveform across conditions and sessions. With this property the StrEP meets an important prerequisite for clinical value. The peaks at different latencies allow separation between the arrival of input at the cortex and subsequent processing of this information. Measurement of the StrEP is feasible in subacute stroke patients and our first exploration of StrEPs in this patient group indicates that even subjects with good motor function may show abnormal StrEP waveforms. We found no clear association between StrEP features and good or poor motor function in this population, leaving the relation between StrEP features and clinical phenotype to be established.

Chapter 7

General Discussion

Motor control involves various parts of the central nervous system (CNS). The lowest level is the spinal cord, that executes 'simple' reflexes; higher levels are the brainstem and the cerebellum. The highest level is the cortex, where several areas are involved in sensory integration, motor planning and motor execution. Motor control requires the formation of functional networks that facilitate the exchange of information, functional connectivity, between neural populations. The formation of functional networks relies on the synchronization of neural oscillations. Several measures exist that quantify the synchronization and thus the connectivity between neural populations based on recording of the population activity.

In this thesis two measures that are currently applied in the context of (corticomuscular) connectivity in motor control were evaluated (chapters 2 and 3). In addition, two novel measures of afferent pathway connectivity in motor control were presented: a frequency domain measure, the position-cortical coherence (PCC) and a time domain measure: the muscle stretch evoked potential (StrEP) (chapters 4 and 6, respectively). These measures can also be obtained in stroke survivors (chapters 5 and 6). In this chapter the results from the previous chapters will be discussed and directions for future research on connectivity in motor control will be provided.

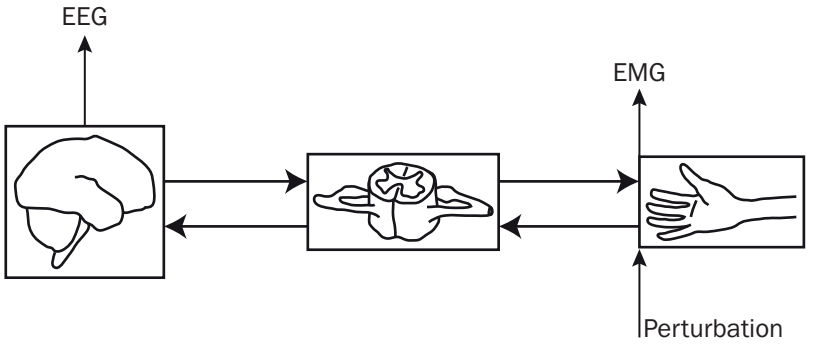

Figure 7.1: Simplified scheme of motor control excited by a mechanical perturbation. The scheme consists of two levels in the central nervous system (CNS): the cortex and the spinal cord, and the efferent and afferent pathways connecting the CNS with the periphery. The electroencephalogram (EEG) and electromyogram (EMG) record cortical and muscle activity respectively. The mechanical perturbation 'enters' the closed loop motor control scheme at the beginning of the afferent pathways.

Motor control requires functional connectivity between neural populations in the cortex and the spinal cord. In most studies this connectivity is quantified by the coherence between EEG (or MEG) and EMG: corticomuscular coherence (CMC). Coherence is the frequency domain equivalent of the cross correlation coefficient and expresses the amount of linear coupling between two signals: zero indicates no linear coupling between the signals at a particular frequency, one indicates perfect, noise free coupling between the signals. Significant CMC is found in the beta band (15 to 30Hz) during static isometric contractions (Halliday et al., 1998; Conway et al., 1995; Mima et al., 2000; Baker, 2007).

The detection of significant CMC shows that there is synchronization between neural populations in the cortex and the spinal cord. It does not provide information about the directionality of the information transfer: both the efferent and afferent pathways contribute to the generation of CMC. The closed loop structure of the motor control system makes it impossible to derive specific properties, such as transmission delays, of the efferent of afferent pathway from CMC (chapter 3).

In order to obtain better measures of connectivity in motor control, the main objective of this thesis was to develop and evaluate measures to quantify pathway connectivity in motor control, based on techniques from the field of system identification. The application of external perturbations 'opens' a closed loop system (Ljung, 1999; Pintelon and Schoukens, 2001).

From the application of external mechanical perturbations two connectivity measures were derived: position-cortical coherence (PCC) and muscle stretch evoked potentials (StrEPs). Because the mechanical perturbation 'enters' the motor control system at the beginning of the afferent pathways (see figure 7.1), integrity of the afferent pathways is required for the detection of PCC and StrEP. Indeed, in a normal subject population all subjects presented both PCC and a StrEP, consistent with a normal integrity of the afferent sensory pathways (chapters 4 and 6).

Corticomuscular connectivity is studied not only to increase the understanding of

physiological motor control; quantifying connectivity after stroke may also provide insight in the role of pathway integrity and neuroplasticity in the recovery of motor function (Grefkes and Ward, 2014). Most clinical studies apply CMC as a measure of corticomuscular connectivity. When applying CMC as a measure of connectivity after stroke the population of stroke survivors that can be studied is limited to individuals with relatively good motor function. A measurable EMG signal and thus voluntary muscle control is a prerequisite for the estimation of CMC. The PCC and StrEP have the advantage that they can also be elicited in absence of muscle activation.

Specific assessment of afferent sensory pathway connectivity may be valuable during recovery of motor function after stroke. In the closed loop structure of motor control sensory feedback is essential. Indeed, recovery of motor function is not only associated with altered activation and reorganisation of cortical motor areas (Grefkes and Ward, 2014) but also with changes in sensory areas (Roiha et al., 2011). Laaksonen et al. (2012) showed that the modulation of motor cortex excitability by sensory input changes during the recovery of motor function, underlining that recovery of motor function requires sensorimotor integration. Moreover, training of sensory function reduces motor impairment after stroke (Schabrun and Hillier, 2009).

Also in (subacute) stroke survivors afferent pathway connectivity can be assessed by PCC or the StrEP. All (subacute) stroke survivors presented PCC (chapter 4) and a StrEP (chapter 6), even those with very poor motor function who were unable to perform an isotonic wrist flexion task. Abnormal StrEP waveforms were seen in subacute stroke subjects, but no significant difference were found between StrEP features of subjects with good and poor function. However, presence of PCC did differ between subacute subjects with good and poor motor function.

7.1 Consider the closed loop

Presenting motor control as a closed loop feedback system is natural from a control engineering point of view. However, even in recent publications on connectivity in motor control the closed loop is overlooked (Petersen et al., 2012; Witham et al., 2011) and this can have consequences for the validity of the conclusions that are drawn from experiments. Although evidence is accumulating that CMC is affected by the properties of the efferent and afferent pathways, many studies use coherency phase analysis to estimate efferent pathway transmission delays.

Phase analysis for the estimation of transmission delays gives unreliable results in closed loop systems (chapter 3). A simplified closed loop feedback model of the corticomuscular system and time delay estimation based on coherency phase (Rosenberg et al., 1989; Halliday et al., 1995), reproduced the range of time delays between EEG and EMG found in experimental studies in literature (Halliday et al., 1998; Brown et al., 1998; Gross et al., 2000; Grosse et al., 2003; Riddle and Baker, 2005; Petersen et al., 2012). As the estimated time delays are affected by the model configuration, strength of the efferent and afferent pathways and the contribution of sensory feedback to the recorded cortical activity, transmission delays estimated from coherency phase analysis are meaningless.

In addition, we evaluated time delay estimation with two Granger causality based measures: the Directed Transfer Function (DTF, Kaminski and Blinowska, 1991) and the Partial

Directed Coherence (DTF, Baccalá and Sameshima, 2001). Both DTF and PDC capture bidirectional connectivity in a multivariate autoregressive model structure, however, only PDC phase resulted in correct estimation of transmission delays in all model configurations. DTF phase does not lead to a correct estimation of the transmission delays in a closed loop feedback system because the DTF expresses the relation between unknown noise sources acting as independent input signals and signals recorded within the closed loop. For a closed loop system, it can be shown that the DTF contains the dynamics of both pathways in the loop (Schouten and Campfens, 2012). Partial directed coherence estimates the transfer function between signals that are all recorded from within the closed loop; in the simple model of the corticomuscular system this leads to correct estimation of the transmission delays. However, this model is a very simplified representation of the actual motor control system and thus also phase delays estimated from PDC phase will represent a lumped time delay.

Estimating the transmission delays between EEG and EMG is a form of system identification: the estimation of specific properties of a system that connects two signals. The closed loop structure of motor control does not only lead to problems in the identification of properties of the efferent and afferent pathways but also impacts other fields of motor control research, e.g. balance control (van der Kooij et al., 2005). System identification of closed loop feedback systems offers several approaches to overcome the specific problems that arise when identifying properties of single pathways in the closed loop. One of these approaches is the fitting of a multivariate autoregressive model, this approach is taken in the application of DTF and PDC. A different approach is the application of an external perturbation exciting the system (Ljung, 1999; Pintelon and Schoukens, 2001). We used this approach in the development of new corticomuscular pathway connectivity measures.

7.2 Reproducibility of connectivity measures

Connectivity measures should first of all be valid for the process that they intend to capture. When measures are applied in study protocols with repeated measurement sessions, such as monitoring subjects during recovery of motor function, connectivity measures should also be reproducible. Intramuscular coherence (IMC) analysis quantifies the common oscillatory drive to different parts of a muscle and beta band IMC is considered to reflect the common oscillatory drive originating from the primary motor cortex (Grosse et al., 2002). Requiring only EMG recordings, IMC analysis is an attractive approach to quantify common drive during functional motor tasks (Bo Nielsen, 2002; Bo Nielsen et al., 2008; Hansen et al., 2005; Barthélemy et al., 2010).

Although it is easy to obtain the required signal and it may be a valid measure of common (supra-spinal) drive (Grosse et al., 2002), the applicability of IMC analysis is limited during the functional task of walking (chapter 2). We showed that the test-retest reliability and agreement of IMC variables were dependent on the applied signal processing steps. The best reliability and agreement were obtained when the subjects walked at slow speed (2.5km/h) and the EMG was rectified prior to coherence analysis. However, even for these settings the reliability was only on the limit of good (ICC = 0.76) and the agreement was low. The smallest real difference, i.e. the smallest change necessary to exceed the measurement error of two repeated measurements, indicated that only large changes in IMC

variables (> 66%) can be shown.

The poor reliability and agreement of the evaluated IMC variables limits the applicability of these measures. Changes in cortical oscillatory drive due to therapeutic interventions are easily obscured by the large variability between sessions. Furthermore, we showed that obtaining longer recordings is not likely to increase the reproducibility of the IMC variables. Differences in length of recordings can even introduce a bias in the estimated IMC variables; including more segments in the analysis increases the area of coherence.

Possibly the reproducibility of coherence variables obtained from other (pairs of) muscles or during other tasks is better than reproducibility of the coherence variables we evaluated. However, this should be shown, not be assumed. Before coherence analysis is used in intervention studies, the reproducibility of the coherence variables should be assessed.

The importance of reproducibility does not only apply to intramuscular coherence analysis. The reproducibility of corticomuscular coherence (CMC) has been assessed by Pohja et al. (2005). They showed that CMC variables obtained from different measurements within one session are similar, but are variable between sessions. Although that study analysed the correlation between CMC variables between measurements and sessions instead of the reliability and agreement, it is likely that between session reproducibility of CMC variables obtained during static isotonic contractions is poor. Reproducibility of the measures for afferent pathway connectivity presented in this thesis has not yet been studied extensively. Such analysis should be included in the continued development of afferent pathway connectivity measures.

7.3 The application of external perturbations: afferent pathway connectivity

Two types of external perturbations were applied to obtain connectivity measures: continuous joint position perturbations and transient joint position perturbations. The different perturbations enabled the the presentation of two measures that quantify the information transfer across the afferent pathways: afferent pathway connectivity. Position-cortical coherence (PCC) was presented as a frequency-domain measure of connectivity in chapter 4. The muscle stretch evoked potential (StrEP) was presented as a time-domain measure of connectivity in chapter 6.

The frequency domain: position-cortical coherence

Position-cortical coherence expresses the synchronization between a continuous position perturbation and cortical activity. In normal subjects, significant PCC was localised at the sensorimotor cortex contralateral to the perturbed wrist. The detection of significant PCC shows that oscillatory cortical activity is synchronized to the perturbation. This can only occur when there is sufficient connectivity between periphery and cortex via the afferent sensory pathways. The process underlying PCC may be compared with how a steady state evoked potentials are elicited in the visual or auditory system (Herrmann, 2001).

Position-cortical coherence has important advantages over the coherence between EEG and EMG during an unperturbed task. Firstly, all normal subjects included in our

study presented significant PCC on at least one stimulus frequency, while not all healthy subjects present significant CMC during a static isotonic motor task (Mendez-Balbuena et al., 2011; Ushiyama et al., 2011). The absence of significant CMC in 50% of the normal healthy population is a serious downside of the applicability of CMC. The normal subjects have normal voluntary motor control and therefore the absence of CMC does not indicate the absence of connectivity between motor cortex and muscles. The inter-individual variability in the presence of significant CMC does indicate that there is a large degree of variability in the strength of oscillatory connectivity during a static motor task (Ushiyama et al., 2011). It was shown that CMC can be elicited by transient mechanical perturbations (McClelland et al., 2012a), or after learning (Mendez-Balbuena et al., 2011; Perez et al., 2006). This implies that the strength of oscillatory connectivity between cortical and spinal neural populations also varies within the same individual.

Secondly, PCC represents connectivity across the afferent sensory pathways as the perturbation 'enters' the motor motor control system via the afferent sensory pathways, while CMC represents the connectivity across the efferent and afferent pathways. PCC is therefore simpler to interpret than CMC. The contribution of efferent and afferent pathways makes it impossible to relate changes in CMC to specific pathway connectivity.

Position-cortical coherence after stroke

All stroke survivors showed significant PCC on the contralateral sensorimotor area in response to affected and unaffected wrist perturbations. Poor function stroke subjects (Fugl-Meyer upper extremity score < 30) had a reduced presence of contralateral PCC in responses to affected side perturbations compared to good function stroke subjects. Contrary to studies on CMC after stroke (Meng et al., 2009; Mima et al., 2001b), no significant differences were found in PCC amplitudes between groups or sides.

In line with the studies evaluating localisation of CMC after stroke (Meng et al., 2009; Rossiter et al., 2013), PCC showed a different spatial pattern after stroke. While in normal subjects PCC was localised predominantly on the sensorimotor area contralateral to the position perturbation, stroke subjects showed a more widespread spatial distribution of PCC. Expressing the balance between contralateral and ipsilateral PCC in the lateralisation index revealed that in poor function stroke subjects contralateral PCC is more dominant in the unaffected wrist tasks, while PCC was distributed more evenly between the hemispheres or was even more dominant in the ipsilateral hemisphere in the affected wrist tasks. The altered distribution of PCC may be related to reorganization of cortical sensory and motor areas.

The time domain: stretch evoked potentials

The StrEP is the cortical activation in response to a transient joint position perturbation. The StrEP provides a time domain measure for afferent sensory pathway connectivity. Normal subjects presented StrEPs with a stereotypical waveform. The StrEP is characterised by an early peak at approximately 40ms after movement onset which is maximal at the sensorimotor cortex contralateral to the perturbed wrist. The early peak is followed by a complex of subsequent peaks between 60 and 300ms after movement onset. The complex of these later peaks reaches maximum amplitude at the vertex at approximately

200ms after movement onset. Recording of cortical activation in response to transient external stimuli is not a new technique, in clinical practice recording of the somatosensory evoked potential (SSEP, i.e. the cortical activation in response to electrical stimulation of for example the median nerve) is common. The difference between the SSEP and StrEP is that the StrEP is elicited by realistic afferent sensory feedback, while the electrical stimulation in SSEP recording provides mixed artificial input. MacKinnon et al. (2000) and Seiss et al. (2002) showed that the StrEP is generated (at least in part) by sources in the primary motor cortex while the electrically elicited SSEP is generated in sensory areas of the cortex.

We showed that the StrEP has a consistent waveform across different task conditions (25ms ramp duration vs. 50ms and active vs. relaxed tasks) and that the similarity between StrEPs elicited in different measurement sessions was large (mean cross correlation coefficient was 0.91 at the contralateral motor cortex and 0.93 at the vertex). The StrEP features that were derived from the StrEP waveform could differ between task conditions. The reliability of the StrEP features between sessions was good to very good.

The StrEP allows the temporal separation between the arrival of afferent sensory input and the subsequent processing of this information. The early peak of the StrEP has a latency that is consistent with the arrival of sensory input at the cortex. As such, this peak gives an indication of the integrity of afferent sensory pathways, similar to the interpretation of the SSEP N20 peak which also signals the arrival of sensory input to the cortex (van Putten, 2012). However, not all normal subjects presented a significant early peak in all task conditions. Only the active 25ms ramp task condition always elicited a significant early peak. Also when no significant early peak was detected the normal subjects showed a complex of later peaks. This shows that sensory input related to the position perturbation reached the cortex and was processed.

Stretch evoked potentials after stroke

StrEPs were also recorded in stroke survivors, including individuals with poor motor function. All stroke subjects showed an early peak in response to affected and unaffected transient wrist movement, consistent with the arrival of afferent sensory input at the cortex. Despite the presence of the early StrEP component in all stroke subjects, the StrEP waveforms in the later interval showed large inter-individual differences, in contrast to normal subjects. In subacute stroke survivors, StrEP waveform and features do not seem to allow discrimination between stroke subjects with good and poor motor function. Stroke subjects with good motor function did not necessarily present more normal StrEP waveforms than subjects with poor function.

Potentially the similarity between StrEP waveforms at the contralesional and ipsilesional hemisphere has discriminative power between good and poor function stroke subjects. The cross correlation coefficients between ipsilesional and contralesional hemisphere StrEPs tended to be lower in poor function stroke subjects, but the difference did not reach significance ($p > 0.14$). Discrimination based on the similarity between ipsilesional and contralesional would be in line with the results Graziadio et al. (2012) obtained using CMC; recovery of motor function after stroke may not necessarily be the restoring of the pre-stroke activation patterns, but could be the restoration of the balance between the hemispheres.

Comparison of position-cortical coherence and stretch evoked potentials

Both PCC and the StrEP measure afferent sensory pathway integrity by eliciting cortical responses to joint position perturbations. The active tasks the healthy subjects performed were the same, only the characteristics of the joint position perturbation were different. As both measures quantify the same afferent pathway connectivity, they should present the same information. Indeed, all normal subjects presented both PCC and a StrEP showing the intactness of the afferent sensory pathways as was expected from normal subjects.

Although the PCC and the StrEP represent connectivity and pathway integrity in different domains, from a system identification perspective they are directly related. Position-cortical coherence is a frequency domain expression of the correlation between perturbation and EEG. The StrEP represents correlation in the time domain. It can be shown that averaging over segments time locked to the onset of wrist manipulator handle movement is similar to estimating the average cross correlation between the EEG and the absolute velocity profile of a block shaped position profile with infinitely small ramp duration. However, the calculation of the StrEPs included steps that would not be included in cross correlating the EEG and an absolute velocity profile and vice versa. The baseline correction that was applied in the StrEP estimation is not part of a cross correlation estimation. On the other hand, cross correlation analysis includes a normalization step which is not included in the StrEP estimation. Presenting the StrEP as a cross correlation measure is therefore not entirely correct from a mathematical point of view. However, looking at the StrEP as a cross correlation between position perturbation and EEG can allow a comparison between PCC and the StrEP as related connectivity measures where the perturbation signals have different characteristics.

As a result of the differences in estimation procedure of PCC and StrEP, the StrEP expresses afferent pathway connectivity over a wider frequency range and includes possible non-linear responses. Position-cortical coherence cannot capture non-linear responses of the afferent pathways because it can only be expressed on frequencies contained in the perturbation signal; non-linear dynamics would result in cross-frequency synchronization (Pintelon and Schoukens, 2001). The frequency content of the StrEP waveform is only limited by the filtering operation applied to the raw EEG and thus responses elicited on frequencies not contained in the perturbation signal do remain present in the StrEP waveform.

The frequency content of the perturbation signals could explain a difference between the StrEP and PCC. Position-cortical coherence was localised predominantly on the contralateral sensorimotor cortex, while the StrEP also contained peaks of considerable amplitude at the vertex. The dominant late peak at the vertex has a duration of approximately 250ms and thus represents a frequency of 4Hz, while the lowest frequency contained in the continuous multisine perturbation signal was 5Hz. The duration of the early StrEP peak was smaller, representing a higher frequency. Possibly the finding that PCC was localized on the contralateral motor cortex resulted from the difference in frequency content between the perturbation signals. Including more (lower) frequencies in the continous perturbation signal may also elicit low frequency responses at the vertex.

Despite that the StrEP is able to express afferent pathway connectivity in a wider frequency range and capture possible non-linear responses, only PCC features (presence of

contralateral PCC) differed between stroke subjects with good and poor motor function. StrEP waveforms differed between normal and stroke subjects but not between good and poor function stroke subjects. Based on the results in this thesis, only PCC has discriminative power between good and poor function stroke subjects. In the development of connectivity measures that are suitable for monitoring afferent pathway connectivity during recovery of motor function after stroke, PCC seems to be the more promising measure.

7.4 Future directions

In this thesis, two novel measures for afferent pathway connectivity in motor control were presented. In the process of developing and evaluating these methods choices were made that had to be reconsidered in a later stage. As a result of this (inevitable) process of continuing new insights, a direct comparison between normal subjects and stroke subjects is hampered. The subject groups have different age characteristics, experimental protocols differed and other choices were made in data analysis. The research presented in this thesis provides a starting point for studying connectivity in motor control combining external perturbations and connectivity measures. This thesis shows that it is feasible to obtain measures of afferent pathway connectivity, also after stroke, but provides directions for future research rather than firm conclusions.

Although StrEPs were already presented in experimental studies on transcortical reflexes over three decades ago (Abbruzzese et al., 1985; Starr et al., 1981), many properties of both PCC and StrEPs are unknown. We need to get to know these measures better before either measure can be considered valuable in clinical practice. Further research needs to reveal how PCC or StrEP features relate to actual afferent pathway connectivity and how they are modulated in various motor task conditions. Furthermore, for application in clinical practice a simple and short measurement protocol is required that can be performed by subjects with various levels of motor function.

Development of connectivity measures

To elicit PCC and the StrEP, we applied a position perturbation during an isotonic force task. However, for stroke subjects with poor motor function, an active motor task was very difficult and it was decided to let stroke subjects with poor motor function relax. StrEP features were compared between active and relaxed tasks in some normal subjects and PCC was evaluated in some stroke subjects. The effect of task type, active vs. relaxed tasks, on afferent pathway connectivity measures should be systematically evaluated in a larger normal subject population. For the development of connectivity measures for clinical applications, inclusion of relax tasks is essential because this task condition can also be performed by subjects without voluntary muscle control.

Possibly, the limited frequency range of the continuous position perturbation used to elicit PCC underlies the difference in localization of the StrEP (contralateral sensorimotor cortex and vertex) and PCC (only contralateral sensorimotor cortex). In the further development of PCC, the bandwidth of the perturbation should be varied, including more low frequencies, to see whether this captures more properties of the afferent pathways.

Extracting relevant features

Recording multiple channels of EEG enables the recording of cortical activity from multiple cortical areas on a millisecond time scale. This provides a valuable window on the brain but when the number of available channels increases the amount of data that potentially contains relevant information increases as well. The extraction of relevant information from the available data can become a challenge. We chose to focus on single electrodes (PCC in chapter 4 and StrEPs in chapter 6) or group several electrodes together (PCC in chapter 5). Grouping multiple electrodes has the advantage that it allows inter-individual differences in the spatial distribution of the connectivity measure. The downside of grouping electrodes is that spatial resolution is lost.

In addition to choosing a spatial focus, the connectivity measures themselves have multiple possible dimensions: presence, amplitude, latency, frequency. Especially in the development of connectivity measures that should be applicable in clinical practice a measure should capture all relevant information in a limited number of outcome measures with a clear meaning. We showed that subacute stroke survivors with poor motor function show significant PCC at less frequencies across the contralateral sensorimotor area than subacute stroke survivors with good motor function. Yet, no difference was found in the amplitude of PCC. Apparently, when PCC exceeds the significance limit the amplitude of PCC contains no additional information. The StrEP features we choose do not differ between good and poor function stroke subjects, while the similarity between StrEP waveforms in ipsilesional and contralesional hemisphere may differ when studying a larger subject population.

In this thesis we analysed cortical activity in a 'sensor space'. Although we referenced the EEG to a Laplacian nearest neighbour derivation to enhance the spatial resolution of the EEG, we did not locate the sources of the cortical activity. However, by applying source localisation techniques, it becomes possible to focus on the connectivity in specific cortical areas. Specific source localisation techniques are available for evoked potentials like the StrEP (Grech et al., 2008) and for coherence (Gross et al., 2001). The 4D-EEG project[1] will combine source localisation techniques, external perturbations and system identification to study the role of different cortical areas in motor control.

An important aspect that should not be overlooked in the extraction of (additional) features from the afferent pathway connectivity measures is reproducibility. Poor reproducibility properties severely limit the applicability of any measure that is applied to assess the effect of an intervention or to follow subjects in a longitudinal study design. We performed a first evaluation of the reliability of StrEP features in a small group of normal subjects. The results of this evaluation were promising, but further analysis in a specifically designed study is recommended.

Towards identification of pathway properties

Although the application of external perturbations is a technique taken from the field of system identification, PCC and the StrEP do not identify properties of a dynamical system. System identification for linear systems includes the estimation of the impulse response

[1] More information on: `http://www.4deeg.eu/`, project headed by prof.dr. F.C.T. van der Helm from Delft Technical University, the Netherlands

(time domain) or frequency response function (frequency domain). A potential difficulty in the extension of the afferent pathways connectivity measures to system identification procedures is that only a very small portion of the cortical activity is linearly related to the perturbation signal. This is best seen in the PCC: maximal PCC seldom exceeded 0.25. This means that at least 75% of the EEG power at a specific stimulus frequency is generated by sources not linearly related to the perturbation. From a linear system identification perspective these other sources are noise; the PCC amplitudes thus indicate a poor signal to noise ratio. As a result, application of linear system identification techniques requires long recordings to allow enough averaging to cancel the noise contributions.

In the development and validation of system identification techniques, modelling of the corticomuscular system can shed light on how properties of the efferent and afferent pathways shape the (non-linear) dynamics of the system. Modelling of the efferent pathways has previously been applied to provide insight in properties of CMC (Williams and Baker, 2009a,b) and to support choices in data analysis, for example regarding the rectification of the EMG (Stegeman et al., 2010; Boonstra and Breakspear, 2012; Farina et al., 2013). As it is evident that motor control involves a closed loop feedback system, both afferent and efferent pathways should be included in a model to evaluate the connectivity measures. Several models have already been developed that may be combined towards the development of a closed loop model. In the context of CMC several models have been developed of the afferent pathways (Williams and Baker, 2009a,b; Stegeman et al., 2010). Furthermore, there are models available that represent the spinal reflex loop (Schuurmans et al., 2009; Stienen et al., 2007).

From connectivity to motor function recovery

Recovery of motor function is a complex process where actual pre-stroke functions can return and new patterns emerge. Various processes, including recovery of penumbra tissue, cortical and subcortical reorganization, utilisation of alternative (ipsilateral) pathways and behaviour compensation strategies, act on different time scales (Kwakkel et al., 2004). It is unknown how these processes interact and shape the recovery process on an individual (Kwakkel et al., 2004). By looking at motor function and impairment only, the addition of the underlying processes is seen, not their separate contribution. Disentangling the mechanisms shaping recovery after stroke may allow the identification of critical time windows where beneficial processes are dominant and thus allow the right therapy at the right time (Kwakkel et al., 2004; Dobkin, 2005).

Assessment of connectivity between neural populations involved in motor control could provide some of this much needed insight in different mechanisms underlying motor function recovery after stroke. The measures of afferent pathway connectivity presented in this thesis are valuable in this context as sensory feedback and sensorimotor integration are vital for motor function (Scott, 2004; Pruszynski and Scott, 2012). Showing the feasibility of obtaining PCC and the StrEP early after stroke opens the possibility to record afferent pathway connectivity after stroke in a longitudinal study design following stroke survivors throughout motor function recovery process. Such a longitudinal study can include subjects with a variety of motor function scores because the measures can also be obtained from individuals with very poor motor function. It is of great importance to include this group of poor function subjects as this group also contains some individ-

uals that make a substantial recovery despite an initial poor prognosis. Especially these individuals are likely to benefit most from intensive therapy at the right time.

Currently, a longitudinal study assessing changes in connectivity during recovery of motor function after stroke is running at the Leiden University Medical Centre and the Free University Medical Centre in the Netherlands: Explore stroke[2]. Recording of afferent pathway connectivity measures is included in the Explore stroke protocol. The first results on longitudinal changes of afferent pathway connectivity in relation to motor function recovery are expected towards the end of 2015. Also the 4D-EEG project will include studies on (pathway) connectivity and recovery of motor function after stroke to improve prediction of motor function outcome and improve rehabilitation therapy.

Bridging the gap between pathway connectivity and recovery will not only provide insight in mechanisms underlying recovery of motor function. It may allow providing individual stroke survivors with a more informed prognosis of their potential motor function recovery and targeted therapy in critical time windows. This is of great value for stroke survivors, who in the end want to make their everyday life as normal as possible again.

[2] More information (in Dutch) on:
`https://wetenschap.hersenstichting.nl/onderzoek/onderzoeken/explore-beroerte`,
project headed by dr. C.G.M. Meskers at the Free University Medical Centre, Amsterdam, the Netherlands.

Bibliography

Abbruzzese, G., Berardelli, A., Rothwell, J.C., Day, B.L. and Marsden, C.D., 1985. 'Cerebral potentials and electromyographic responses evoked by stretch of wrist muscles in man.' *Experimental Brain Research*, 58(3):544–551.

Abbruzzese, G., Ratto, S., Favale, E. and Abbruzzese, M., 1981. 'Proprioceptive modulation of somatosensory evoked potentials during active or passive finger movements in man.' *Journal of Neurology, Neurosurgery, and Psychiatry*, 44(10):942–949.

Akaike, H., 1971. 'Autoregressive model fitting for control'. *Annals of the Institute of Statistical Mathematics*, 23(2):163–180.

Al-Rawi, M.A.W., Hamdan, F.B. and Abdul-Muttalib, A.K., 2009. 'Somatosensory evoked potentials as a predictor for functional recovery of the upper limb in patients with stroke.' *Stroke*, 18(4):262–8.

Allison, T., Hume, a.L., Wood, C.C. and Goff, W.R., 1984. 'Developmental and aging changes in somatosensory, auditory and visual evoked potentials.' *Electroencephalography and Clinical Neurophysiology*, 58(1):14–24.

Allison, T., McCarthy, G., Wood, C.C. and Jones, S.J., 1991. 'Potentials Evoked in Human and Monkey Cerebral Cortex By Stimulation of the Median Nerve'. *Brain*, 114(6):2465–2503.

Amtage, F., Henschel, K., Schelter, B., Vesper, J., Timmer, J., Lücking, C.H. et al., 2009. 'High functional connectivity of tremor related subthalamic neurons in Parkinson's disease.' *Clinical Neurophysiology*, 120(9):1755–1761.

Astolfi, L., Cincotti, F., Mattia, D., Marciani, M.G., Baccalá, L.A., de Vico Fallani, F. et al., 2007. 'Comparison of different cortical connectivity estimators for high-resolution EEG recordings.' *Human Brain Mapping*, 28(2):143–157.

Baccalá, L.A. and Sameshima, K., 2001. 'Partial directed coherence: a new concept in neural structure determination.' *Biological Cybernetics*, 84(6):463–74.

Baker, S.N., 2007. 'Oscillatory interactions between sensorimotor cortex and the periphery.' *Current Opinion in Neurobiology*, 17(6):649–655.

Baker, S.N., Chiu, M. and Fetz, E.E., 2006. 'Afferent encoding of central oscillations in the monkey arm.' *Journal of Neurophysiology*, 95(6):3904–3910.

Baker, S.N., Olivier, E. and Lemon, R.N., 1997. 'Coherent oscillations in monkey motor cortex and hand muscle EMG show task-dependent modulation.' *Journal of Physiology*, 501(1):225–241.

Barthélemy, D., Willerslev-Olsen, M., Lundell, H., Conway, B.A., Knudsen, H., Biering-Sø rensen, F. et al., 2010. 'Impaired transmission in the corticospinal tract and gait disability in spinal cord injured persons.' *Journal of Neurophysiology*, 104(2):1167–76.

Beckerman, H., Roebroeck, M.E., Lankhorst, G.J., Becher, J.G., Bezemer, P.D. and Verbeek, A.L., 2001. 'Smallest real difference, a link between reproducibility and responsiveness.' *Quality of Life Research*, 10(7):571–8.

Bo Nielsen, J., 2002. 'Motoneuronal drive during human walking.' *Brain Research Reviews*, 40(1-3):192–201.

Bo Nielsen, J.B., Brittain, J.S., Halliday, D.M., Marchand-Pauvert, V., Mazevet, D. and Conway, B.A., 2008. 'Reduction of common motoneuronal drive on the affected side during walking in hemiplegic stroke patients.' *Clinical Neurophysiology*, 119(12):2813–8.

Bohannon, R.W. and Smith, M.B., 1987. 'Interrater reliability of a modified Ashworth scale of muscle spasticity.' *Physical Therapy*, 67(2):206–7.

Boonstra, T.A., Schouten, A.C. and van der Kooij, H., 2013. 'Identification of the contribution of the ankle and hip joints to multi-segmental balance control.' *Journal of Neuroengineering and Rehabilitation*, 10(1):23.

Boonstra, T.W. and Breakspear, M., 2012. 'Neural mechanisms of intermuscular coherence: implications for the rectification of surface electromyography.' *Journal of Neurophysiology*, 107(3):796–807.

Bortel, R. and Sovka, P., 2007. 'Approximation of statistical distribution of magnitude squared coherence estimated with segment overlapping'. *Signal Processing*, 87(5):1100–1117.

Braun, C., Staudt, M., Schmitt, C., Preissl, H., Birbaumer, N. and Gerloff, C., 2007. 'Crossed cortico-spinal motor control after capsular stroke.' *European Journal of Neuroscience*, 25(9):2935–2945.

Brown, P., Farmer, S.F., Halliday, D.M., Marsden, J. and Rosenberg, J.R., 1999. 'Coherent cortical and muscle discharge in cortical myoclonus.' *Brain*, 122 (Pt 3:461–72.

Brown, P., Salenius, S., Rothwell, J.C. and Hari, R., 1998. 'Cortical Correlate of the Piper Rhythm in Humans'. *Journal of Neurophysiology*, 80:2911–2917.

Bruns, A., 2004. 'Fourier-, Hilbert- and wavelet-based signal analysis: are they really different approaches?' *Journal of Neuroscience Methods*, 137(2):321–332.

Campfens, S.F., Schouten, A.C., van der Kooij, H. and van Putten, M.J.A.M., 2011. 'P7.11 Corticomuscular system tunes to external perturbations during a motor task as revealed by corticomuscular coherence'. *Clinical Neurophysiology*, 122 (Supl 1):S92.

Campfens, S.F., Schouten, A.C., van Putten, M.J.A.M. and van der Kooij, H., 2013. 'Quantifying connectivity via efferent and afferent pathways in motor control using coherence measures and joint position perturbations.' *Experimental Brain Research*, 228(2):141–153.

Carter, G.C., 1987. 'Coherence and time delay estimation'. *Proceedings of the IEEE*, 75:1235–1246.

Connell, L.A., Lincoln, N.B. and Radford, K.A., 2008. 'Somatosensory impairment after stroke: frequency of different deficits and their recovery.' *Clinical Rehabilitation*, 22(8):758–67.

Conway, B.A., Halliday, D.M., Farmer, S.F., Shahani, U., Maas, P., Weir, A.I. et al., 1995. 'Synchronization between motor cortex and spinal motoneuronal pool during the performance of a maintained motor task in man.' *Journal of Physiology*, 489(3):917–924.

Cramer, S.C., Sur, M., Dobkin, B.H., O'Brien, C., Sanger, T.D., Trojanowski, J.Q. et al., 2011. 'Harnessing neuroplasticity for clinical applications.' *Brain*, 134(Pt 6):1591–609.

de Ruiter, C.J., de Korte, A., Schreven, S. and de Haan, A., 2010. 'Leg dominancy in relation to fast isometric torque production and squat jump height.' *European Journal of Applied Physiology and Occupational Physiology*, 108(2):247–55.

de Vet, H.C.W., Terwee, C.B., Knol, D.L. and Bouter, L.M., 2006. 'When to use agreement versus reliability measures.' *Journal of Clinical Epidemiology*, 59(10):1033–9.

den Otter, a.R., Geurts, a.C.H., Mulder, T. and Duysens, J., 2004. 'Speed related changes in muscle activity from normal to very slow walking speeds.' *Gait and Posture*, 19(3):270–8.

Desmedt, J.E. and Tomberg, C., 1989. 'Mapping early somatosensory evoked potentials in selective attention: critical evaluation of control conditions used for titrating by difference the cognitive P30, P40, P100 and N140.' *Electroencephalography and Clinical Neurophysiology*, 74(5):321–46.

Dobkin, B.H., 2005. 'Rehabilitation after Stroke'. *New England Journal of Medicine*, 352(16):1677–1684.

Dukelow, S.P., Herter, T.M., Moore, K.D., Demers, M.J., Glasgow, J.I., Bagg, S.D. et al., 2010. 'Quantitative assessment of limb position sense following stroke.' *Neurorehabilitation and Neural Repair*, 24(2):178–87.

Fang, Y., Daly, J.J., Sun, J., Hvorat, K., Fredrickson, E., Pundik, S. et al., 2009. 'Functional corticomuscular connection during reaching is weakened following stroke.' *Clinical Neurophysiology*, 120(5):994–1002.

Farina, D., Negro, F. and Jiang, N., 2013. 'Identification of common synaptic inputs to motor neurons from the rectified electromyogram.' *Journal of Physiology*, 591(Pt 10):2403–18.

Farmer, S.F., Bremner, F.D., Halliday, D.M., Rosenberg, J.R. and Stephens, J.A., 1993. 'The frequency content of common synaptic inputs to motoneurones studied during voluntary isometric contraction in man'. *Journal of Physiology*, 470:127–155.

Feys, H., Van Hees, J., Bruyninckx, F., Mercelis, R. and De Weerdt, W., 2000. 'Value of somatosensory and motor evoked potentials in predicting arm recovery after a stroke.' *Journal of Neurology, Neurosurgery, and Psychiatry*, 68(3):323–31.

Florin, E., Gross, J., Pfeifer, J., Fink, G.R. and Timmermann, L., 2010a. 'The effect of filtering on Granger causality based multivariate causality measures.' *NeuroImage*, 50:577–588.

Florin, E., Gross, J., Pfeifer, J., Fink, G.R. and Timmermann, L., 2011. 'Reliability of multivariate causality measures for neural data.' *Journal of Neuroscience Methods*, 198(2):344–358.

Florin, E., Gross, J., Reck, C., Maarouf, M., Schnitzler, A., Sturm, V. et al., 2010b. 'Causality between local field potentials of the subthalamic nucleus and electromyograms of forearm muscles in Parkinson's disease.' *European Journal of Neuroscience*, 31:491–498.

Fries, P., 2005. 'A mechanism for cognitive dynamics: neuronal communication through neuronal coherence.' *Trends in Cognitive Sciences*, 9(10):474–480.

Fugl-Meyer, A.R., Jääskö, L., Leyman, I., Olsson, S. and Steglind, S., 1975. 'The post-stroke hemiplegic patient. 1. a method for evaluation of physical performance.' *Scandinavian Journal of Rehabilitation Medicine*, 7(1):13–31.

Gourévitch, B., Bouquin-Jeannès, R.L. and Faucon, G., 2006. 'Linear and nonlinear causality between signals: methods, examples and neurophysiological applications.' *Biological Cybernatics*, 95(4):349–369.

Granger, C., 1969. 'Investigating Causal Relations by Econometric Models and Cross-spectral Methods'. *Econometrica*, 37(3):424–438.

Graziadio, S., Tomasevic, L., Assenza, G., Tecchio, F. and Eyre, J.A., 2012. 'The myth of the 'unaffected' side after unilateral stroke: Is reorganisation of the non-infarcted corticospinal system to re-establish balance the price for recovery?' *Experimental Neurology*, 238(2):168–175.

Grech, R., Cassar, T., Muscat, J., Camilleri, K.P., Fabri, S.G., Zervakis, M. et al., 2008. 'Review on solving the inverse problem in EEG source analysis.' *Journal of NeuroEngineering and Rehabilitation*, 5:25.

Grefkes, C. and Ward, N.S., 2014. 'Cortical Reorganization After Stroke: How Much and How Functional?' *The Neuroscientist*, 20(June):56–70.

Gross, J., Kujala, J., Hamalainen, M., Timmermann, L., Schnitzler, A. and Salmelin, R., 2001. 'Dynamic imaging of coherent sources: Studying neural interactions in the human brain.' *Proceeding of the National Academy of Sciences of the United States of America*, 98(2):694–699.

Gross, J., Tass, P.A., Salenius, S., Hari, R., Freund, H.J. and Schnitzler, A., 2000. 'Cortico-muscular synchronization during isometric muscle contraction in humans as revealed by magnetoencephalography.' *Journal of Physiology*, 527 Pt 3:623–631.

Grosse, P., Cassidy, M. and Brown, P., 2002. 'EEG-EMG, MEG-EMG and EMG-EMG frequency analysis: physiological principles and clinical applications.' *Clinical Neurophysiology*, 113(10):1523–1531.

Grosse, P., Guerrini, R., Parmeggiani, L., Bonanni, P., Pogosyan, A. and Brown, P., 2003. 'Abnormal corticomuscular and intermuscular coupling in high-frequency rhythmic myoclonus.' *Brain*, 126(Pt 2):326–342.

Gwin, J.T. and Ferris, D.P., 2012. 'Beta- and gamma-range human lower limb corticomuscular coherence.' *Frontiers in Human Neuroscience*, 6(September):258.

Halliday, D.M., Conway, B.A., Christensen, L.O.D., Hansen, N.L., Petersen, N.P. and Nielsen, J.B., 2003. 'Functional coupling of motor units is modulated during walking in human subjects.' *Journal of Neurophysiology*, 89(2):960–8.

Halliday, D.M., Conway, B.A., Farmer, S.F. and Rosenberg, J.R., 1998. 'Using electroencephalography to study functional coupling between cortical activity and electromyograms during voluntary contractions in humans.' *Neuroscience Letters*, 241(1):5–8.

Halliday, D.M. and Farmer, S.F., 2010. 'On the need for rectification of surface EMG.' *Journal of Neurophysiology*, 103(6):3547; author reply 3548–9.

Halliday, D.M., Rosenberg, J.R., Amjad, a.M., Breeze, P., Conway, B.A. and Farmer, S.F., 1995. 'A framework for the analysis of mixed time series/point process data–theory and application to the study of physiological tremor, single motor unit discharges and electromyograms.' *Progress in Biophysics and Molecular Biology*, 64(2-3):237–278.

Hansen, N.L., Conway, B.A., Halliday, D.M., Hansen, S., Pyndt, H.S., Biering-Sørensen, F. et al., 2005. 'Reduction of common synaptic drive to ankle dorsiflexor motoneurons during walking in patients with spinal cord lesion.' *Journal of Neurophysiology*, 94(2):934–42.

Hansen, N.L., Hansen, S., Christensen, L.O.D., Petersen, N.T. and Nielsen, J.B., 2001. 'Synchronization of Lower Limb Motor Unit Activity During Walking in Human Subjects Synchronization of Lower Limb Motor Unit Activity During Walking in Human Subjects'. *Journal of Neurophysiology*, 86:1266–1276.

Haufe, S., Nikulin, V.V., Müller, K.R. and Nolte, G., 2013. 'A critical assessment of connectivity measures for EEG data: a simulation study.' *NeuroImage*, 64:120–33.

Hausdorff, J.M., 2007. 'Gait dynamics, fractals and falls: finding meaning in the stride-to-stride fluctuations of human walking.' *Human Movement Science*, 26(4):555–89.

Hausdorff, J.M., Peng, C.K., Ladin, Z., Wei, J.Y. and Goldberger, A.L., 1995. 'Is walking correlations a random walk? Evidence for long-range in stride interval of human gait'. *Journal of Applied Physiology*, 78(1):349–358.

Herrmann, C.S., 2001. 'Human EEG responses to 1-100 Hz flicker: resonance phenomena in visual cortex and their potential correlation to cognitive phenomena'. *Experimental Brain Research*, 137(3-4):346–353.

Horwitz, B., 2003. 'The elusive concept of brain connectivity.' *NeuroImage*, 19(2 Pt 1):466–470.

Jain, S., Gourab, K., Schindler-Ivens, S. and Schmit, B.D., 2013. 'EEG during pedaling: Evidence for cortical control of locomotor tasks.' *Clinical Neurophysiology*, 124(2):379–390.

Johnson, A.N., Wheaton, L.a. and Shinohara, M., 2011. 'Attenuation of corticomuscular coherence with additional motor or non-motor task.' *Clinical Neurophysiology*, 122(2):356–363.

Josiassen, R.C., Shagass, C., Roemer, R.a., Slepner, S. and Czartorysky, B., 1990. 'Early cognitive components of somatosensory event-related potentials.' *International Journal of Psychophysiology*, 9(2):139–49.

Kaminski, M.J. and Blinowska, K.J., 1991. 'A new method of the description of the information flow in the brain structures.' *Biological Cybernetics*, 65(3):203–210.

Kandel, E.R., Schwartz, J.H. and Jessell, T.M., 2000. *Principles of neural science, 4/e*. McGraw-Hill Medical.

Kato, H., Sugawara, Y., Ito, H., Onodera, K., Sato, C. and Kogure, K., 1991. 'Somatosensory evoked potentials following stimulation of median and tibial nerves in patients with localized intracerebral hemorrhage: correlations with clinical and CT findings.' *Journal of the Neurological Sciences*, 103(2):172–8.

Kottner, J., Audigé, L., Brorson, S., Donner, A., Gajewski, B.J., Hróbjartsson, A. et al., 2011. 'Guidelines for Reporting Reliability and Agreement Studies (GRRAS) were proposed.' *Journal of Clinical Epidemiology*, 64(1):96–106.

Kristeva, R., Patino, L. and Omlor, W., 2007. 'Beta-range cortical motor spectral power and corticomuscular coherence as a mechanism for effective corticospinal interaction during steady-state motor output.' *NeuroImage*, 36(3):785–792.

Kristeva-Feige, R., Fritsch, C., Timmer, J. and Lücking, C.H., 2002. 'Effects of attention and precision of exerted force on beta range EEG-EMG synchronization during a maintained motor contraction task.' *Clinical Neurophysiology*, 113(1):124–131.

Kwakkel, G., Kollen, B. and Lindeman, E., 2004. 'Understanding the pattern of functional recovery after stroke: facts and theories.' *Restorative Neurology and Neuroscience*, 22(3-5):281–99.

Kwakkel, G., Kollen, B.J., van der Grond, J. and Prevo, A.J.H., 2003. 'Probability of regaining dexterity in the flaccid upper limb: impact of severity of paresis and time since onset in acute stroke.' *Stroke*, 34(9):2181–6.

Laaksonen, K., Kirveskari, E., Mäkelä, J.P., Kaste, M., Mustanoja, S., Nummenmaa, L. et al., 2012. 'Effect of afferent input on motor cortex excitability during stroke recovery.' *Clinical neurophysiology*, 123(12):2429–36.

Lachaux, J.P., Rodriguez, E., Martinerie, J. and Varela, F.J., 1999. 'Measuring phase synchrony in brain signals.' *Human Brain Mapping*, 8(4):194–208.

Langdon, A.J., Boonstra, T.W. and Breakspear, M., 2011. 'Multi-frequency phase locking in human somatosensory cortex.' *Progress in Biophysics and Molecular Biology*, 105(1-2):58–66.

Lincoln, N.B., Crow, J.L., Jackson, J.M., Waters, G.R., Adams, S.A. and Hodgson, P., 1991. 'The unreliability of sensory assessments'. *Clinical Rehabilitation*, 5:273–282.

Lindemann, M., Raethjen, J., Timmer, J., Deuschl, G. and Pfister, G., 2001. 'Delay estimation for cortico-peripheral relations.' *Journal of Neuroscience Methods*, 111(2):127–39.

Ljung, L., 1999. *System Identification: Theory for the users, 2nd ed.* Prentice Hall PTR.

MacKinnon, C.D., Verrier, M.C. and Tatton, W.G., 2000. 'Motor cortical potentials precede long-latency EMG activity evoked by imposed displacements of the human wrist.' *Experimental Brain Research*, 131(4):477–490.

Masakado, Y. and Nielsen, J.B., 2008. 'Task-and phase-related changes in cortico-muscular coherence.' *Keio Journal of Medicine*, 57(1):50–56.

Matthews, P.B., 1993. 'Interaction between short- and long-latency components of the human stretch reflex during sinusoidal stretching.' *Journal of Physiology*, 462:503–527.

McClelland, V.M., Cvetkovic, Z. and Mills, K.R., 2012a. 'Modulation of corticomuscular coherence by peripheral stimuli.' *Experimental Brain Research*, 219(2):275–292.

McClelland, V.M., Cvetkovic, Z. and Mills, K.R., 2012b. 'Rectification of the EMG is an unnecessary and inappropriate step in the calculation of Corticomuscular coherence.' *Journal of Neuroscience Methods*, 205(1):190–201.

Mendez-Balbuena, I., Huethe, F., Schulte-Mönting, J., Leonhart, R., Manjarrez, E. and Kristeva, R., 2011. 'Corticomuscular Coherence Reflects Interindividual Differences in the State of the Corticomuscular Network During Low-Level Static and Dynamic Forces.' *Cerebral Cortex*, 22(3):628–638.

Meng, F., Tong, K.Y., Chan, S.T., Wong, W.W., Lui, K.H., Tang, K.W. et al., 2009. 'Cerebral plasticity after subcortical stroke as revealed by cortico-muscular coherence.' *IEEE Transactions on Neural Systems and Rehabilitation Engineering*, 17(3):234–243.

Mima, T., Matsuoka, T. and Hallett, M., 2001a. 'Information flow from the sensorimotor cortex to muscle in humans.' *Clinical Neurophysiology*, 112(1):122–126.

Mima, T., Simpkins, N., Oluwatimilehin, T. and Hallett, M., 1999. 'Force level modulates human cortical oscillatory activities.' *Neuroscience Letters*, 275(2):77–80.

Mima, T., Steger, J., Schulman, A.E., Gerloff, C. and Hallett, M., 2000. 'Electroencephalographic measurement of motor cortex control of muscle activity in humans.' *Clinical Neurophysiology*, 111(2):326–337.

Mima, T., Terada, K., Maekawa, M., Nagamine, T., Ikeda, A. and Shibasaki, H., 1996. 'Somatosensory evoked potentials following proprioceptive stimulation of finger in man.' *Experimental Brain Research*, 111(2):233–245.

Mima, T., Toma, K., Koshy, B. and Hallett, M., 2001b. 'Coherence Between Cortical and Muscular Activities After Subcortical Stroke'. *Stroke*, 32(11):2597–2601.

Mugge, W., Abbink, D.A., Schouten, A.C., Dewald, J.P.A. and van der Helm, F.C.T., 2010. 'A rigorous model of reflex function indicates that position and force feedback are flexibly tuned to position and force tasks.' *Experimental Brain Research*, 200(3-4):325–340.

Myers, L.J., Lowery, M., O'Malley, M., Vaughan, C.L., Heneghan, C., Gibson, A.S.C. et al., 2003. 'Rectification and non-linear pre-processing of EMG signals for cortico-muscular analysis.' *Journal of Neuroscience Methods*, 124(2):157–165.

Negro, F. and Farina, D., 2011. 'Linear transmission of cortical oscillations to the neural drive to muscles is mediated by common projections to populations of motoneurons in humans.' *Journal of Physiology*, 589(Pt 3):629–637.

Neto, O.P. and Christou, E.A., 2010. 'Rectification of the EMG signal impairs the identification of oscillatory input to the muscle.' *Journal of Neurophysiology*, 103(2):1093–1103.

Nijland, R.H.M., van Wegen, E.E.H., Harmeling-van der Wel, B.C. and Kwakkel, G., 2010. 'Presence of finger extension and shoulder abduction within 72 hours after stroke predicts functional recovery: early prediction of functional outcome after stroke: the EPOS cohort study.' *Stroke*, 41(4):745–50.

Nitsche, M.A. and Paulus, W., 2008. 'Sustained excitability elevations induced by transcranial DC motor cortex stimulation in humans'. *Neurology*, 57:1899–1901.

Nolte, G., Bai, O., Wheaton, L., Mari, Z., Vorbach, S. and Hallett, M., 2004. 'Identifying true brain interaction from EEG data using the imaginary part of coherency.' *Clinical Neurophysiology*, 115(10):2292–2307.

Nolte, G., Ziehe, A., Nikulin, V.V., Schlögl, A., Krämer, N., Brismar, T. et al., 2008. 'Robustly estimating the flow direction of information in complex physical systems.' *Physical Review Letters*, 100(23):234101.

Norton, J.A., 2008. 'Higher neural control is required for functional walking.' *Clinical Neurophysiology*, 119(12):2675–6.

Norton, J.A. and Gorassini, M.a., 2006. 'Changes in cortically related intermuscular coherence accompanying improvements in locomotor skills in incomplete spinal cord injury.' *Journal of Neurophysiology*, 95(4):2580–9.

Norton, J.A., Wood, D.E. and Day, B.L., 2004. 'Is the spinal cord the generator of 16-Hz orthostatic tremor?' *Neurology*, 62(4):632–4.

Norton, J.A., Wood, D.E., Marsden, J.F. and Day, B.L., 2003. 'Spinally generated electromyographic oscillations and spasms in a low-thoracic complete paraplegic.' *Movement Disorders*, 18(1):101–6.

Omlor, W., Patino, L., Hepp-Reymond, M.C. and Kristeva, R., 2007. 'Gamma-range corticomuscular coherence during dynamic force output.' *NeuroImage*, 34(3):1191–1198.

Oostenveld, R., Fries, P., Maris, E. and Schoffelen, J.M., 2011. 'FieldTrip: Open source software for advanced analysis of MEG, EEG, and invasive electrophysiological data.' *Computational Intelligence and Neuroscience*, 2011:156869.

Oostenveld, R. and Praamstra, P., 2001. 'The five percent electrode system for high-resolution EEG and ERP measurements.' *Clinical Neurophysiology*, 112(4):713–719.

Pasma, J.H., Boonstra, T.A., Campfens, S.F., Schouten, A.C. and van der Kooij, H., 2012. 'Sensory reweighting of proprioceptive information of the left and right leg during human balance control.' *Journal of Neurophysiology*, 108(4):1138–48.

Perez, M.A., Lundbye-Jensen, J. and Nielsen, J.B., 2006. 'Changes in corticospinal drive to spinal motoneurones following visuo-motor skill learning in humans.' *Journal of Physiology*, 573(Pt 3):843–855.

Petersen, T.H., Kliim-Due, M., Farmer, S.F. and Nielsen, J.B., 2010. 'Childhood development of common drive to a human leg muscle during ankle dorsiflexion and gait.' *Journal of Physiology*, 588(Pt 22):4387–400.

Petersen, T.H., Willerslev-Olsen, M., Conway, B.A. and Nielsen, J.B., 2012. 'The motor cortex drives the muscles during walking in human subjects.' *Journal of Physiology*, 590(Pt 10):2443–52.

Pintelon, R. and Schoukens, J., 2001. *System Identification. A frequency domain approach*. IEEE Press.

Pohja, M. and Salenius, S., 2003. 'Modulation of cortex-muscle oscillatory interaction by ischaemia-induced deafferentation.' *Neuroreport*, 14(3):321–324.

Pohja, M., Salenius, S. and Hari, R., 2005. 'Reproducibility of cortex-muscle coherence.' *NeuroImage*, 26(3):764–770.

Porcaro, C., Coppola, G., Pierelli, F., Seri, S., Di Lorenzo, G., Tomasevic, L. et al., 2013. 'Multiple frequency functional connectivity in the hand somatosensory network: An EEG study.' *Clinical Neurophysiology*, 124(6):1216–24.

Portney, L.G. and Watkins, M.P., 2009. *Foundations of clinical research*. Prentice Hall.

Potvin, J.R. and Brown, S.H.M., 2004. 'Less is more: high pass filtering, to remove up to 99the surface EMG signal power, improves EMG-based biceps brachii muscle force estimates.' *Journal of Electromyography and Kinesiology*, 14(3):389–99.

Power, H.A., Norton, J.a., Porter, C.L., Doyle, Z., Hui, I. and Chan, K.M., 2006. 'Transcranial direct current stimulation of the primary motor cortex affects cortical drive to human musculature as assessed by intermuscular coherence.' *Journal of Physiology*, 577(Pt 3):795–803.

Prabhakaran, S., Zarahn, E., Riley, C., Speizer, A., Chong, J.Y., Lazar, R.M. et al., 2008. 'Inter-individual variability in the capacity for motor recovery after ischemic stroke.' *Neurorehabilitation and Neural Repair*, 22(1):64–71.

Priestley, M.B., 1983. *Spectral analysis and time series*. Academic Press.

Pruszynski, J.A. and Scott, S.H., 2012. 'Optimal feedback control and the long-latency stretch response.' *Experimental Brain Research*, 218(3):341–59.

Riddle, C.N., Baker, M.R. and Baker, S.N., 2004. 'The effect of carbamazepine on human corticomuscular coherence.' *NeuroImage*, 22(1):333–340.

Riddle, C.N. and Baker, S.N., 2005. 'Manipulation of peripheral neural feedback loops alters human corticomuscular coherence.' *Journal of Physiology*, 566(Pt 2):625–639.

Riddle, C.N. and Baker, S.N., 2006. 'Digit displacement, not object compliance, underlies task dependent modulations in human corticomuscular coherence.' *NeuroImage*, 33(2):618–627.

Rogers, L.M., Madhavan, S., Roth, H. and Stinear, J.W., 2011. 'Transforming neurorehabilitation of walking following stroke: the promise of non-invasive brain stimulation–a review.' *Restorative Neurology and Neuroscience*, 29(6):507–16.

Roiha, K., Kirveskari, E., Kaste, M., Mustanoja, S., Mäkelä, J.P., Salonen, O. et al., 2011. 'Reorganization of the primary somatosensory cortex during stroke recovery.' *Clinical Neurophysiology*, 122(2):339–45.

Rosenberg, J.R., Amjad, A.M., Breeze, P., Brillinger, D.R. and Halliday, D.M., 1989. 'The Fourier approach to the identification of functional coupling between neuronal spike trains.' *Progress in Biophysics and Molecular Biology*, 53(1):1–31.

Rossiter, H.E., Eaves, C., Davis, E., Boudrias, M.H., Park, C.h., Farmer, S. et al., 2013. 'Changes in the location of cortico-muscular coherence following stroke'. *NeuroImage: Clinical*, 2:50–55.

Rothwell, J.C., Thompson, P.D., Day, B.L., Boyd, S. and Marsden, C.D., 1991. 'Stimulation of the human motor cortex through the scalp'. *Experimental Physiology*, 76:159–200.

Roy, R.R., Garfinkel, A., Ounjian, M., Payne, J., Hirahara, A., Hsu, E. et al., 1995. 'Three-dimensional structure of cat tibialis anterior motor units.' *Muscle and Nerve*, 18(10):1187–1195.

Schabrun, S.M. and Hillier, S., 2009. 'Evidence for the retraining of sensation after stroke: a systematic review.' *Clinical Rehabilitation*, 23(1):27–39.

Schneider, T. and Neumaier, A., 2001. 'Algorithm 808: ARfit—a matlab package for the estimation of parameters and eigenmodes of multivariate autoregressive models'. *ACM Transactions on Mathematical Software*, 27(1):58–65.

Schoffelen, J.M., Oostenveld, R. and Fries, P., 2005. 'Neuronal coherence as a mechanism of effective corticospinal interaction.' *Science*, 308(5718):111–113.

Schoffelen, J.M., Poort, J., Oostenveld, R. and Fries, P., 2011. 'Selective movement preparation is subserved by selective increases in corticomuscular gamma-band coherence.' *Journal of Neuroscience*, 31(18):6750–6758.

Schouten, A.C. and Campfens, S.F., 2012. 'Directional coherence disentangles causality within the sensorimotor loop, but cannot open the loop.' *Journal of Physiology*, 590(Pt 10):2523–2529.

Schouten, A.C., de Vlugt, E., van Hilten, J.J.B. and van der Helm, F.C.T., 2008. 'Quantifying Proprioceptive Reflexes During Position Control of the Human Arm'. *IEEE Transactions on Biomedical Engineering*, 55(1):311–321.

Schuurmans, J., de Vlugt, E., Schouten, A.C., Meskers, C.G.M., de Groot, J.H. and van der Helm, F.C.T., 2009. 'The monosynaptic Ia afferent pathway can largely explain the stretch duration effect of the long latency M2 response.' *Experimental Brain Research*, 193(4):491–500.

Scott, S.H., 2004. 'Optimal feedback control and the neural basis of volitional motor control.' *Nature Reviews. Neuroscience*, 5(7):532–46.

Seiss, E., Hesse, C.W., Drane, S., Oostenveld, R., Wing, A.M. and Praamstra, P., 2002. 'Proprioception-related evoked potentials: origin and sensitivity to movement parameters.' *NeuroImage*, 17(1):461–468.

Serrien, D.J., Strens, L.H.a., Cassidy, M.J., Thompson, A.J. and Brown, P., 2004. 'Functional significance of the ipsilateral hemisphere during movement of the affected hand after stroke.' *Experimental Neurology*, 190(2):425–32.

Severens, M., Nienhuis, B., Desain, P. and Duysens, J., 2012. 'Feasibility of measuring event related desynchronization with electroencephalography during walking.' *Conference Proceedings - IEEE Engineering in Medicine and Biology Society.*, 2012:2764–7.

Spieser, L., Meziane, H.B. and Bonnard, M., 2010. 'Cortical mechanisms underlying stretch reflex adaptation to intention: a combined EEG-TMS study.' *NeuroImage*, 52(1):316–325.

Stam, C.J., Nolte, G. and Daffertshofer, A., 2007. 'Phase lag index: assessment of functional connectivity from multi channel EEG and MEG with diminished bias from common sources.' *Human Brain Mapping*, 28(11):1178–93.

Stam, C.J. and van Straaten, E.C.W., 2012. 'The organization of physiological brain networks.' *Clinical Neurophysiology*, 123(6):1067–1087.

Starr, A. and Cohen, L.G., 1985. ''Gating' of somatosensory evoked potentials begins before the onset of voluntary movement in man.' *Brain Research*, 348(1):183–6.

Starr, A., Mckeon, B., Skuse, N. and Burke, D., 1981. 'Cerebral potentials evoked by muscle stretch in man'. *Brain*, 104:149–166.

Staudenmann, D., Potvin, J.R., Kingma, I., Stegeman, D.F. and van Dieën, J.H., 2007. 'Effects of EMG processing on biomechanical models of muscle joint systems: sensitivity of trunk muscle moments, spinal forces, and stability.' *Journal of Biomechanics*, 40(4):900–9.

Stegeman, D.F., van de Ven, W.J.M., van Elswijk, G.A., Oostenveld, R. and Kleine, B.U., 2010. 'The alpha-motoneuron pool as transmitter of rhythmicities in cortical motor drive.' *Clinical Neurophysiology*, 121(10):1633–42.

Stienen, A.H.A., Schouten, A.C., Schuurmans, J. and van der Helm, F.C.T., 2007. 'Analysis of reflex modulation with a biologically realistic neural network.' *Journal of Computational Neuroscience*, 23(3):333–48.

Stolk-Hornsveld, F., Crow, J.L., Hendriks, E.P., van der Baan, R. and Harmeling-van der Wel, B.C., 2006. 'The Erasmus MC modifications to the (revised) Nottingham Sensory Assessment: a reliable somatosensory assessment measure for patients with intracranial disorders.' *Clinical Rehabilitation*, 20(2):160–172.

Tallon-Baudry, C., Bertrand, O. and Fischer, C., 2001. 'Oscillatory synchrony between human extrastriate areas during visual short-term memory maintenance.' *Journal of Neuroscience*, 21(20):RC177.

Tass, P., Rosenblum, M.G., Weule, J., Kurths, J., Pikovsky, A., Volkmann, J. et al., 1998. 'Detection of n:m Phase Locking from Noisy Data: Application to Magnetoencephalography'. *Physical Review Letters*, 81(15):3291–3294.

Tecchio, F., Pasqualetti, P., Pizzella, V., Romani, G. and Rossini, P.M., 2000. 'Morphology of somatosensory evoked fields: inter-hemispheric similarity as a parameter for physiological and pathological neural connectivity.' *Neuroscience Letters*, 287(3):203–6.

Tsumoto, T., Hirose, N., Nonale, S. and Takahashi, M., 1973. 'Cerebrovascular disease changes in somatosensory evoked potentials associated with unilateral lesions'. *Electroencephalography and Clinical Neurophysiology*, 35:463–473.

Tzvetanov, P. and Rousseff, R.T., 2003. 'Median SSEP changes in hemiplegic stroke: long-term predictive values regarding ADL recovery.' *NeuroRehabilitation*, 18(4):317–24.

Ushiyama, J., Suzuki, T., Masakado, Y., Hase, K., Kimura, A., Liu, M. et al., 2011. 'Between-subject variance in the magnitude of corticomuscular coherence during tonic isometric contraction of the tibialis anterior muscle in healthy young adults.' *Journal of Neurophysiology*, 106(3):1379–1388.

van Asseldonk, E.H.F., Buurke, J.H., Bloem, B.R., Renzenbrink, G.J., Nene, A.V., van der Helm, F.C.T. et al., 2006. 'Disentangling the contribution of the paretic and non-paretic ankle to balance control in stroke patients.' *Experimental Neurology*, 201(2):441–451.

van der Helm, F.C.T., Schouten, A.C., de Vlugt, E. and Brouwn, G.G., 2002. 'Identification of intrinsic and reflexive components of human arm dynamics during postural control.' *Journal of Neuroscience Methods*, 119(1):1–14.

van der Kooij, H., van Asseldonk, E. and van der Helm, F.C.T., 2005. 'Comparison of different methods to identify and quantify balance control.' *Journal of Neuroscience Methods*, 145(1-2):175–203.

van der Meer, J.N., Schouten, A.C., Bour, L.J., de Vlugt, E., van Rootselaar, A.F., van der Helm, F.C.T. et al., 2010. 'The intermuscular 3-7 Hz drive is not affected by distal proprioceptive input in myoclonus-dystonia.' *Experimental Brain Research*, 202(3):681–691.

van Putten, M.J.A.M., 2012. 'The N20 in post-anoxic coma: are you listening?' *Clinical Neurophysiology*, 123(7):1460–4.

van Rootselaar, A.F., Maurits, N.M., Koelman, J.H.T.M., van der Hoeven, J.H., Bour, L.J., Leenders, K.L. et al., 2006. 'Coherence analysis differentiates between cortical myoclonic tremor and essential tremor.' *Movement Disorders*, 21(2):215–222.

van Strien, J.W., 1992. 'Classificatie van links- en rechtshandige proefpersonen'. *Nederlands tijdschrift voor de Psychologie*, 47:88–92.

Varela, F., Lachaux, J.P., Rodriguez, E. and Martinerie, J., 2001. 'The brainweb: phase synchronization and large-scale integration.' *Nature Reviews. Neuroscience*, 2(4):229–239.

Vinck, M., van Wingerden, M., Womelsdorf, T., Fries, P. and Pennartz, C.M.A., 2010. 'The pairwise phase consistency: a bias-free measure of rhythmic neuronal synchronization.' *NeuroImage*, 51(1):112–22.

Wagner, J.M., Rhodes, J.a. and Patten, C., 2008. 'Reproducibility and minimal detectable change of three-dimensional kinematic analysis of reaching tasks in people with hemiparesis after stroke.' *Physical Therapy*, 88(5):652–63.

Ward, N.J., Farmer, S.F., Berthouze, L. and Halliday, D.M., 2013. 'Rectification of EMG in low force contractions improves detection of motor unit coherence in the beta-frequency band.' *Journal of Neurophysiology*, 110(8):1744–50.

Ward, N.S., 2003. 'Neural correlates of outcome after stroke: a cross-sectional fMRI study'. *Brain*, 126(6):1430–1448.

Weiss, S. and Mueller, H.M., 2003. 'The contribution of EEG coherence to the investigation of language'. *Brain and Language*, 85(2):325–343.

Williams, E.R. and Baker, S.N., 2009a. 'Circuits generating corticomuscular coherence investigated using a biophysically based computational model. I. Descending systems.' *Journal of Neurophysiology*, 101(1):31–41.

Williams, E.R. and Baker, S.N., 2009b. 'Renshaw cell recurrent inhibition improves physiological tremor by reducing corticomuscular coupling at 10 Hz.' *Journal of Neuroscience*, 29(20):6616–6624.

Williams, E.R., Soteropoulos, D.S. and Baker, S.N., 2009. 'Coherence between motor cortical activity and peripheral discontinuities during slow finger movements.' *Journal of Neurophysiology*, 102(2):1296–1309.

Witham, C.L. and Baker, S.N., 2012. 'Reply from C.L. Witham and S.N. Baker'. *The Journal of Physiology*, 590(10):2531–2533.

Witham, C.L., Riddle, C.N., Baker, M.R. and Baker, S.N., 2011. 'Contributions of descending and ascending pathways to corticomuscular coherence in humans.' *Journal of Physiology*, 589(Pt 15):3789–3800.

Witham, C.L., Wang, M. and Baker, S.N., 2007. 'Cells in somatosensory areas show synchrony with beta oscillations in monkey motor cortex.' *European Journal of Neuroscience*, 26(9):2677–86.

Witte, M., Patino, L., Andrykiewicz, A., Hepp-Reymond, M.C. and Kristeva, R., 2007. 'Modulation of human corticomuscular beta-range coherence with low-level static forces.' *European Journal of Neuroscience*, 26(12):3564–3570.

Yang, Q., Fang, Y., Sun, C.K., Siemionow, V., Ranganathan, V.K., Khoshknabi, D. et al., 2009. 'Weakening of functional corticomuscular coupling during muscle fatigue.' *Brain Research*, 1250:101–112.

Yang, Q., Siemionow, V., Yao, W., Sahgal, V. and Yue, G.H., 2010. 'Single-Trial EEG-EMG Coherence Analysis Reveals Muscle Fatigue-Related Progressive Alterations in Corticomuscular Coupling.' *IEEE Transactions on Neural Systems and Rehabilitation Engineering*, 18(2):97–106.

Yao, B., Salenius, S., Yue, G.H., Brown, R.W. and Liu, J.Z., 2007. 'Effects of surface EMG rectification on power and coherence analyses: an EEG and MEG study.' *Journal of Neuroscience Methods*, 159(2):215–223.

Yao, J. and Dewald, J.P.A., 2006. 'Cortico-muscular communication during the generation of static shoulder abduction torque in upper limb following stroke.' *Conference Proceedings - IEEE Engineering in Medicine and Biology Society*, 1:181–184.

Dankwoord

Na vijf jaar ben ik op het punt gekomen dat ik het meest gelezen stuk van mijn proefschrift kan gaan schrijven: het dankwoord. Er is mij tijdens mijn promotie wel eens gevraagd of het niet eenzaam is om alleen met een onderzoek bezig te zijn. Nu ben ik natuurlijk wel een aanzienlijke periode voornamelijk met één onderzoek bezig geweest, alleen of eenzaam was ik zeker niet. Het is een voorrecht om mij op deze plek te richten tot de mensen met wie ik gedurende de afgelopen jaren heb samengewerkt en die mijn promotietraject in vele opzichten een memorabele periode hebben gemaakt.

De meest directe bijdrage is geleverd door mijn begeleiders en promotoren: Herman, Michel en Alfred. Drie heel verschillende begeleiders; de verschillende invalshoeken vormden soms een uitdaging. Terugkijkend kan ik alleen maar zeggen dat het juist door de verschillen beter is geworden en dat ik van elk van jullie heel veel heb geleerd. Herman, waarschijnlijk ben jij de belangrijkste man in mijn academische opleiding; begeleider tijdens mijn bachelor opdracht, tijdens mijn master opdracht en promotor. In al die fases heb ik je begeleiding zeer plezierig gevonden: kritisch, niet zomaar tevreden, maar altijd constructief. Zelf heb ik nog wel eens getwijfeld of ik dit project wel tot een goed einde zou weten te brengen, het was op die momenten een enorme geruststelling te weten dat jij er in elk geval vertrouwen in had. Alfred, jij werd kort na het begin van mijn master opdracht aan mijn begeleidingsteam toegevoegd en ik was blij dat Herman je ook voor mijn promotie erbij haalde. Slechts eens per twee weken in Enschede, maar altijd bereikbaar voor allerhande vragen van apparatuur aan de praat helpen tot wiskundige ins en outs van signaalverwerking, en waar nodig zijn opbeurende woorden paraat. Ik denk dat je geduld oneindig is. Tot slot Michel, jou ken ik 'pas' sinds het begin van mijn promotie. Direct vanaf het begin werd ik ook in jouw leerstoel-in-oprichting opgenomen. Ik heb veel van je geleerd over de wonderen van ons brein en verwerk nu vanzelf het commentaar dat jij als taalkenner bij mijn eerste schrijfsels zette.

Gedurende het project ontstond de mogelijkheid om samen te werken met de afdeling revalidatiegeneeskunde op het LUMC. Carel, je hebt een enorme bijdrage geleverd door de patiëntstudies mogelijk te maken en van input vanuit de revalidatie te voorzien. Je bent enorm druk met patiëntenzorg en onderzoek maar bent toch in staat geweest om inhoudelijk mee te (blijven) denken. Ook Sarah heeft voor die patiëntstudies een enorme hoeveelheid werk verzet. Ik had de metingen aan de CVA patiënten alleen lang zo goed niet kunnen doen, het was heel fijn dat jij daarbij kon ondersteunen en input kon leveren. Ik wens je heel veel succes met de vervolgmetingen en je promotieonderzoek.

Ook Edwin wil ik hier graag noemen, ook jij was betrokken bij de begeleiding van mijn bachelor en master opdracht. Je hebt zeker bijgedragen aan mijn interesse in onderzoek

naar de aansturing van bewegingen. Tijdens mijn promotie kon ik nog steeds voor allerhande zaken bij je terecht. Van een fijne begeleider tijdens mijn studie naar een fijne collega tijdens mijn promotie, met een gezamenlijke publicatie. Die publicatie is er natuurlijk ook gekomen dankzij de inzet van Stan, waarvoor dank.

De mensen die hiervoor genoemd staan hebben allemaal direct een inhoudelijke bijdrage geleverd aan dit proefschrift. Dat was allemaal zinloos geweest als we geen data hadden kunnen meten van een heleboel vrijwilligers. In het bijzonder wil ik de CVA patiënten bedanken, zij waren bereid om zich belangeloos te onderwerpen aan metingen die niet altijd even aangenaam waren.

Tijdens mijn promotie had ik als onderdeel van twee vakgroepen een hele groep leuke collega's. Het grootste deel van mijn tijd bij Biomedische Werktuigbouw en een dag per week bij Clinical Neurophysiology. Ik heb met beide groepen enorm geboft en het heeft ervoor gezorgd dat de afgelopen vijf jaar ook bijzonder gezellig zijn geweest met lunches, wandelingen, congressen, borrels, etentjes, koffie, koekjes en vakgroepuitjes. Ik kan niet iedereen bij naam noemen, ik vertrouw erop dat iedereen zich in voldoende mate aangesproken weet. Ik maak een paar uitzonderingen. De mensen met wie ik lange tijd mijn werkplekken heb gedeeld verdienen vermelding: Tjitske, Ard en Alexander bij BW (a.k.a. de gezellige kamer); Esther, Marleen, Jessica en Cecile bij CNPH. Binnen een kantoor deel je toch nog net iets meer lief en leed dan in de koffiepauze. Ook voor Lianne wil ik een uitzondering maken: je bent de afgelopen jaren een enorme steun geweest, niet alleen op praktisch vlak maar ook persoonlijk. Bedankt dat ik met alle bloed, zweet, tranen en hoogtepunten bij je terecht kon.

Zelfs nu mijn proefschrift bijna klaar is, en ik dit dankwoord schrijf, kan ik me nog maar moeilijk voorstellen dat ik op 9 oktober daadwerkelijk mijn proefschrift zal verdedigen. Gelukkig weet ik wel dat ik die dag bijgestaan zal worden door twee mensen die ik bewonder en mij erg dierbaar zijn. Mijn paranimfen hebben vaak klaar gestaan om mijn promotie-perikelen aan te horen, te relativeren en me ervan af te leiden. Tjitske: afstudeerbegeleider, kamergenoot en vriendin. Ik gun je van harte dat je binnenkort een avontuur in het buitenland kan ondernemen, maar ik zal je dan wel ontzettend missen. Thijs: studiegenoot, stapmaatje en vriend. Amsterdam en Enschede zouden dichter bij elkaar moeten liggen.

Zo richting het einde van dit dankwoord wil ik graag ook al mijn vrienden en familie bedanken voor alle getoonde interesse en geboden afleiding. Werk is niet het belangrijkste in het leven en ik prijs mij gelukkig met veel mensen om mij heen die mij daar regelmatig aan herinneren. In het bijzonder wil ik mijn (schoon) familie noemen: Tonny en Laurens, Roos en Peter, Piet en Carla, Saskia en Geert. Jullie bijdrage aan wie ik ben en wat ik bereikt heb, is groter dan ik hier onder woorden kan brengen.

En als afsluiting van dit dankwoord wil ik mij nog tot de - voor mij - belangrijkste persoon richten. Michel, allerliefste, jij vindt alles wat je de afgelopen tijd voor me hebt gedaan vanzelfsprekend, ik vind dat zeker niet. Bedankt voor je steun, ontspanning en liefde. Naast jou kan ik de wereld aan.

Floor Campfens

About the author

Sanne Floor Campfens (January 18th 1985, Amsterdam) studied Biomedical Engineering at the University of Twente, Enschede, the Netherlands. During her Bachelor assignment she developed an interest in scientific research on motor control. She performed an international research internship at the Montpellier Laboratory of Computer Science, Robotics and Microelectronics (LIRMM) on modelling of muscle activation by electrical stimulation. In June 2009 she obtained her Master of Science degree cum laude. Her master assignment at the Laboratory of Biomechanical Engineering was on proprioceptive reweighting between the left and right leg in maintaining upright balance.

Following the finishing of her master thesis, Floor started as a PhD student under the joint supervision of prof.dr.ir. Michel van Putten (Clinical Neurophysiology Chair), prof.dr.ir. Herman van der Kooij (Laboratory of Biomechanical Engineering) and dr.ir. Alfred Schouten (Laboratory of Biomechanical Engineering) at the University of Twente. This thesis describes the result of the research project on identification of corticomuscular connectivity in motor control. For measurements on stroke survivors she also collaborated with the dr. Carel Meskers at the Leiden University Medical Center.

Since December 2013, Floor works as a lecturer and applied researcher at Saxion University of Applied Science within the educational program of Mechatronics.

Journal publications

S.F. Campfens, H. van der Kooij and A.C. Schouten, 2014. 'Face to phase: pitfalls in time delay estimation from coherency phase.' *Journal of Computational Neuroscience*, 37(1):1-8

E.H.F. van Asseldonk, S.F. Campfens, S.J.F. Verwer, M.J.A.M. van Putten and D.F. Stegeman, 2014. 'Reliability and agreement of intramuscular coherence in tibialis anterior muscle.' *PLoS ONE*, 9(2):e88428

S.F. Campfens, A.C. Schouten, M.J.A.M. van Putten and H. van der Kooij, 2013. 'Quantifying connectivity via efferent and afferent pathways in motor control using coherence measures and joint position perturbations.' *Experimental Brain Research*, 228(2):141-153

J.H. Pasma, T.A. Boonstra, S.F. Campfens, A.C. Schouten and H. van der Kooij, 2012. 'Sensory reweighting of proprioceptive information of the left and right leg during human balance control.' *Journal of Neurophyiology*, 108(4):1138-1148

A.C. Schouten and S.F. Campfens, 2012. 'Directional coherence disentangles causality within the sensorimotor loop, but cannot open the loop.' *Journal of Physiology*, 590(Pt 10):2529-2530

A.C. Schouten, T.A. Boonstra, F. Nieuwenhuis, S.F. Campfens and H. van der Kooij, 2009. 'A bilateral ankle manipulator to investigate human balance control.' *IEEE Transactions on Neural Systems & Rehabilitation Engineering*, 19(6):660-669

Conference contributions

A.C. Schouten, S.F. Campfens and H. van der Kooij, 2013 'Time delays cannot be estimated from the phase-frequency relationship of coherence.' *1st International Conference on Basic and Clinical Multimodal Imaging*.

A.C. Schouten and S.F. Campfens, 2012. 'Disentangling causality of corticomuscular coherence within the sensorimotor loop.' *Annual meeting of the Society of Neuroscience*.

S.F. Campfens, A.C. Schouten, M.J.A.M. van Putten and H. van der Kooij, 2012. 'Reproducability of corticomuscular coherence: a comparison between static and perturbed tasks.' *Annual meeting of the Society of Neuroscience*.

S.F. Campfens, A.C. Schouten, H. van der Kooij and M.J.A.M. van Putten, 2011. 'Corticomuscular system tunes to external perturbations during a motor task as revealed by corticomuscular coherence.' *14th European Congress on Clinical Neurophysiology*.

S.F. Campfens, M.J.A.M. van Putten, A.C. Schouten and H. van der Kooij, 2011. 'Corti-

comuscular coupling: different coupling measures and system identification.' *3rd Dutch BME conference*.

S.F. Campfens, T.A. Boonstra, A.C. Schouten, E.H.F. van Asseldonk and H. van der Kooij, 2009. 'Proprioceptive sensory reweighting in the left and right leg during balance control.' *Annual meeting of the Society for Neuroscience*.

A.C. Schouten, S.F. Campfens, T.A. Boonstra and H. van der Kooij, 2009. 'Unloading responses in the ankle during balance: The afferent contribution to balance.' *Annual meeting of the Society for Neuroscience*.

S.F. Campfens, M. Papaiordanidou, D. Guiraud, M. Hayashibe and A. Varray, 2008. 'An activation model of motor response and H-reflex under FES.' *13th Annual Conference of the International Functional Electrical Stimulation Society*.